

AD-A054 043

GENERAL ELECTRIC CO PHILADELPHIA PA SPACE DIV
METHODS OF FABRICATING CERAMIC MATERIALS.(U)
NOV 77 A GATTI, M J NOONE

F/G 11/2

F33615-74-C-4073

UNCLASSIFIED

AFML-TR-77-135

NL

1 OF 2

AD
A054043



FOR FURTHER TRAN ~~FILE~~

2

AD A 054043

AFML-TR-77-135

METHODS OF FABRICATING CERAMIC MATERIALS

GENERAL ELECTRIC COMPANY
SPACE SCIENCES LABORATORY
P. O. BOX 8555
PHILADELPHIA, PA. 19101

— use Space Div

405025

AD No.
DDC FILE COPY

NOVEMBER 1977

TECHNICAL REPORT AFML-TR-77-135
Final Report for Period April 1974 – April 1977

Approved for public release; distribution unlimited.

AIR FORCE MATERIALS LABORATORY
AIR FORCE WRIGHT AERONAUTICAL LABORATORIES
AIR FORCE SYSTEMS COMMAND
WRIGHT-PATTERSON AIR FORCE BASE, OHIO 45433

DDC
RECEIVED
MAY 16 1978
D

NOTICE

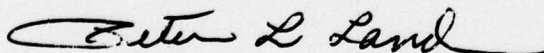
When Government drawings, specifications, or other data are used for any purpose other than in connection with a definitely related Government procurement operation, the United States Government thereby incurs no responsibility nor any obligation whatsoever; and the fact that the government may have formulated, furnished, or in any way supplied the said drawings, specifications, or other data, is not to be regarded by implication or otherwise as in any manner licensing the holder or any other person or corporation, or conveying any rights or permission to manufacture, use, or sell any patented invention that may in any way be related thereto.

This final report was prepared under Contract No. AF33615-74-C-4073 "Methods of Fabricating Ceramic Materials" performed under the direction of the Processing and High Temperature Materials Branch, Metallurgy and Ceramics Division, Air Force Materials Laboratory.

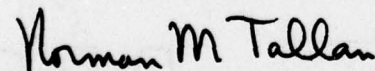
This report has been reviewed by the Information Office (IO) and is releasable to the National Technical Information Service (NTIS). At NTIS, it will be available to the general public, including foreign nations.

This technical report has been reviewed and is approved for publication.

P.L. LAND
Project Engineer



FOR THE COMMANDER



NORMAN M. TALLAN
Chief, Processing and High Temperature
Materials Branch
Metals & Ceramics Division

Copies of this report should not be returned unless return is required by security considerations, contractual obligations, or notice on a specific document.

⑨ Final rept. 15 Apr 74 - 15 Apr 77

SECURITY CLASSIFICATION OF THIS PAGE (When Data Entered)

19 REPORT DOCUMENTATION PAGE		READ INSTRUCTIONS BEFORE COMPLETING FORM
1. REPORT NUMBER 18 AFML-TR-77-135	2. GOVT ACCESSION NO.	3. RECIPIENT'S CATALOG NUMBER
4. TITLE (and Subtitle) 6 METHODS OF FABRICATING CERAMIC MATERIALS.		5. TYPE OF REPORT & PERIOD COVERED 15 April 1974 to Final: 15 April 1977
7. AUTHOR(s) 10 Arno Gatti Michael J. Noone		6. PERFORMING ORG. REPORT NUMBER
9. PERFORMING ORGANIZATION NAME AND ADDRESS General Electric Co. ✓ Space Sciences Laboratory P.O. Box 8555, Phila, Penna. 19101		8. CONTRACT OR GRANT NUMBER(s) 15 F33615-74-C-4073
11. CONTROLLING OFFICE NAME AND ADDRESS Air Force Materials Laboratory (LLM) AF Wright Aeronautical Laboratories, AFSC Wright-Patterson Air Force Base, Ohio 45433		10. PROGRAM ELEMENT, PROJECT, TASK AREA & WORK UNIT NUMBERS 61102F 17 16 2306 2306P, 2306P204
14. MONITORING AGENCY NAME & ADDRESS (if different from Controlling Office)		12. REPORT DATE 11 Nov 1977
		13. NUMBER OF PAGES 118 12 137p
		15. SECURITY CLASS. (of this report) Unclassified
		15a. DECLASSIFICATION/DOWNGRADING SCHEDULE
16. DISTRIBUTION STATEMENT (of this Report) Approved for public release; distribution unlimited.		
17. DISTRIBUTION STATEMENT (of the abstract entered in Block 20, if different from Report)		
18. SUPPLEMENTARY NOTES		
19. KEY WORDS (Continue on reverse side if necessary and identify by block number) Si-Al-Q-N, Sialons, Structural Ceramics, Pressureless Sintering, Mineralizing, Ceramics for Gas Turbines, Radomes, Fabrication, Slip-Casting, Jigging, Bend Strength, Oxidation.		
20. ABSTRACT (Continue on reverse side if necessary and identify by block number) Processing parameters are described which allow the fabrication of high density "Sialon" compositions using conventional ceramic technology amenable to low-cost large-scale production. A processing technique, "mineralization" is used to incorporate sintering aids into the Al ₂ O ₃ component of the sialon which facilitates control and minimization of the amount of such additives while simultaneously extending the firing range of the materials. Sialons containing up to 87% by weight of Si ₃ N ₄ are densified by pressureless sintering in an atmosphere of N ₂ +H ₂ with negligible weight loss. Properties discussed include bend strength of up to 60,000 psi at room temperature with good strength retention in several compositions to 1400 C and oxidation		

DD FORM 1 JAN 73 1473 EDITION OF 1 NOV 65 IS OBSOLETE

SECURITY CLASSIFICATION OF THIS PAGE (When Data Entered)

405 025

JOB

resistance superior to hot pressed Si_3N_4 . The fabrication of Radome Shapes by slip casting and jiggering and of turbine blade shapes by injection molding are demonstrated.

ACCESSION NO.	
NTIS	White Section <input checked="" type="checkbox"/>
DOC	Blue Section <input type="checkbox"/>
UNANNOUNCED	<input type="checkbox"/>
JUSTIFICATION	
BT	
DISTRIBUTION/AVAILABILITY CODES	
RICL	AVAIL. AND/OR SPECIAL
A	

FOREWORD

This is a Final Technical Report submitted under Contract No. F33615-74-C-4073, "Methods of Fabricating Ceramic Materials". Project 2306, Task 2306P2, Work Unit No. 2306P204. The report covers the period 15 April 1974 to 15 April 1977. Submitted by the authors June 30, 1977.

This program was performed at the General Electric Company's Space Sciences Laboratory, Valley Forge, Pa., in the Materials Research and Development Section, managed by Mr. Louis R. McCreight; Dr. Michael J. Noone was Program Manager and Principal Investigator. Mr. Arno Gatti was co-investigator on the program and was responsible for the development of Sialon fabrication technology, Mr. William Laskow was the fabrication specialist, Mr. T. A. Harris, Jr., was responsible for x-ray analysis of fabricated specimens, Mr. M. I. Birenbaum assisted with metallography, and Mr. Robert Grosso performed mechanical testing.

This program was sponsored by the Processing and High Temperature Materials Branch, Metals and Ceramics Division, Air Force Materials Laboratory, Air Force Wright Aeronautical Laboratories, Air Force Systems Command, Wright-Patterson Air Force Base, Ohio.

Dr. James M. Wimmer and later Dr. Peter L. Land, Research Physicists, AFML/LLM, Metals and Ceramics Division of the Air Force Materials Laboratory were project engineers.

TABLE OF CONTENTS

<u>SECTION</u>	<u>PAGE</u>
I INTRODUCTION	1
II EXPERIMENTAL PROCEDURES	8
1. Power Processing	8
a. Waring Blender Mixing	8
b. Milling	10
c. Firing	13
d. Hot Pressing	15
III RESULTS AND DISCUSSION	17
1. Preliminary Experiments	17
a. Preparation of sialon powders	17
b. Sialon sintering studies	17
c. Microstructural Studies	20
d. Sialon Formed from Amorphous Si_3N_4 manufactured by DuPont	20
e. Sialons containing AlN only	22
f. Hot pressed sialons	23
g. Thermal expansion of sialon materials	29
h. Oxidation studies	32
i. Mechanical Properties of MgO doped sialons	34
j. Nitrogen atmosphere sintering experiments	38
k. Sintering behavior of sialon containing CeO_2 , ZrO_2 and La_2O_3	38

TABLE OF CONTENTS (cont'd)

SECTION	PAGE
1. Sintering behavior of sialon using GTE-Sylvania and Plessey Si ₃ N ₄ powders	39
2. Controlled Sialon Processing Employing Milling Techniques	42
a. Particle size studies	42
b. Pre-reacted sialon materials-MX series	42
(1) Milling	42
(2) Sintering studies	43
(3) The role of AlN in Mx sialon	46
(4) Microstructure analysis of Mx material	47
(5) Mechanical test of Mx material	47
c. Unreacted sialon material studies	49
(1) "W" series	49
(2) Fabrication of sialon grinding media	55
(3) SM series	57
(a) Sintering behavior of SM-15	59
(b) Strength of SM-15	60
(4) Studies on sialon bodies other than SM-15	60
(5) #102 material	65
(6) Sialons containing Y ₂ O ₃ and ZrO ₂	73
(7) Milled sialons	73
(a) Screening experiments using #128 sialon	78
(b) Firing studies	80
(c) Mechanical testing	84
(d) Young's modulus	88
(e) Oxidation of sialons	91
(f) Electrical properties of sialons	95

TABLE OF CONTENTS (cont'd)

SECTION	PAGE
3. Hardware Fabrication	102
a. Radome shapes - by cold pressing and sintering procedures	102
b. Radome shapes - by slip casting procedure	102
c. Radome shapes - by jigging procedures	104
d. JT 79 Turbine Blade Shapes - Injection molding procedure	106
4. Deliverables	106
IV CONCLUSIONS	113
REFERENCES	116

LIST OF ILLUSTRATIONS

	PAGE
Figure 1. The Si_3N_4 - AlN - SiO_2 Ternary Showing Locus of Compositions Used by Lumby et al to Establish the Formula $\text{Si}_{6-z}\text{Al}_z\text{O}_z\text{N}_{5-z}$ For the Single-Phase Sialon Materials(8).	3
Figure 2. Isothermal Section Si_3N_4 - AlN - Al_2O_3 of the System Si - Al - O - N at 1700°C . (Dashed lines are tentative for a temperature slightly below 1760°C) after Gauckler et al (15).	3
Figure 3. The Si_3N_4 - AlN - Al_2O_3 - SiO_2 System based on Research at Newcastle (after Jack - Ref. 16).	4
Figure 4. Flow diagrams of Sialon Powder Processing followed (a) when using Waring Blender (R) mixing technique, (b) when using high alumina mills and (c) when milling in polyurethane-lined mill using sialon grinding media.	9
Figure 5. Showing (a) Schematic view of molybdenum retort used to final fire MgO doped Sialons during preliminary studies, (b) Schematic view of molybdenum retort used to final fire all later Sialon compositions and (c) photograph of the high temperature retort fabricated from molybdenum and stainless steel. This retort was inserted into the 4" ID x 48" long Al_2O_3 tube furnace equipped with Mo winding and H_2 atmosphere.	14
Figure 6. (a) X-ray trace of sialon sintered in N_2/H_2 atmosphere. Some X phase but no Y phase. (b) X-ray trace of sialon + 13.3% MgO showing multiplicity of phases due to incomplete reaction of starting powders after 1 hour at 1700°C in N_2/H_2 atmosphere. (c) Same specimen as (b) but sintered for 2 hours at 1700°C . Note more complete reaction of α - Si_3N_4 .	21
Figure 7. (a) Micro-structure of hot-pressed 8% MgO sialon and (b) x-ray diffractometer trace of the same structure showing multiple phases α and β Si_3N_4 , β' and MgAl_2O_4 .	25
Figure 8. Typical microstructure of a 60:40 sialon (doped with 5% MgO) processed under standard conditions. The grain structure on the polished section is not readily distinguished and, except for islands of porosity and metallic inclusions, the material appears essentially single-phased.	26

LIST OF ILLUSTRATIONS

		<u>PAGE</u>
Figure 9.	(a) Microstructure of hot-pressed 8% MgO material (same specimen as Figure 7) after a homogenizing heat treatment at 1700°C for 2 hours in N ₂ -H ₂ , (b) x-ray diffractometer trace of structure shown in (a). β' Sialon is the only phase detected.	27
Figure 10.	X-ray diffractometer trace of hot-pressed 13.3% MgO Sialon under conditions which produced "Y" phase, β' Si ₃ N ₄ and large quantities of glass.	28
Figure 11.	Thermal expansion behavior of various Sialon compositions and hot-pressed Si ₃ N ₄ (NC-132).	30
Figure 12.	Thermal Expansion Coefficient of 60:40 Sialon as a function of MgO content at 800°C.	31
Figure 13.	Weight gain (in Mg /cm ²) vs time at 1400°C in still air for several MgO doped Sialon compositions.	33
Figure 14.	Assembled apparatus for elevated temperature testing with close-up view of specimen in place in the alumina ceramic 3-point bend-test fixture.	35
Figure 15.	The relationship between strength retention as measured at 1200°C and magnesia content of Sialon materials.	36
Figure 16.	Linear shrinkage, % weight loss and measured final density of Sialon containing CeO ₂ and La ₂ O ₃ sintered in H ₂ -H ₂ at 1700°C for 2 hours.	40
Figure 17.	X-ray diffractometer traces from Sialon material containing (a) 20 W/O CeO ₂ , (b) 10 W/O La ₂ O ₃ , (c) 10 W/O ZrO ₂ .	41
Figure 18.	X-ray diffractometer traces of (a) pre-reacted 8% MgO sialon, (b) as-milled Mx showing original 8% MgO sialon pattern and additional Al ₂ O ₃ . (c) Mx after sintering showing β' sialon and Mg Al ₂ O ₄ , and (d) "X" phase, β' sialon, and no Al ₂ O ₃ after "aging" heat treatment.	44

LIST OF ILLUSTRATIONS

	<u>PAGE</u>
Figure 19. Cross sections of Mx sialon after sintering in N ₂ -H ₂ for 2 hours at (a) 1450°C, (2) 1500°C, (3) 1550°C, (4) 1600°C, (5) 1625°C, (6) 1650°C, (7) 1675°C, (8) 1700°C, (9) 1700°C + 5 AlN, (10) 1700°C + 10% AlN, (11) 1700°C + 15% AlN.	45
Figure 20. Optical microstructure and electron microprobe images obtained from Mx material fired at 1600°C for 2 hours in N ₂ -H ₂ .	49
Figure 21. X-ray diffractometer traces of "W" series Sialon fired for 2 hours at 1700°C in N ₂ -H ₂ showing β' Sialon and unreacted alumina.	50
Figure 22. Optical microstructure and electron-microprobe images of "W" material milled for 72 hours and fired at 1700°C for 2 hours in N ₂ -H ₂ showing Mg concentration in sialon phase.	51
Figure 23. X-ray diffraction traces of "W" material milled for 24 hours then (a) fired at 1700°C for 2 hours and (b) Si ₃ N ₄ added, milled and fired for 2 hours at 1700°C showed that unreacted alumina still persists after this treatment.	54
Figure 24. Photographs of sialon cylinders and sialon balls for use in rubber or soft urethane-lined mills to minimize contamination, all "W" material, milled 24 hours.	56
Figure 25. X-ray diffractometer traces of SM series sialon showing relationships between β' sialon, "X" phase, AlN and Al ₂ O ₃ .	58
Figure 26. X-ray diffractometer traces of Sm-15 showing affect of temperature on formation of β' sialon phase.	62
Figure 27. X-ray diffractometer traces of sialon materials in which the glass forming volume was varied by adjusting the Al ₂ O ₃ - SiO ₂ - MgO content showing single phase β' sialon formation as specimen numbers increase.	63
Figure 28. Typical microstructure of #102 Sialon material after firing for 2 hours at 1700°C.	66

LIST OF ILLUSTRATIONS

	<u>PAGE</u>
Figure 29. (a) A typical x-ray diffractometer trace of #102 Sialon material fired at 1700°C for 1 hour, (b) after aging for 16 hours at 1400°C all in N ₂ -H ₂ atmosphere. Showing broadening of β' Sialon peaks after aging.	67
Figure 30. Density vs. sintering time data for #102 material sintered at 1700°C using the standard firing procedure with Mo retort and N ₂ -H ₂ atmosphere.	69
Figure 31. X-ray diffractometer traces of #102 material sintered at 1700°C for increasing times showing progressive elimination of α Si ₃ N ₄ (see also Figure 30).	71
Figure 32. X-ray diffractometer traces of #102 material fired in N ₂ atmosphere at AFML. A - AFML trace, B ¹ - GE trace.	72
Figure 33. X-ray diffractometer traces of Sialon sintered with additives of (a) Y ₂ O ₃ and (b) ZrO ₂ showing free Al ₂ O ₃ but no free ZrO ₂ or Y ₂ O ₃ .	74
Figure 34. X-ray diffractometer traces of Sialons #127, #128, #129 showing retained ZrO ₂ (127), single-phased β' Sialon (128) and single-phase β' Sialon and α - Si ₃ N ₄ (129).	76
Figure 35. Photomicrographs of Sialons #128, #129, #130 showing increasing porosity with increasing Si ₃ N ₄ content for identical firing procedures.	77
Figure 36. Photographs of #128 material showing variation in shrinkage during firing as a function of milling time, i.e. as a function of "actual" composition. A = 8 hours milling, B = 72 hours milling.	79
Figure 37. Schematic view of a screening apparatus capable of passing only particles of small diameter (after Prochaska (36)).	81
Figure 38. Microstructure of Sialon #128 made from -10μm starting powder. Showing absence of "evidence of coarse" particulates but remnant porosity persists.	82

LIST OF ILLUSTRATIONS

	<u>PAGE</u>
Figure 39. Schematic view of the four point bending apparatus used during this study. 15/16" outer span, 3/8" inner span.	85
Figure 40. High temperature strength behavior of #102 Sialon with data on aged #102 materials, #128 Sialon and ZrO_2 and Y_2O_3 Sialons added. (All in 4-point bending).	87
Figure 41. SEM images of a fracture area of #128 Sialon showing fracture initiation site at a large particle.	89
Figure 42. Fractograph of #128 Sialon showing typical evidence of slow crack growth behavior.	90
Figure 43. Oxidation behavior of Sialon materials in still air at 1400°C.	92
Figure 44. X-ray diffraction trace of layer formed during oxidation of Sialons showing mullite as the only detectable crystalline phase but also evidence for amorphous material in the broad background distortion.	94
Figure 45. Comparison of specular reflectance of $\beta - Si_3N_4$ (NC132) with #102 and #129 Sialons. Showing reflectance peaks proportional to Si_3N_4 content.	97
Figure 46. Dielectric constant as a function of temperature for several sialons and hot-pressed Si_3N_4 (data obtained by Westphal at MIT for AFML).	100
Figure 47. Loss tangent as a function of temperature for several sialons and hot-pressed Si_3N_4 (data obtained by Westphal of MIT for AFML).	101
Figure 48. As-Fired IR dome shape made from #102 sialon.	103
Figure 49. Slip cast IR dome shapes made from sialon materials. (Shown after binder removal ready for final firing).	105

LIST OF ILLUSTRATIONS

	<u>PAGE</u>
Figure 50. (a) Metal forms, plaster mold and cotton liners used to "jigger" radome shapes, (b) radome shape formed by "jiggering" technique.	107
Figure 51. Fired IR dome shapes produced from sialon compositions.	108
Figure 52. Photograph showing material container positioned ready for injection into mold for formation of turbine blade shape.	109
Figure 53. Injection molded sialon-wax JT79 turbine blade.	110
Figure 54. A sialon JT79 blade after firing to 1700°C for 2 hours (minus shroud portion).	111
Figure 55. Fired sialon #128 body on right and two sialon #129 bodies on left before machining into flat plate specimens for laser irradiation and rain erosion testing.	112

LIST OF TABLES

	PAGE
1. Materials Used During This Study	11
2. Preliminary Sialon Compositions (W/O) and Density and Weight Changes after Firing at 1700 C for Various Times	17
3. Compositions of Sialons Containing MgO (W/O) with Shrinkage and Weight Loss Data after Firing at 1700 C.	19
4. Sialon Compositions Containing DuPont Si_3N_4 (W/O)	22
5. Effect of AlN On Firing Shrinkage of 60/40 $\text{Si}_3\text{N}_4/\text{Al}_2\text{O}_3$ Sialon Discs	23
6. Three Point Bend Test Results for MgO-doped Sialons. (All based on 60/40 $\text{Si}_3\text{N}_4/\text{Al}_2\text{O}_3$ by weight).	37
7. Four Point Bend Strength of Mx Material at 20 C and 1200 C.	49
8. Weight Loss (%) and Shrinkage (%) vs. Firing Temperature ($^{\circ}\text{C}$) for SM-15 Material.	61
9. Four Point Bend Strength results on SM-15 Material.	61
10. Compositions of Sialon Bodies Processed with Varying Amounts of "Glass-Formers".	64
11. Compositions, Firing Schedules and Final Sintered Density of High- Si_3N_4 content Sialons	82
12. Four-point Strength Data of $-10\mu\text{m}$ Screened #128 Sialon Material.	82
13. Compositions and Final Densities of High- Si_3N_4 Content Sialons (fired by both GE and AFML).	83
14. Four Point Bend Strength Results for Various Sialon Materials at Several Temperatures.	86
15. Elastic Modulus and Density of Various Sialon Compositions at Room Temperature.	91
16. Composition in Weight Percent of Sialons Used During Oxidation Studies.	93
17. Cyclic Oxidation Behavior of Several Sialon Compositions.	95
18. Summary of Dielectric Properties of Sialons (after Land (43)).	99

SUMMARY

This report presents the results of a three-year effort to study the ceramic processing of the silicon-aluminum-oxygen-nitrogen materials (Sialons) funded by the Air Force Materials Laboratory, Wright-Patterson Air Force Base, Ohio. Processing studies were necessary because detailed knowledge of the "new" sialon systems was not generally available. There was also a need to reproducibly fabricate sizeable specimens for test and evaluation. Finally, the sintering mechanism was complicated because it involved a liquid phase which could vary in composition by both choice of starting materials and processing techniques. This liquid phase in turn had a profound effect on the mechanical properties, particularly at high temperatures, of the materials developed. This report first describes the initial fabrication and properties of compositions with deliberate additives and culminates in the description of the fabrication of Si_3N_4 -based ceramics of up to 82 M/O Si_3N_4 with a minimum of second phase content and hence, good strength retention at high temperatures.

Initial processing studies centered on careful mixing of fine particles of starting materials to limit processing contamination by using a Waring blender technique which was found to be useful in previous work. MgO was added as a sintering aid in quantities up to 13.5 M/O to promote a silica-magnesia glass phase which greatly enhanced consolidation during firing.

The series of MgO doped materials sintered erratically as a result of the low viscosity silica-magnesia glass phase which generated "foamy" microstructures during high temperature firing by decomposition of silicon nitride. The firing of these compositions was controlled by mineralizing the alumina addition so that the components of the glass phase were already incorporated

into the starting "powder" materials. Mineralization ensured that the necessary liquid phase for sintering was made available at the right place, at the right time, and of a more favorable viscosity (or reactivity) range; this markedly increased the practical firing range of the resulting sialon bodies. Fully dense bodies without size limitation (other than furnace capacity) were fabricated using the mineralization technique.

Processing studies were also made using the "technique" reported most in the literature (intentionally or inferred) of allowing grinding media to contaminate the starting materials. This program, however, introduced one important variation in that the grinding media used during this study were sialon balls formed previously by the mineralization process. This method for adding sintering aids was very effective when pick-up during milling was controlled by weighing the mill charge as a function of time. A 10% pick-up by weight was needed to ensure sintering to high density with sialon compositions of up to 87 W/O (i.e. to over 80% by volume) silicon nitride.

Other processing variables were evaluated during this work including the effect of aluminum nitride additions on sintering rate and the effect of various sintering atmospheres on ultimate density. The dual role of AlN was interesting in that it provided a means for removal of excess silica to form sialon while simultaneously controlling sintering mechanisms. Increasing AlN additions decreased sintering ability since AlN combined rapidly with available silica and prevented adequate liquid-phase formation. Since this was counter to enhanced densification during initial sintering, it was found desirable to place AlN within the sialon mix in a manner which would delay this reaction until after densification was completed. Mineralizing was used

as one approach, using composition-controlled grinding media was a second approach (actually, mineralizing the sintering aid would be a better description of this mechanism). Simple mixed (unground) sialon compositions would not readily densify without an abundance of sintering aids and the concomitant problem of "foaming" which would result from the presence of excess liquid at high temperature.

The strength of sialon materials made on this program was up to 400 MPa (60 KSI) in 4-point bending at room temperature. All testing was done on specimens cut from bulk material rather than on individually fabricated small test bars and thus better represents realistic engineering properties which may be expected in larger scale component fabrication. High temperature mechanical behavior was dependent upon the nature of the grain-boundary phase after sintering. When this remained glassy, viscous flow along grain boundaries would be expected and was observed. When the boundary phase was assimilated into the grains or converted to a refractory crystalline second phase, the material would remain strong at high temperatures. Material tested during this work behaved in a similar manner to hot-pressed Si_3N_4 as a function of test temperature indicating the presence of a glassy phase which allowed the material to flow plastically above 1200°C . Thermal aging experiments on some materials indicated that higher stress levels could be attained without deformation presumably as the remnant glassy phase was crystallized.

The oxidation behavior of sialons with few exceptions was better (lower weight change) than hot-pressed Si_3N_4 . Thermal expansion was essentially the same as hot-pressed Si_3N_4 while elastic modulus was lower and was proportional to the Si_3N_4 content.

During the latter part of the program, the processing study was focussed on application of sialons to radomes and IR dome structures. Accordingly, the best material developed to that date was used to show feasibility of fabrication of such shapes by slip casting and jiggering. Many samples were delivered to AFML for evaluation of reflectivity, microwave properties and rain erosion resistance. These tests are continuing at AFML under the direction of Dr. P. L. Land.

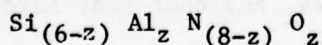
PRECEDING PAGE BLANK - FILMED

SECTION I

INTRODUCTION

This program was designed to investigate methods of fabricating ceramic materials with structurally useful thermal and mechanical properties from solid solutions of silicon, nitrogen, and metal oxides. The investigations included studies of the relationship of precursor powders and processing methods to the resulting composition and microstructure of fabricated specimens and, in turn, the relationship of these compositions and microstructures to the mechanical properties of the fabricated specimens. Emphasis was placed throughout the program on the use of conventional but controlled ceramic powder processing, fabrication of green shapes, and firing procedures, to achieve high density in the components using pressureless sintering techniques. Materials studied on the program were formed exclusively from compositions within the silicon-aluminum-oxygen-nitrogen system which are generally referred to as sialons.

The stimulus for this work was the data reported almost simultaneously by Jack (1,2,3) and Oyama (4,5,6) that the extensive solid solutions which exist in the $\text{Si}_3\text{N}_4\text{-Al}_2\text{O}_3$ system result in materials which may have unique properties and may be readily fabricated to high density by pressureless sintering techniques. Studies of sialons at Lucas in England (7,8) showed that materials with attractive mechanical and thermochemical properties could be produced, at least by the hot-pressing route, and that single-phase materials existed over only a narrow range of compositions represented by the formula:



The potential for development and exploitation of sialon materials particularly by the pressureless sintering approach led to the initiation of this work and several similar programs^(9,10,11,12). During the course of this work it has been demonstrated here and elsewhere, particularly at Lucas⁽¹³⁾, that dense materials can be achieved by pressureless sintering from a wide range of compositions and with properties amenable to exploitation in hazardous thermal, chemical, and friction and wear environments.

Tsuge et al⁽¹⁴⁾ showed that β - Si_3N_4 could accommodate up to about 60% by weight of Al_2O_3 in solid solution without major change of crystal structure but with increasing 'a' and 'c' unit-cell dimensions as the Al_2O_3 concentration increased. The phase diagram for the sialon system was established by Gauckler et al⁽¹⁵⁾ and further work has been performed by Jack⁽¹⁶⁾, Layden⁽¹⁰⁾, and Land et al⁽¹²⁾. Somewhat different phase diagrams have been determined by Land et al⁽¹²⁾ and by Layden⁽¹⁰⁾ from pressureless sintering studies but such differences are to be expected given the wide variety of processing conditions and potential mechanism for compositional changes. No specific phase equilibria studies were performed on this program and the compositions and fabrication procedures were designed as far as was practical to be consistent with the formula established by Lumby and the narrow phase field for achievement of single-phase structures observed by him (Figure 1) and developed in more detail by Gauckler (Figure 2)⁽¹⁵⁾. The wide range of phase stability previously outlined by Jack^(1,3) were no doubt multi-phased compositions involving at least some silicate glass. It has been shown that other stable single-phase materials of increasing solid solubility can be obtained in the Si-O-Be-N system⁽¹⁷⁾ as well as in the Si-O-Al-N system⁽¹⁵⁾ in directions which extend along lines of constant cation/anion ratio other than 3/4, and that many interesting materials may exist in these and similar systems⁽¹⁶⁾. The current phase diagram for the sialon system based on the work at Newcastle is shown in Figure 3⁽¹⁶⁾.

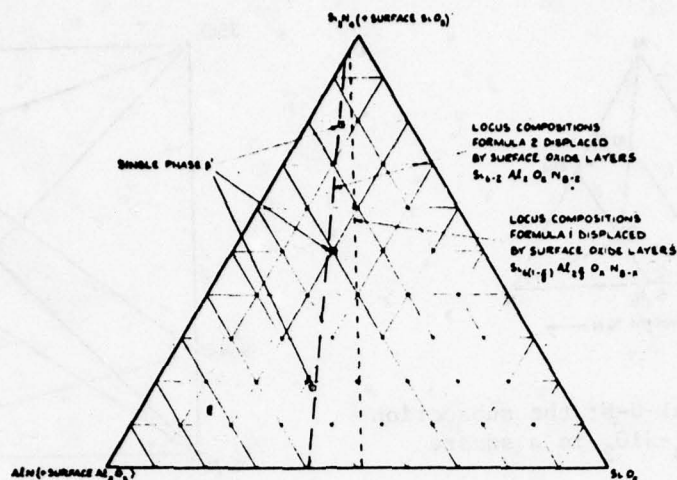


Figure 1. The $\text{Si}_3\text{N}_4\text{-AlN-SiO}_2$ Ternary Showing Locus of Compositions used by Lumby et al, to Establish the Formula $\text{Si}_{6-2}\text{Al}_z\text{O}_z\text{N}_{8-2}$ for the Single-Phase Sialon Materials (8)

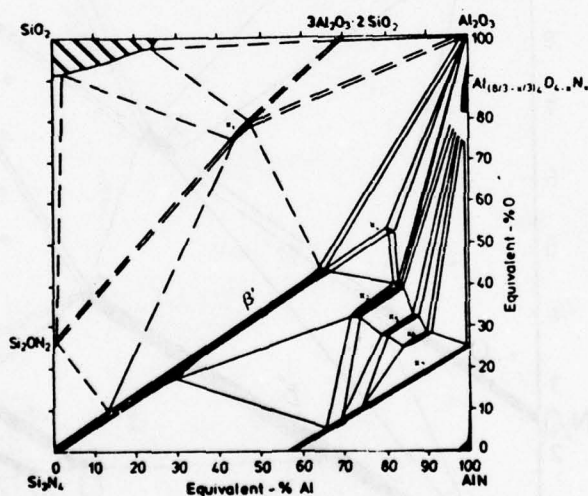
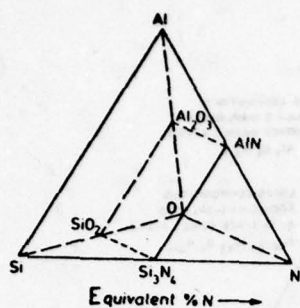
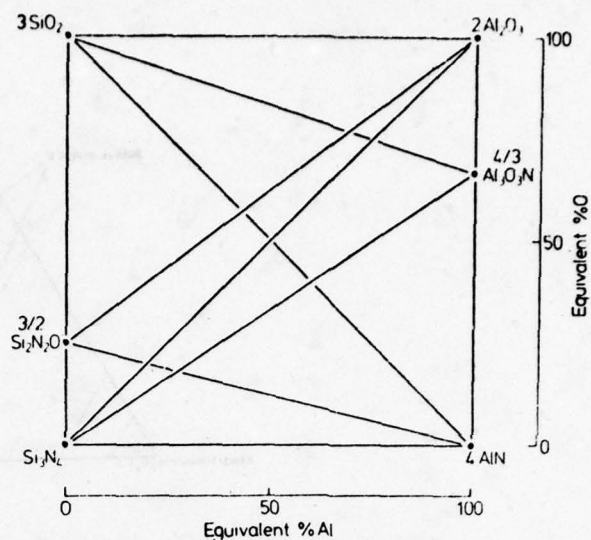


Figure 2. Isothermal Section $\text{Si}_3\text{N}_4\text{-AlN-Al}_2\text{O}_3$ of the System Si-Al-O-N at 1760°C . (Dashed lines are tentative for a temperature slightly below 1760°C) after Gauckler et al (15).



The system Si-Al-O-N; the subsection Si_3N_4 -AlN-Al₂O₃-SiO₂ is a square plane.



The square representation of the Si-Al-O-N system using equivalent concentrations.

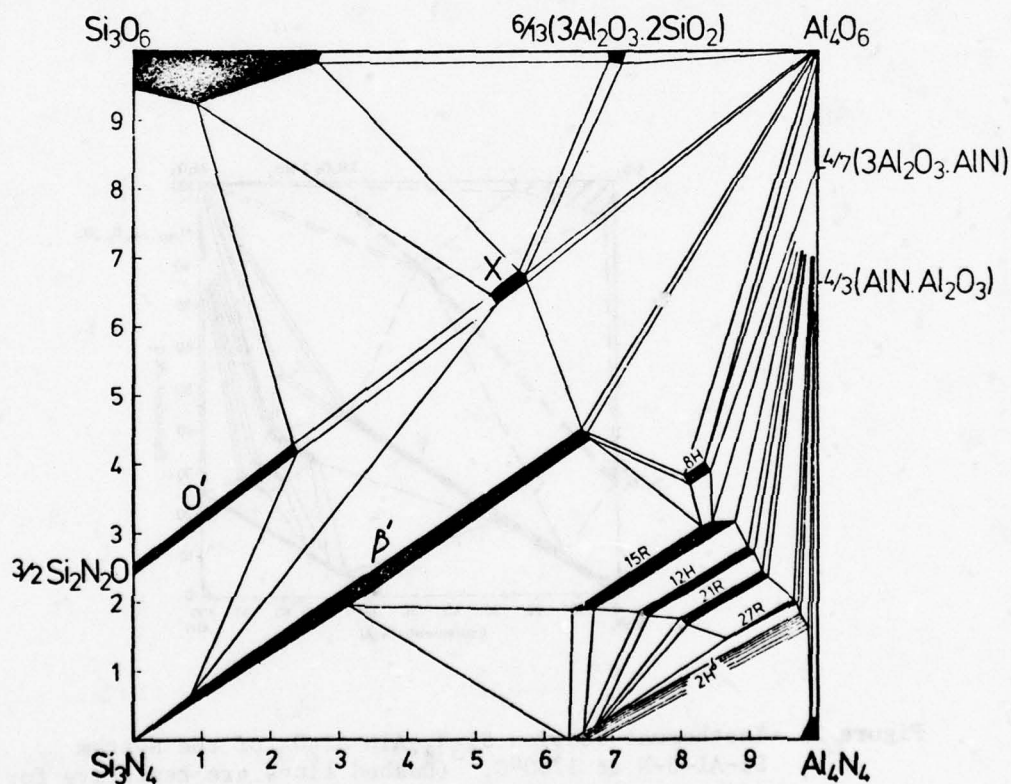


Figure 3. The Si_3N_4 -AlN-Al₂O₃-SiO₂ system based on research at Newcastle (after Jack Ref. 16).

The rapid formation of the β' solid solution in sialon systems and the ease with which impure "sialon" compositions could be densified by sintering were manifestations of the operation of a liquid phase sintering mechanism. It was clear at the outset of this work that a primary objective must be to achieve densification with a minimum of impurities or densification aids and to eliminate or at least minimize the presence of a liquid phase at the conclusion of the densification process. In previous studies the present authors had exploited this type of technology to develop dense sintered spinels in which additives were used to encourage liquid phase sintering in the initial densification stages and then removed or included into the solid solution by careful control of temperature and atmosphere in the final stages of densification (18,19). As will be discussed, this mechanism was made to operate in "sialon" systems and has more recently been termed "transient liquid phase sintering" in other studies in the sialon system (10,11,20) taking advantage of the low melting compositions which exist in the SiO_2 -rich corners of the phase diagram (Figure 3).

The present work explored fabrication variables in the sialon system so as to obtain an understanding of the means whereby dense single-phase materials might be achieved. It will be shown that materials in the sialon system can be readily fabricated by conventional ceramic processing and fired under controlled conditions to produce structural ceramics which, except for lower as-fabricated strengths, have properties comparable to Si_3N_4 -based materials produced by more complex and expensive methods. The properties of the materials described have not yet been optimized by concentrating on the production of any single composition. However, sufficient data have been attained to indicate that

materials in the sialon family warrant further study for an application in which their attributes of low-cost large-scale fabrication and insensitivity to specific starting materials may be focussed on, and the properties optimized for, the requirements of that particular applications.

The work to be described is divided into two major sections. Section III-1 discusses preliminary experiments which covered the first half of the program and involves the preparation of 'sialon' materials using simple blending techniques in an effort to avoid contamination which accompanies ball milling techniques. Section III-2 covers the latter half of the program in which variants of ball milling techniques were used to produce sialons using various mineralizing techniques based on the results of the preliminary experiments in which the important processing variables were identified and their roles evaluated.

Discussions of the properties of sialons are separated between these two sections since the two general families of materials differed significantly. The preliminary work generally produced glass-bonded materials with inferior high temperature properties and glassy oxidation products. It was, nevertheless, shown that simple processing techniques could be employed to produce sizeable components of a single crystalline phase content (β' - Si_3N_4 solid solution with generally low Si_3N_4 content of the order of 50%). The later studies particularly those employing sialon milling media demonstrated that compositions rich in Si_3N_4 could be readily fabricated with a minimum of glassy grain boundary phase and hence with properties appropriate to several potential structural applications. These materials also possessed essentially only

one crystalline phase (β Si_3N_4 solid solution) and as a result of improvements in firing techniques, the reproducibility of specimen preparation was assured. Compositions from this phase of the program are being studied further in other ongoing programs at GE and AFML.

SECTION II

EXPERIMENTAL PROCEDURES

1. Powder Processing

Three basic methods of powder processing were used during this study. These were: mixing of powders with a Waring blender (R), milling of powders separately in a high alumina mill and combining them into appropriate compositions, and milling sialon mixtures using a polyurethane-lined mill with sialon grinding media.

a. Waring Blender Mixing

Figure 4(a) shows a flow diagram of the processing steps used to produce sialon material by the Waring Blender (R) approach. This technique provided a rapid means for making low containment powder mixtures when the blade material was chosen carefully. For powder mixtures containing alumina an aluminum blade was an ideal choice in this respect. The addition of paraffin as a pressing lubricant and inclusion of a pelletizing step in the powder processing produced specimens of highest green density which led to highest fired density. Materials with sintered densities of 95-98% were not uncommon for MgO-doped sialon bodies processed by this method.

It was also noted that pre-firing (at 1000°C for 2 hours in air) reduced the amount and incidence of bloating during final firing for sialon compositions based on 60% Si_3N_4 containing up to 13.3% MgO by weight. This pre-reaction step appeared to convert the simple powder mixture into a more stable, refractory form avoiding some liquid intermediate phases. Subsequent x-ray analysis did confirm the formation of magnesium aluminate spinel in pre-firing. As it turned out, pre-firing partially accomplished a form of "mineralization" of the simple oxide components and the liquid portion of the sintering system during firing which is deemed essential for densification of sialon materials.

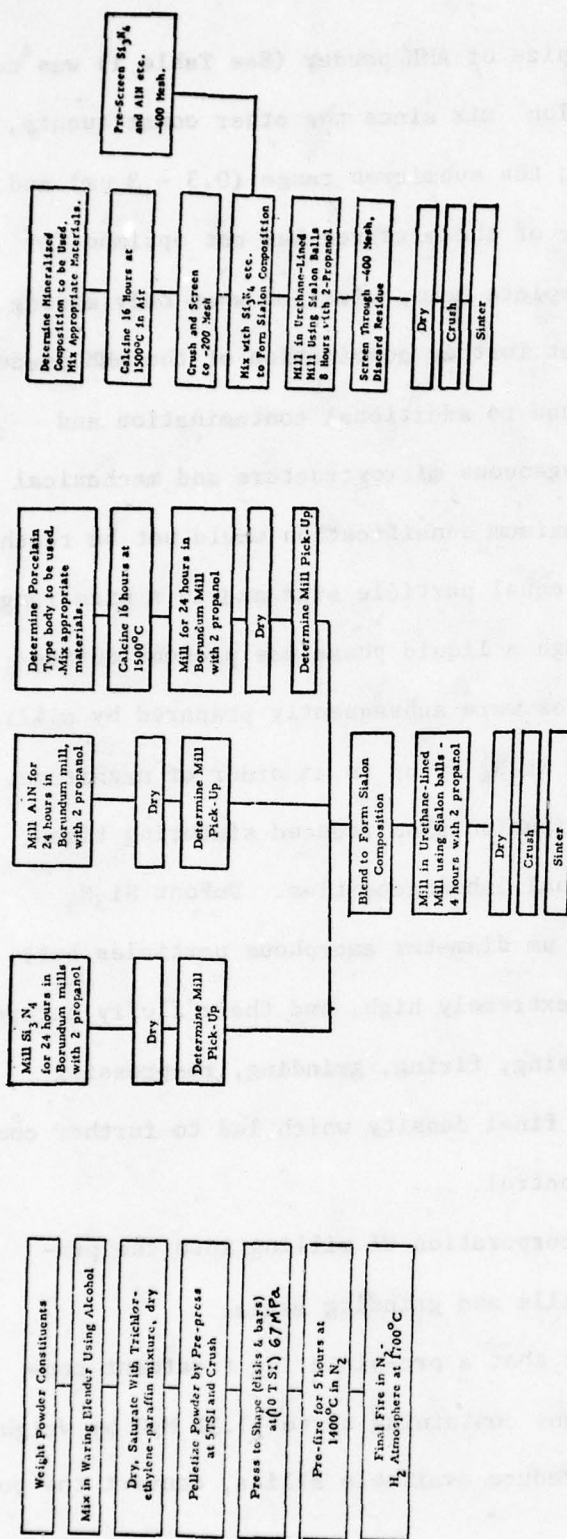


Figure 4. Flow diagrams of Sialon Powder Processing followed (a) when using Waring Blender (R) mixing technique, (b) when using high alumina mills and (c) when milling in polyurethane-lined mill using Sialon grinding media.

b. Milling

The -325 mesh particle size of AME powder (See Table 1) was not ideal for incorporation into the sialon mix since the other constituents, Linde A alumina and Baker MgO, were in the submicron range ($0.3 - 3 \mu\text{m}$) and thus the mixing and sintering behavior of the mixtures was not optimum for ceramic processing. This led to incomplete homogenization when only mixing by blending. Although it was felt that further comminution of the AME powder to a comparable particle size would lead to additional contamination and further degradation in terms of inhomogeneous microstructure and mechanical properties, it became apparent that maximum densification would not be reached unless starting powders were of about equal particle size and in a size range to promote active sintering, even though a liquid phase was present during sintering. Therefore, sialon mixtures were subsequently prepared by milling to reduce the particle size of the AME Si_3N_4 by up to an order of magnitude. The more favorable particle size distribution also reduced sintering times, sintering temperatures, and compositional inhomogeneities. DuPont Si_3N_4 powders (Table 1) were supplied as $0.1 \mu\text{m}$ diameter amorphous particles but, unfortunately, the silica content was extremely high, and their fluffy nature necessitated double processing by pressing, firing, grinding, re-pressing and firing again to achieve reasonable final density which led to further contamination and loss of compositional control.

Figure 4(b) shows the incorporation of milling into the processing schedules using high alumina mills and grinding media.

It was determined earlier that a pre-sintering treatment controlled bloating in the 60% Si_3N_4 sialons containing up to 13.3% MgO by weight. This pre-reaction step was thought to reduce available silica, convert the powder

TABLE I MATERIALS USED DURING THIS STUDY

Material	Vendor	Remarks
Si_3N_4	AME (England)	85% α , -325 mesh
Si_3N_4	DuPont	Amorphous, Submicron
Si_3N_4	GTE - Sylvania	Amorphous
Si_3N_4	GTE - Sylvania	α
Si_3N_4	Plessey (Frenchtown)	
Al_2O_3	Linde, Air Products Division	α aluminum, 0.3 μm particle size
MgO	Bakers Reagent Grade	0.1 - 0.3 μm particle size
AlN	Cerac/Pure	-200 mesh
Y_2O_3	Ceram/Pure	-325 mesh
CeO_2	Fisher Scientific	99.5%
ZrO_2	Fisher Scientific	"Purified"
La_2O_3	Moly Corp.	99.9%

mixture into a more stable refractory form, and avoid a liquid intermediate phase. It is now believed that the pre-sintering step caused agglomeration of the Si_3N_4 with whatever MAS glass ($\text{MgO-Al}_2\text{O}_3\text{-SiO}_2$) was available at that point in the processing.

Figure 4(c) shows the flow diagram of the processing followed when a polyurethane-lined mill, sialon balls, and a mineralization technique were used to control the liquid phase sintering additives. Rather than rely on mill wear to add glass-forming contaminants such as silica, magnesia and calcium, these materials were added to the alumina component of the sialon composition, calcined for "mineralization" (and homogenization) and milled to a fine particle size during sialon mixing. This technique led to sialon compositions with a broad firing range and with "liquid" phases less susceptible to low temperature AlN reactions which would otherwise reduce the total liquid (SiO_2 and silicates) volume available to aid densification. As the study progressed, the amount of liquid formers was reduced to a minimum in order to maximize high temperature properties. This phase of the work utilized only sialon ball wear itself to furnish the "liquid" necessary for sintering to high density, i.e. no sintering aids added separately.

As will be discussed later, another reaction occurred simultaneously during processing in the form of a consistent reduction of available AlN due to oxidation and water reaction to form NH_3 (gas) and Al(OH)_3 . As will be discussed, and has been shown by others⁽²⁰⁾, the reduction of available AlN in the system in effect results in greater liquid content since the SiO_2 content is not reduced by AlN reaction and thus remains available as liquid silicates to enhance sintering. This inhibition of AlN activity occurs both by direct conversion of AlN to Al(OH)_3 and by indirectly reducing the activity of AlN by coating each particle with an Al(OH)_3 (Al_2O_3) reaction layer.

c. Firing

Firing of sialon compositions was performed in a molybdenum box packed loosely with "sialon" powder and covered with a molybdenum lid. The retort was covered with molybdenum foil and the assembly fired in a hydrogen furnace to temperatures up to 1770 C for various times. Figure 5(a) is a schematic of the technique used. The Sialon packing material tends to adhere to the surfaces of rectangular blocks of fired Sialon but removal of this excess "scale" by grinding operations is not difficult. However, intricate shapes such as turbine blades and domes are less readily cleaned-up if adhering scales persist after firing - particularly if the components have thin walls. Pure Si_3N_4 was used in several attempts to achieve a non-sintering and readily removable packing material but this led to excessive silicon formation (in the H_2 ambient) and reaction with the molybdenum boat and firing retort. A parting compound was required which would allow the fired component to be readily removed from the packing material and at the same time avoid problems with silicon. A duplex coating was developed which both aided in scale removal and helped to prevent silicon depletion in the surface of the fired sialon. A thin layer (~.050") alumina-alcohol slurry was first sprayed or painted onto the unfired sialon component followed by another thicker layer of a blended slurry consisting of $1/3 \text{ Si}_3\text{N}_4$ - $1/3 \text{ Al}_2\text{O}_3$ - $1/3 \text{ AlN}$ (by weight). The part was then packed in the loose sialon mix as shown in Figure 5(b) and fired. Although samples were originally inserted into the furnace at 1500 C and the temperature then rapidly raised to 1700 C, further studies showed that a slow fire, starting at 1200 C and increasing to 1700 C at 50 C/hr. was more beneficial. It was shown that the slower firing schedule in effect allowed more time to presinter (densify) the bodies: some densification was observed at temperatures of 1500 - 1600 C before complete conversion to β' -sialon. This pre-sintering

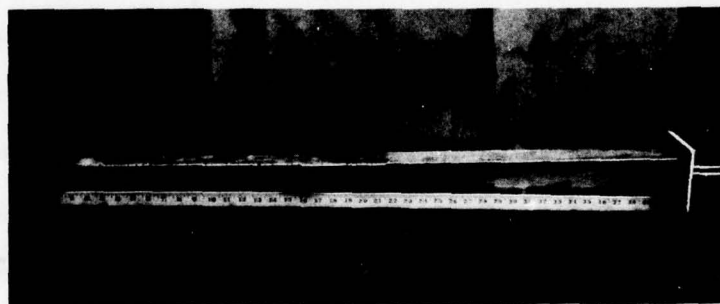
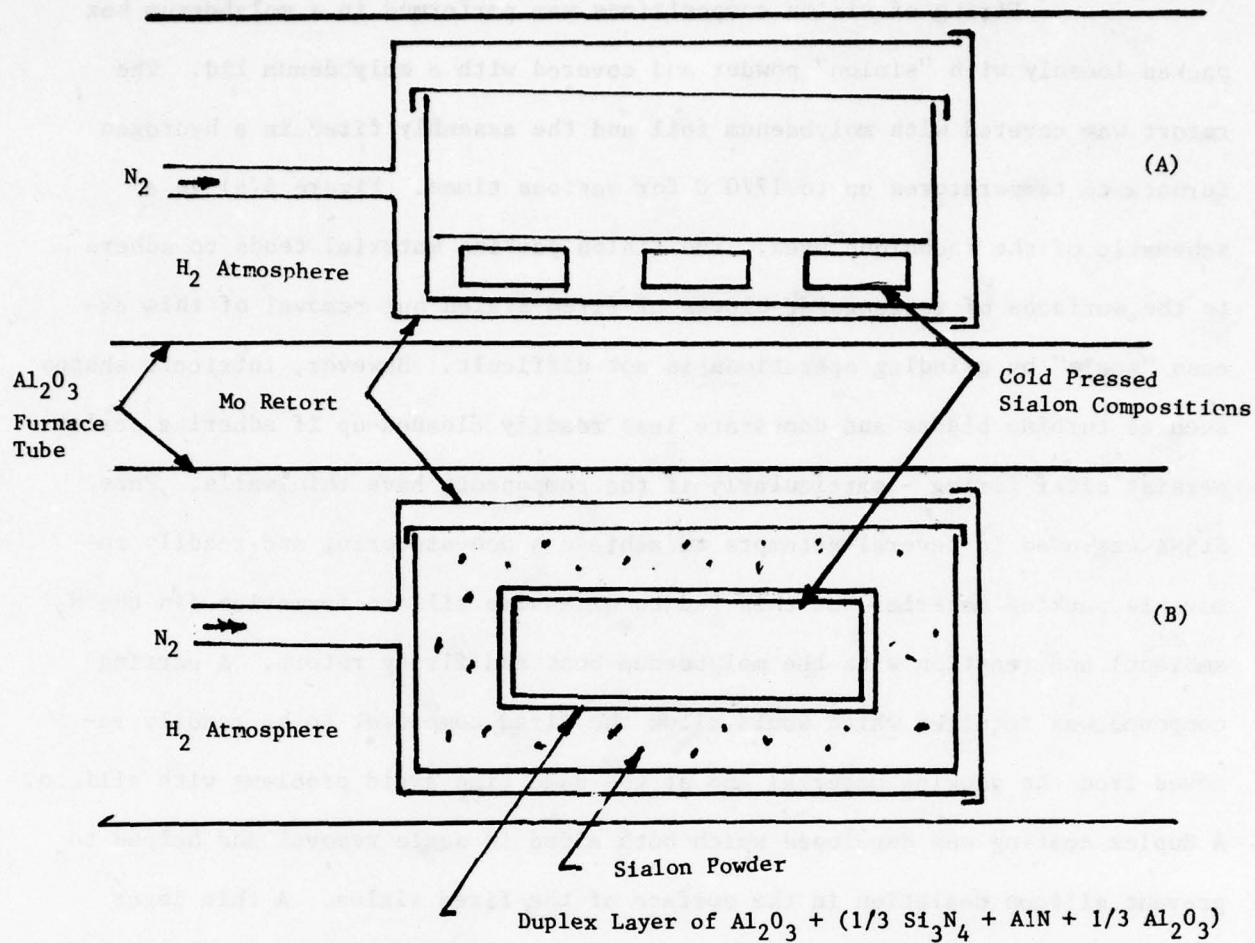


Figure 5. Showing (a) Schematic view of molybdenum retort used to final fire MgO doped Sialons during preliminary studies, (b) Schematic view of molybdenum retort used to final fire all later Sialon compositions and (c) photograph of the high temperature retort fabricated from molybdenum and stainless steel. This retort was inserted into the 4" ID x 48" long Al_2O_3 tube furnace equipped with Mo winding and H_2 atmosphere.

resulted in a very low weight loss. The initial procedure of plunging specimens into the furnace at 1500 C caused excessive volatilization from the low density, open structure, and, although the later compositional practice prevented such volatilization, the slower firing was adopted and preferred for maximum fired density. Fired samples were usually withdrawn directly from 1700 C into a water-cooled entrance compartment of the furnace; however, larger blocks suffered thermal shock damage when rapidly cooled, therefore, the larger samples were allowed to cool in the furnace before removal (about 12 hours to room temperature).

A firing retort was designed and fabricated with a sealable loading port using molybdenum for the high temperature chamber and 304 stainless steel for the portions of the retort which extend into the water-cooled furnace chamber. This retort is also shown in Figure 5(c). A high temperature chamber 2-1/4" x 2-1/4" x 20" long was thus available for controlled atmosphere sintering. Weight loss was completely controlled and minimized using this retort with specimens surrounded by sialon powders as described above. Dense single-phase materials were prepared in both retort systems shown in Figure 5(b) and 5(c) when specimens were packed in sialon powders and N₂/H₂ atmosphere control was imposed.

d. Hot Pressing

Brief studies of densification under pressure at 1500 C and 1700 C were performed during preliminary work to facilitate removal of porosity from compositions for which optimized sintering conditions were not then achieved. These specimens were pressed in boron nitride coated carbon dies at 20 MPa (3000 psi) for times to one hour in a Vacuum Industries, Inc. hot press apparatus.

Densification under pressure was readily achieved in compositions containing MgO, however, only a minimal effort was expended on this process during this program since high density was achieved by pressureless sintering of similar compositions under appropriate conditions. It appears that hot pressing is not necessary for the fabrication of sialon compositions of high density and good mechanical properties even with compositions as rich as 87 W/O Si₃N₄ as will be shown later. Recent work at Lucas has confirmed that properties previously attained and reported in hot-pressed sialon materials,⁽⁷⁾ including excellent creep resistance, have been achieved by pressureless sintering (13) although processing details have not been released.

SECTION III

RESULTS AND DISCUSSION

1. Preliminary Experiments

a. Preparation of sialon powders.

Patent procedures (21,22) were followed in an attempt to form Si_3N_4 which in turn might react with added Al_2O_3 to form sialons in-situ. Although some Si_3N_4 was always produced, no sialons were ever detected and further, the Si_3N_4 reactions never went to completion. It was concluded that using available Si_3N_4 powder starting materials would be a more fruitful approach to sialon production and this phase of the study was terminated.

b. Sialon Sintering Studies

Table 2 shows some of the preliminary "sialon" compositions studied and the weight loss and fired densities attained from these compositions after 1 hour and 3 hours at 1700 C in N_2/H_2 .

TABLE 2 - PRELIMINARY SIALON COMPOSITIONS (IN WEIGHT PERCENT) AND DENSITY AND WEIGHT CHANGES AFTER FIRING AT 1700 C FOR VARIOUS TIMES.

Si_3N_4	Al_2O_3	Wt. Loss %		Density (gm/cc) at 1700°C		
		1 hr	3 hr	As pressed	After 1 hr.	After 3 hrs.
90	10	7	10	1.5	1.6	1.6
80	20	7	10	1.5	1.65	1.65
70	30	7	10	1.5	1.70	1.70
60	40	5	8	1.5	1.80	1.80
50	50	4	7	1.6	2.0	2.0
40	60	3	5	1.65	2.3	2.3
30	70	3	4	1.7	2.6	2.6
20	80	3	4	1.7	2.8	2.8
10	90	3	4	1.8	3.4	3.4

Fifty gram batches of each composition were mixed using powders of Linde-A Al_2O_3 and AME Si_3N_4 in an aluminum bladed Waring Blender with alcohol as previously discussed. X-rays confirmed Jack's results (4) that more than 70% alumina by weight could be dissolved in Si_3N_4 . However, unlike others (9,12) no "X" phase could be detected in any sintered material (including MgO-doped material).

Since no reducers of silica such as carbon or aluminum nitride were added, it was speculated that the back-diffusion of hydrogen during final sintering was responsible for the lack of oxygen-containing phases since hydrogen is a potent reducer of SiO_2 at high temperatures. Weight loss measurements indicated that material was volatilizing as a function of both time at temperature and of composition. This weight loss was in part the silica associated with Si_3N_4 and MgO in the case of MgO -containing materials. Sintered bodies had a white surface layer a few mils thick which was depleted of both silicon and nitrogen.

These preliminary sialon bodies did not achieve high density until excessive amounts of alumina were added. Also, all of the shrinkage occurred within the first hour at temperature confirming that sintering in this system was indeed rapid, presumably involving liquid phases. X-ray evidence nevertheless indicated that the nature, amount, and distribution of the crystalline phase could be changed and homogenized by firing for longer times. The addition of magnesia as a sintering aid to sialon and silicon nitride compositions has been well documented, (1,4,9) and bodies have been readily sintered to densities of 95 to 98% of theoretical which makes the material attractive from a fabrication standpoint. However, poor creep resistance at high temperatures has discouraged this approach because films of glass or low-melting silicates form at grain boundaries by reaction of MgO with the silica associated with Si_3N_4 particles.

Table 3 is a list of the MgO -containing compositions which were evaluated and shows the final densities (fired shrinkage) achieved after various times. The Si_3N_4 content was maintained constant at 60 W/O and the alumina-magnesia ratio was varied. Additions greater than 5% MgO do not show appreciably greater shrinkage after one hour pre-fire in N_2 followed by $\text{N}_2\text{-H}_2$ firing. It was noticed, however, that the 10.8 and 13.3 W/O MgO mixtures bloated after final firing. Prefiring these mixtures for longer times accomplished two objectives:

(a) bloating was reduced and (b) higher final densities were achieved.

TABLE 3 - COMPOSITIONS OF SIALONS CONTAINING MgO IN WEIGHT PERCENT WITH SHRINKAGE AND WEIGHT LOSS DATA FIRING AT 1700°C

Si ₃ N ₄	Al ₂ O ₃	MgO	% Linear Shrinkage at 1700 C			Wt. Loss % 1 hr/1700 C
			1 hr.	2 hrs.	3 hrs.	
60	40	1/4	7	10	11	13
60	39	1	9	10	10	
60	37	3	10	11	12	12
60	40	5	13	15	16	10
60	32	8	14	16	16	8
60	29.2	10.8	14	16	16	5
60	26.6	13.3	14	15	15	2

(Compositions with 10.8 and 13.3 W/O MgO were chosen to provide a stoichiometric magnesium aluminate spinel with the available Al₂O₃ in the case of the 10.8 material and a magnesia-rich spinel for the 13.3 material).

The weight loss of 60% Si₃N₄ sialon material as a function of MgO content shows that more dense bodies lose less weight under the used N₂/H₂ atmosphere.

Other investigators (9,10) had employed sintering atmospheres with access to carbon from furnace hardware or pressing dies during formation of sialons. To approximate this condition, a mixture of 10 parts carbon, 10 parts silicon and 50 parts alumina by weight was used to cover the specimens during pre-fire and final firing. The weight-loss using this approach was reduced by a factor of 2 but examination of fired microstructures showed that a "rind" of dense (silica-rich) material had formed, trapping less dense material inside. This result is similar to that described by Lange⁽⁹⁾. It was concluded that although the material loss might be reduced by adding carbon to the system, the trapping of porosity was not desirable.

The above experiments were repeated using AME Si₃N₄ powder as a covering material during firing. This technique produced material with no

loss in weight but which remained porous and retained a "rind" effect.

An average bend strength of 293 MPa (44,000 psi) was measured for 13.3 W/O MgO material at room temperature.

c. Microstructural Studies

Preliminary examination of polished sections of fired specimens showed evidence for a general multi-phase structure particularly in specimens induced to densify by the addition of MgO. Areas of varying reflectivity, of much greater size than the initial particle size in some instances, were observed. The nature of these phases was studied primarily by x-ray diffraction analysis as summarized in the next section. Polished sections showed that all specimens contained remnant porosity. Essentially single-phase materials were observed in low density specimens with no (or small) MgO additions.

Figure 6(a) is an x-ray scan of the 50/50 composition from Table II. This composition contains only Si_3N_4 and Al_2O_3 . Notice the presence of "X" phase. Figure 6(b) shows the multi-phased structure of the 13.3 W/O MgO composition after 1 hour at 1700 C while Figure 6(c) shows the structure after 2 hours at 1700 C. Notice the marked decrease in intensity of the MgAl_2O_4 lines and the lack of α Si_3N_4 as compared to 6(b). These results suggest that longer times at temperature would further homogenize this composition and most probably other sialons .

d. Sialons Formed From Amorphous Si_3N_4 Manufactured by DuPont

DuPont Si_3N_4 appeared ideal from a powder morphology standpoint since it was of uniform sub-micron size which fitted the criteria for sintering to high density more closely than the -325 mesh AME material normally used. Accordingly, mixtures containing Al_2O_3 + 8 weight percent MgO and AlN were made as summarized in Table IV. These mixtures were fired to 1550 C⁽²³⁾ in a standard N_2 - H_2 atmosphere. The MgO-bearing material sintered well but the material without

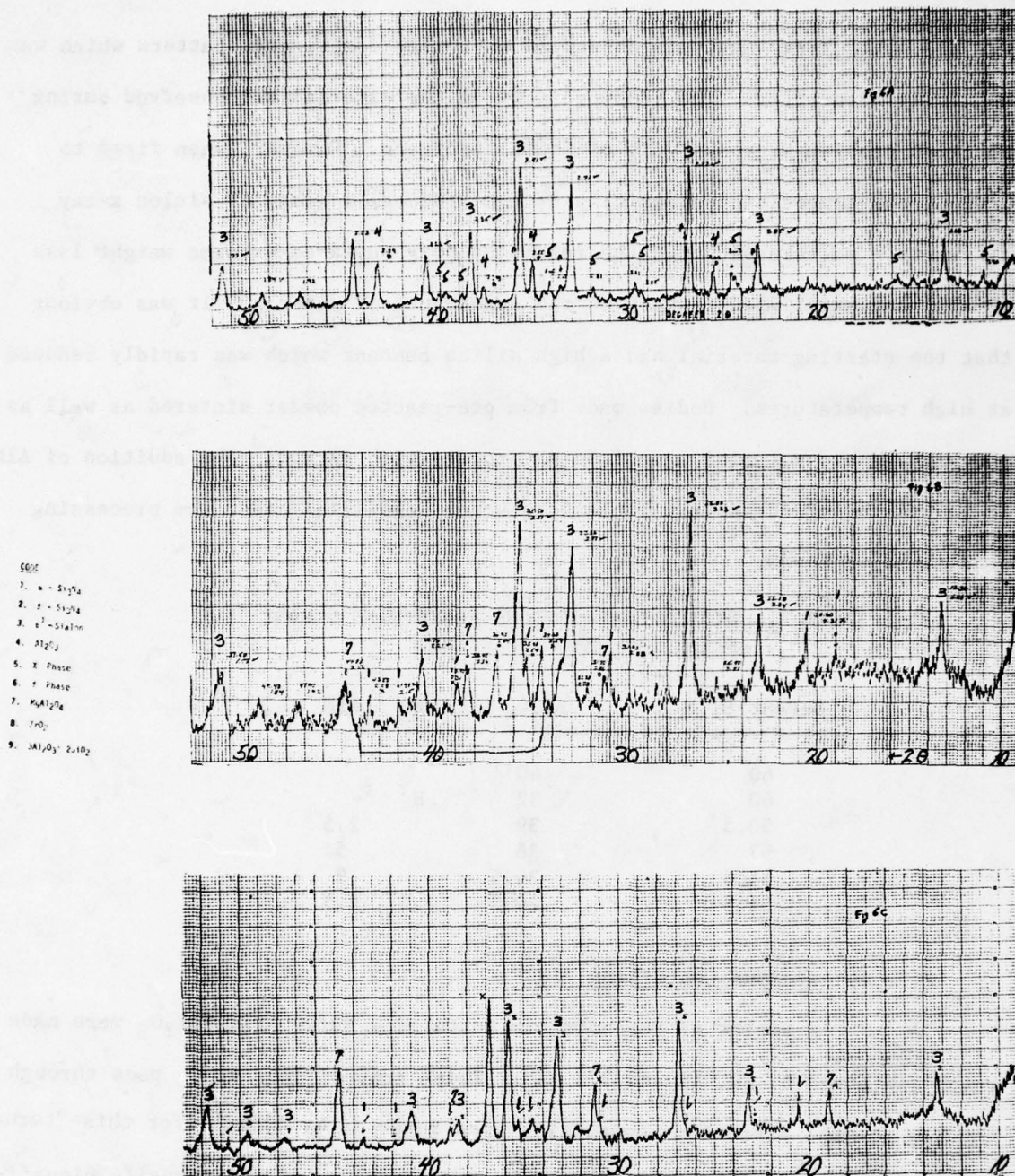


Figure 6. (a) X-ray trace of sialon sintered in N_2/H_2 atmosphere. Some X phase but no Y phase. (b) X-ray trace of sialon + 13.3% MgO showing multiplicity of phases due to incomplete reaction of starting powders after 1 hour at 1700°C in N_2/H_2 atmosphere. (c) Same specimen as (b) but sintered for 2 hours at 1700°C . Note more complete reaction of α - Si_3N_4 .

MgO did not. X-ray analysis showed an extremely complicated pattern which was not fully identified. The inhomogeneity of the material was observed during electron probe microanalysis of these specimens. However, when fired to 1700 C, the composition containing 8% MgO produces a clean β' sialon x-ray diffraction pattern although the resulting body suffered extreme weight loss (~20%) and exfoliated taking on the appearance of popcorn. It was obvious that the starting material had a high silica content which was rapidly reduced at high temperatures. Bodies made from pre-reacted powder sintered as well as the pre-reacted material made from AME powder with 8% MgO. The addition of AlN to any of the mixtures from Table 4 was not beneficial under the processing conditions employed.

TABLE 4. SIALON COMPOSITIONS CONTAINING DuPONT Si_3N_4 (IN WEIGHT PERCENT)

DuPont Si_3N_4	Al_2O_3	MgO	AlN
60	40		
60	32	8	
58.5	39		2.5
57	38		5
54.5	36.5		9
54.5	29.2	7.3	4.5

e. Sialons Containing AlN

A series of compositions containing 60/40 $\text{Si}_3\text{N}_4/\text{Al}_2\text{O}_3$ were made which contained 5, 10, 15 and 20% AlN. These compositions would pass through the low thermal expansion composition area reported by Oyama⁽⁴⁾ for this "ternary" system. Specimens fabricated from these compositions did not densify significantly indicating the adverse effect of AlN on sintering as shown in Table 5: thermal expansion measurements were not made on these porous materials. As will be shown later, such compositions could not sinter without additional sintering aids and/or mineralizing of sintering aids within the alumina component so as to

retard the reaction rate of $\text{SiO}_2\text{-AlN}$ and thus prevent the reduction of available sintering liquid.

TABLE 5. EFFECT OF AlN ON FIRING SHRINKAGE OF
60/40 $\text{Si}_3\text{N}_4/\text{Al}_2\text{O}_3$ DISCS

Weight % AlN	Firing Linear Shrinkage %
0	10
5	10
10	7
15	5.5
20	3

f. Hot-Pressed Sialons

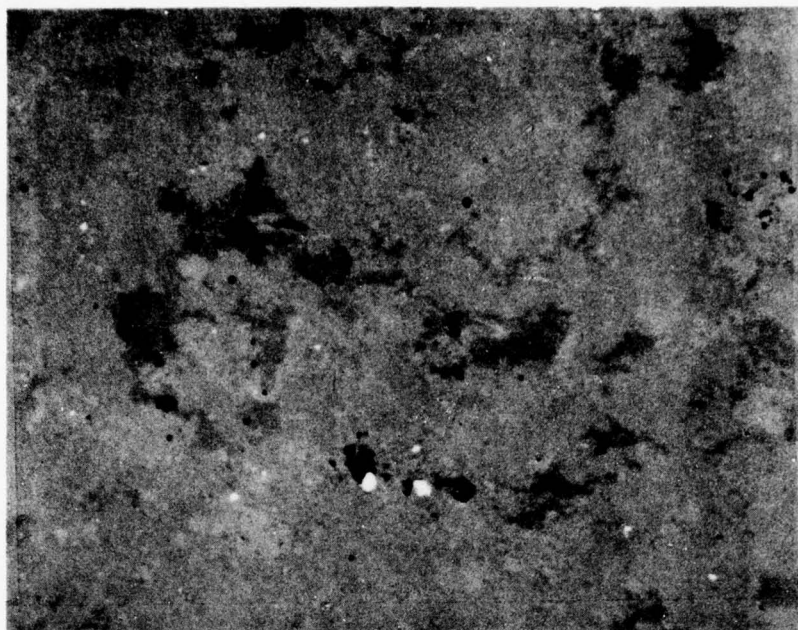
Hot-pressing affords the opportunity to produce ceramic specimens in closed systems less subject to volatilization phenomena and provides the ability to achieve densification without reliance on significant amounts of sintering aids. The presence of SiO_2 and the formation of MAS glass in the sialon compositions containing MgO as a sintering aid is a decided advantage during hot pressing since the well-distributed liquid makes an excellent intergranular "glue". Further, because the die isolates and confines the samples, volatilization is not a serious problem when compared to sialon densification by conventional sintering. However, the retention of in-situ siliceous films on grain boundaries and the formation of uncontrolled multi-phased structures ("X" phase, "Y" phase, etc.) may not be desirable for optimum properties of fired bodies.

Hot-pressing can only approximate structures produced by sintering and, although the starting compositions may be identical, the final compositions may differ markedly because of differences in material lost from the die, or from the open system. For these studies, however, dense pore-free specimens were

required from compositions under investigation in the sintering program before optimized pressureless sintering conditions had been developed. Hot-pressing appeared to be an acceptable and rapid processing method and a few samples of MgO-containing material were densified by this process.

Samples 36 mm in diameter by about 6 mm thick of 8% and 1% MgO compositions were fabricated by hot pressing in a BN-coated graphite die at 10 MPa (1500 psi) for 30 minutes at 1700 C in 10^{-4} torr vacuum. The ability to maintain vacuum was influenced by volatilization of the specimen unless pressure was applied early to isolate it in the die; specimens of 13.3% MgO were fabricated in N_2 . Figure 7 shows the typical microstructure of hot-pressed 8% MgO and the x-ray diffraction data for this material. When compared with normally sintered material (Figure 8) the coarse multiphased structure obtained by hot-pressing is readily apparent. A portion of this material was "homogenized" by heating in N_2 - H_2 atmosphere at 1700 C for three hours. Figure 9 shows the microstructure and x-ray results after this treatment. It is apparent that both the microstructure and the phase composition was altered by the homogenization treatment. X-ray results from hot pressed 13.3% MgO materials are shown in Figure 10.

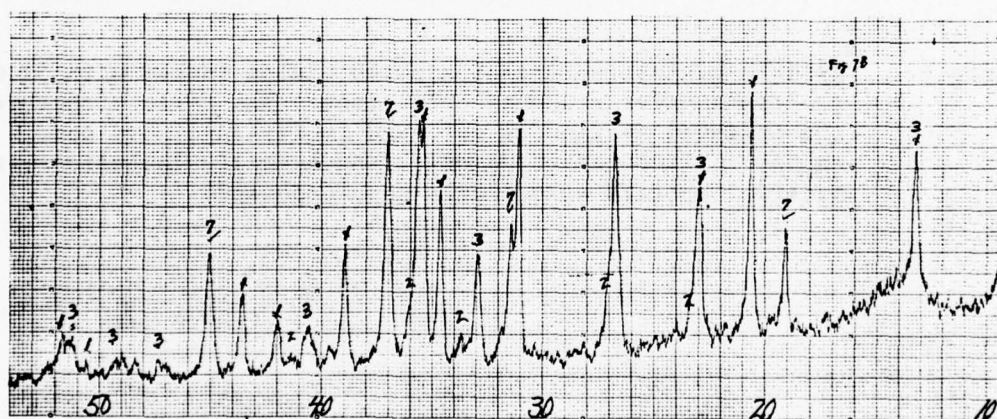
Hot pressing of various compositions proved a useful method of comparing materials; however, it was clear that compositions should be modified if good single-phased β' sialon materials were to be obtained by hot pressing since, in the absence of atmospheric removal of SiO_2 , significant additions of AlN would be required to compensate for the SiO_2 present in the initial mixture. It was clear that correlation of sintering and hot-pressing data in the sialon system could not be made on the basis of starting compositions. Considerable weight loss has been reported for hot pressed materials ⁽¹¹⁾ and the final compositions are unknown. This is of course also true for conventional sintering processes with weight losses



(a)

5000

1. α - Si_3N_4
2. β - Si_3N_4
3. β' - Sialon
4. Al_2O_3
5. γ Phase
6. γ Phase
7. MgAl_2O_4
8. ZrO_2
9. $3\text{Al}_2\text{O}_3 \cdot 2\text{SiO}_2$



(b)

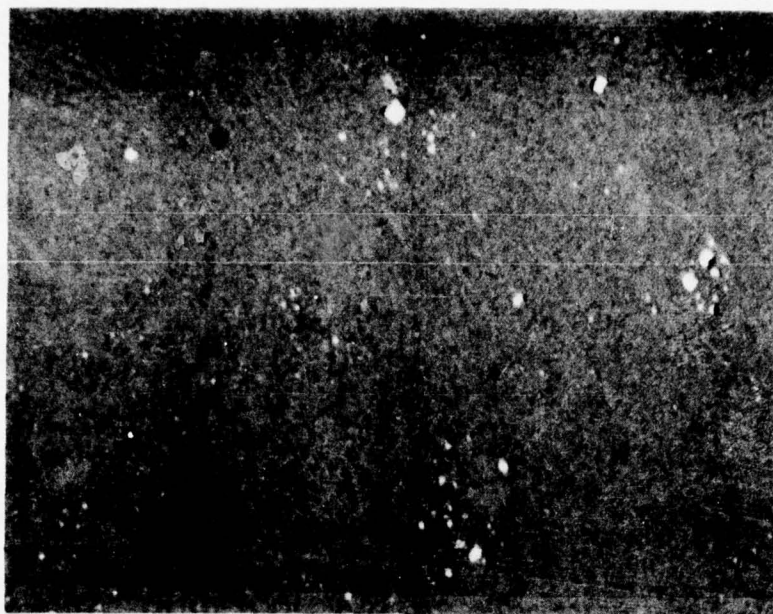
Figure 7.

(a) Micro-structure of hot-pressed 8% MgO Sialon and (b) x-ray diffractometer trace of the same structure showing multiple phases α and β Si_3N_4 , β' and MgAl_2O_4 .



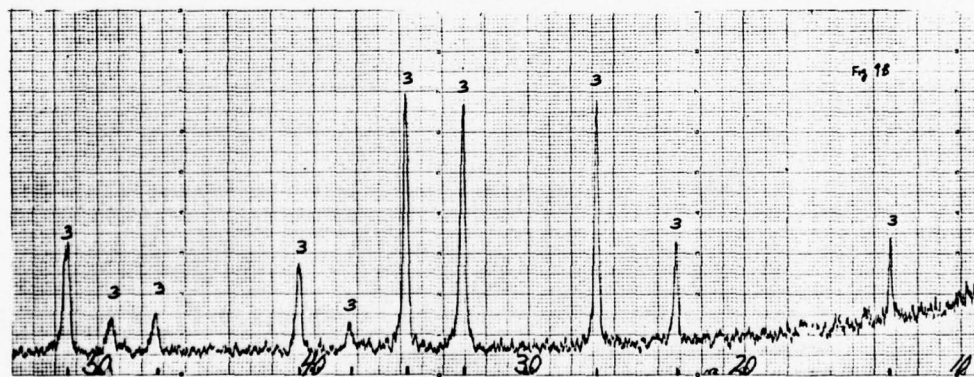
10μm

Figure 8. Typical microstructure of a 60:40 Sialon (doped with 5% MgO) processed under standard conditions. The grain structure on the polished section is not readily distinguished and, except for islands of porosity and metallic inclusions, the material appears essentially single-phased.



(a)

CODE
1. α - Si_3N_4
2. β - Si_3N_4
3. β' - Sialon
4. Al_2O_3
5. ZrO_2
6. Y_2O_3
7. MgAl_2O_4
8. ZrO_2
9. SiAl_2O_5 , 2SiO_2



(b)

Figure 9.

(a) Microstructure of hot-pressed 8% MgO material (same specimen as Figure 7) after a homogenizing heat treatment at 1700°C for 2 hours in $\text{N}_2\text{-H}_2$, (b) x-ray diffractometer trace of structure shown in (a). β' Sialon is the only phase detected.

- 6205E
1. α - Si_3N_4
 2. β - Si_3N_4
 3. β' - Sialon
 4. Al_2O_3
 5. X Phase
 6. Y Phase
 7. MgAl_2O_4
 8. ZrO_2
 9. $3\text{Al}_2\text{O}_3 \cdot 2\text{SiO}_2$

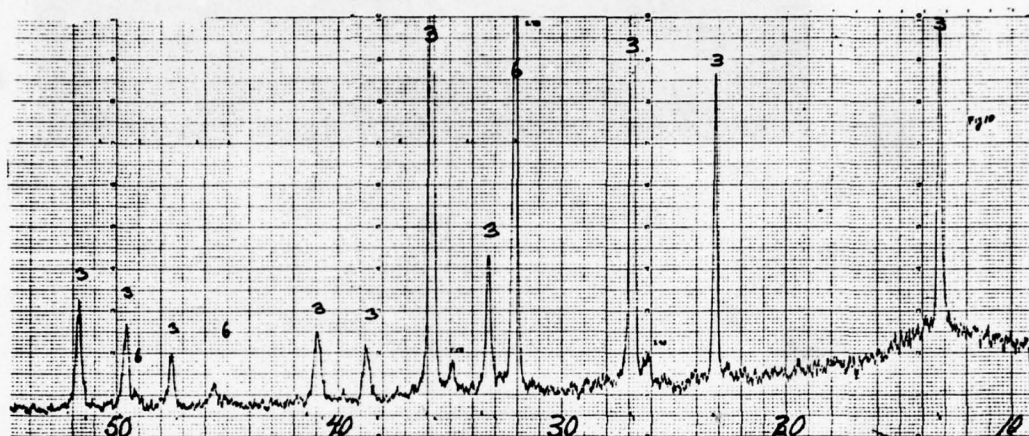


Figure 10. X-ray diffractometer trace of hot-pressed 13.3% MgO Sialon under conditions which produced "Y" phase, β' Si_3N_4 and large quantities of glass.

but the mechanisms may differ and be more sensitively influenced by the ambient atmosphere. Therefore, although densification may be facilitated by hot pressing and this may be useful in some specific experimental studies, the major emphasis of this program was on conventional sintering enhanced by ambient atmosphere control and the use of fugitive sintering aids which may be removed in final-stage sintering or incorporated into the final crystalline product. Therefore, hot pressing was not pursued in any more detail.

g. Thermal Expansion of Sialon Materials

A summary of the thermal expansion data accumulated during the initial work is shown in Figure 11, and Figure 12 shows the data plotted as a function of MgO W/O content at a constant temperature of 800 C. Notice the absence of any trend which would indicate that sialons of nominal 60/40 composition could have thermal expansion coefficients less than hot-pressed Si_3N_4 . (Norton NC-132 used as reference material). The data were all obtained on a commercial Theta differential dilatometer at a heating rate of 2 C/min. (This apparatus is capable of accuracies greater than 1 ppm).

Jack⁽¹⁻³⁾ and Oyama⁽⁴⁻⁶⁾ previously reported expansion coefficients for sialons less than $\beta\text{-Si}_3\text{N}_4$ while the experience of Lange⁽⁹⁾ and Arrol⁽⁷⁾ is similar to that reported here. Present speculation is that "low expansion" hot-pressed materials produced by Oyama contained large amounts of silica-containing second phases ("X", glass, etc.) which may have inherently lower expansion coefficients than the crystalline Sialon phases. Sialons made in this work were relatively free of silica-bearing phases largely because of firing differences, therefore, the data may be more representative of single-phase crystalline sialon materials. Attempts to make low-expansion samples from compositions reported by Oyama, for example, were not possible since the sintering

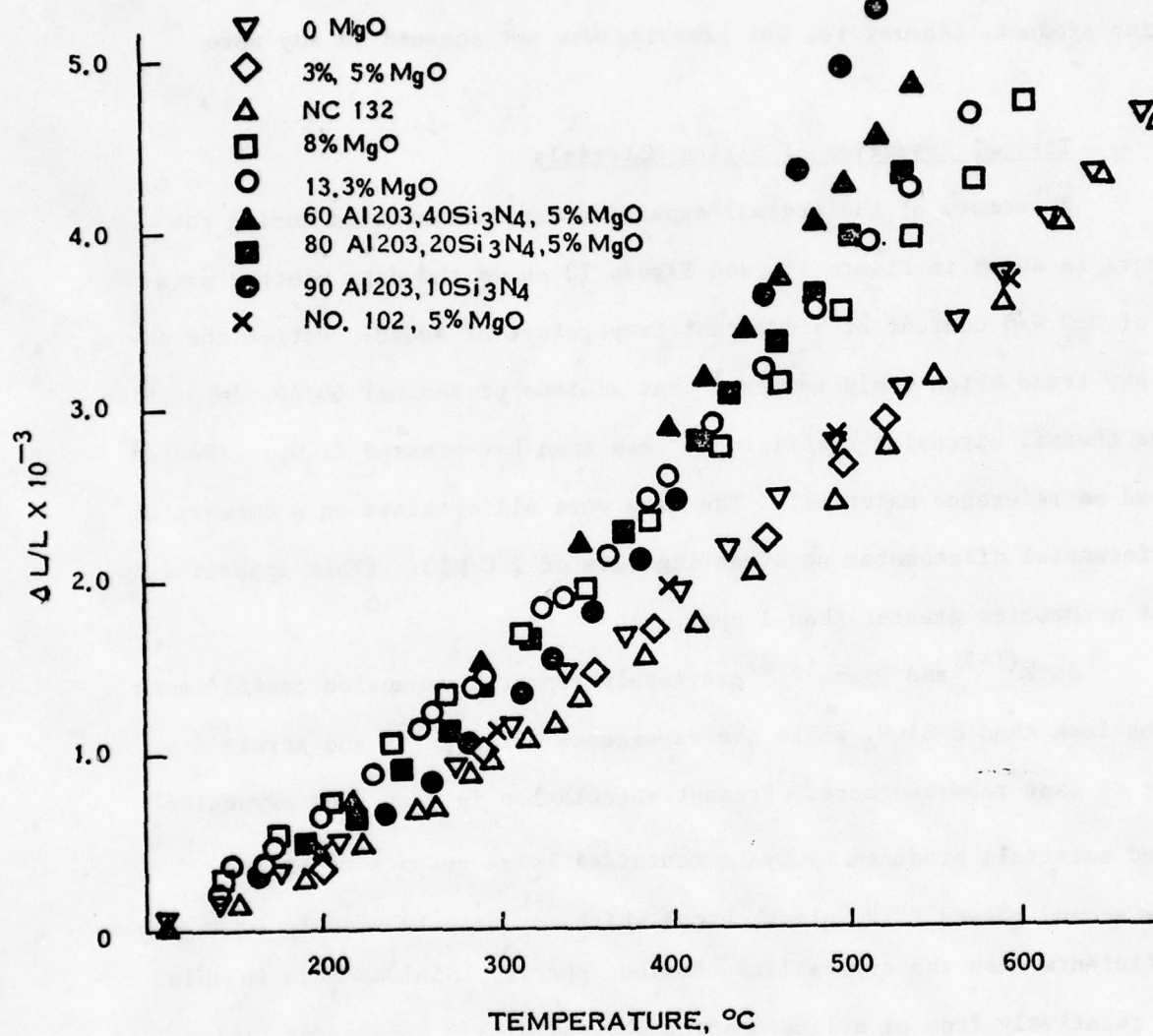


Figure 11. Thermal expansion behavior of various Sialon compositions (all 60/40) and hot-pressed Si₃N₄ (NC-132).

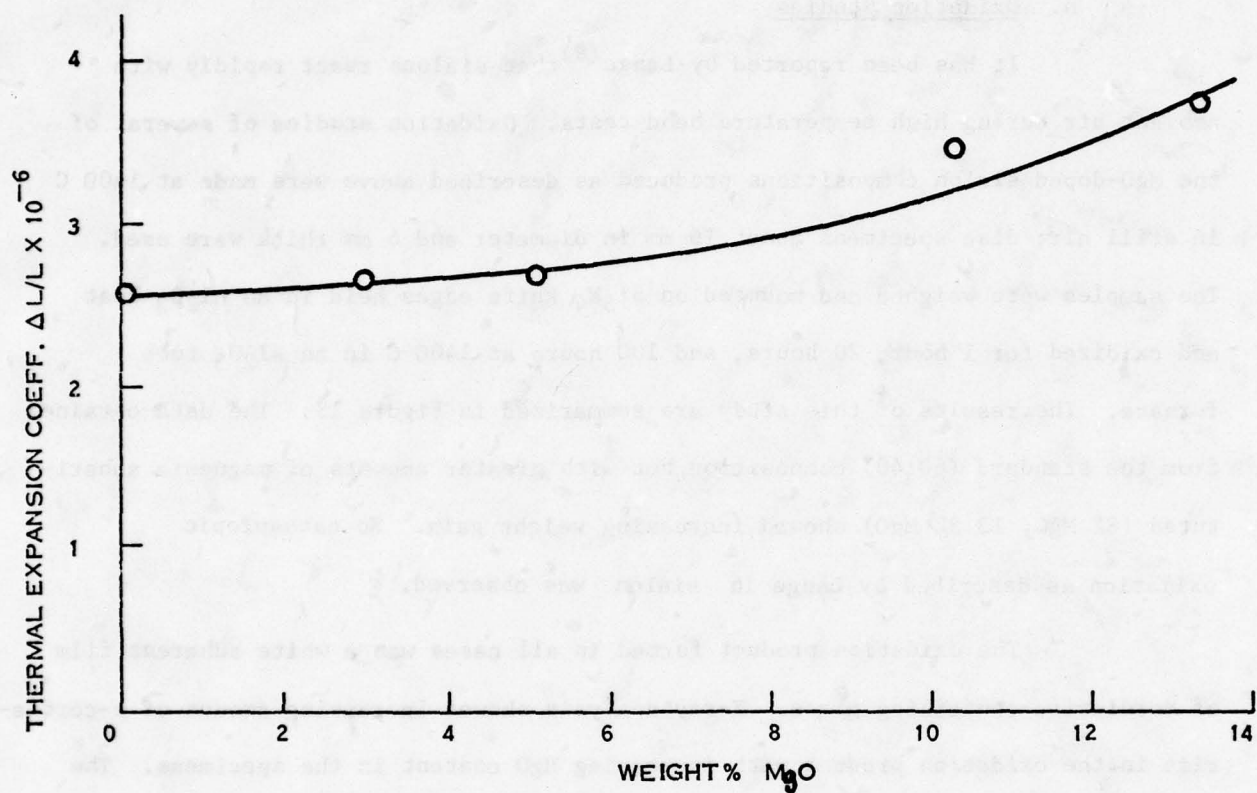


Figure 12. Thermal Expansion Coefficient of 60:40 Sialon as a function of MgO content at $800^{\circ}C$.

technology produced specimens with greatly different final composition and microstructure. It is speculated that the final composition of Oyama's low-expansion material was far removed from the initial material composition and was probably highly siliceous and glassy. More study of the potential for achievement of lower expansion coefficients in other crystalline sialon compositions may be warranted.

h. Oxidation Studies

It has been reported by Lange⁽⁹⁾ that sialons react rapidly with ambient air during high temperature bend tests. Oxidation studies of several of the MgO-doped sialon compositions produced as described above were made at 1400 C in still air; disc specimens about 16 mm in diameter and 6 mm thick were used. The samples were weighed and mounted on Si₃N₄ knife edges held in an Al₂O₃ boat and oxidized for 1 hour, 20 hours, and 100 hours at 1400 C in an Al₂O₃ tube furnace. The results of this study are summarized in Figure 13. The data obtained from the standard (60:40) composition, but with greater amounts of magnesia substituted (8% MgO, 13.3% MgO), showed increasing weight gain. No catastrophic oxidation as described by Lange in sialon was observed.

The oxidation product formed in all cases was a white adherent film of cordierite-containing glass. X-ray analysis showed increasing amount of α -cordierite in the oxidation product with increasing MgO content in the specimens. The specimens were cycled three times during testing and no spalling or cracking of the film was observed. The glassy nature of the reaction product was observed to be modified by contact with Al₂O₃ refractories. Initial studies with specimens supported on an Al₂O₃ boat resulted in much more fluid "foamy glass" reaction products. The data reported above were obtained on specimens supported on Si₃N₄ bars. The reasons for the interaction with Al₂O₃ are not clear but may relate to glass formation in the MAS system at "high" alumina contents.

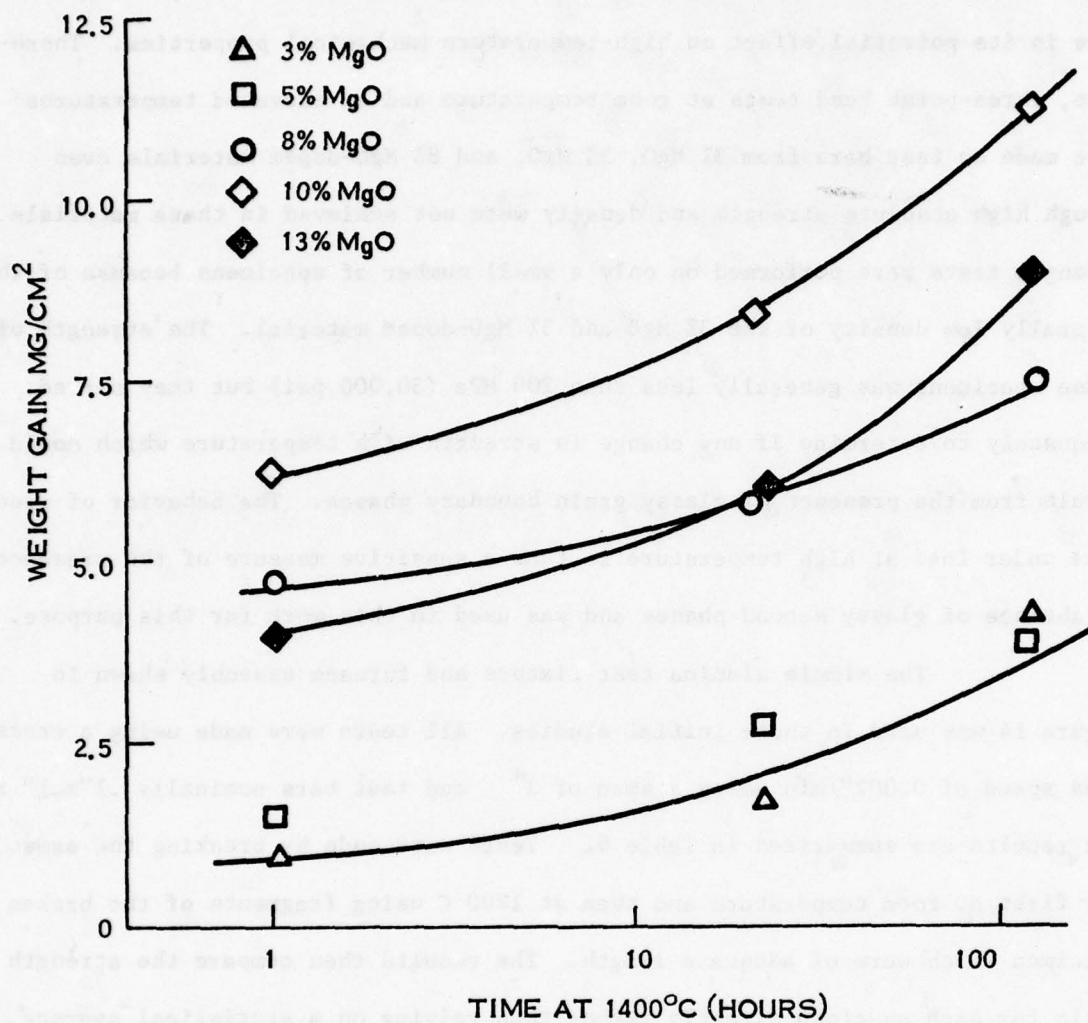


Figure 13. Weight gain (in Mg/cm^2) vs. time at 1400°C in still air for several MgO doped 60/40 Sialon compositions.

1. Mechanical Properties of MgO-Doped Sialons

The practical importance of a glassy phase in sialon materials lies in its potential effect on high-temperature mechanical properties. Therefore, three-point bend tests at room temperature and at elevated temperatures were made on test bars from 3% MgO, 5% MgO, and 8% MgO-doped materials even though high absolute strength and density were not achieved in these materials. Strength tests were performed on only a small number of specimens because of the generally low density of the 3% MgO and 5% MgO-doped material. The strength of these specimens was generally less than 200 MPa (30,000 psi) but they served adequately to determine if any change in strength with temperature which could result from the presence of glassy grain boundary phases. The behavior of specimens under load at high temperature is thus a sensitive measure of the presence or absence of glassy second phases and was used in this work for this purpose.

The simple alumina test fixture and furnace assembly shown in Figure 14 was used in these initial studies. All tests were made using a cross-head speed of 0.002"/min using a span of 1" and test bars nominally .1"x.1" x 2". The results are summarized in Table 6. Tests were made by breaking the same bar first at room temperature and then at 1200 C using fragments of the broken specimen which were of adequate length. The results then compare the strength ratio for each specimen directly rather than relying on a statistical average. Normalized data, which uses only the ratio of the strength at the elevated test temperature to the strength at room temperature are plotted as a function of MgO content in Figure 15.

The data show that adding MgO up to the 8% level both decreases the strength of sialons and shows detectable flow under load. However, at 10.8% MgO and 13.3% MgO "sialon" there is a return to brittle behavior without flow and at an increased strength level. It is believed that when the MgO level was

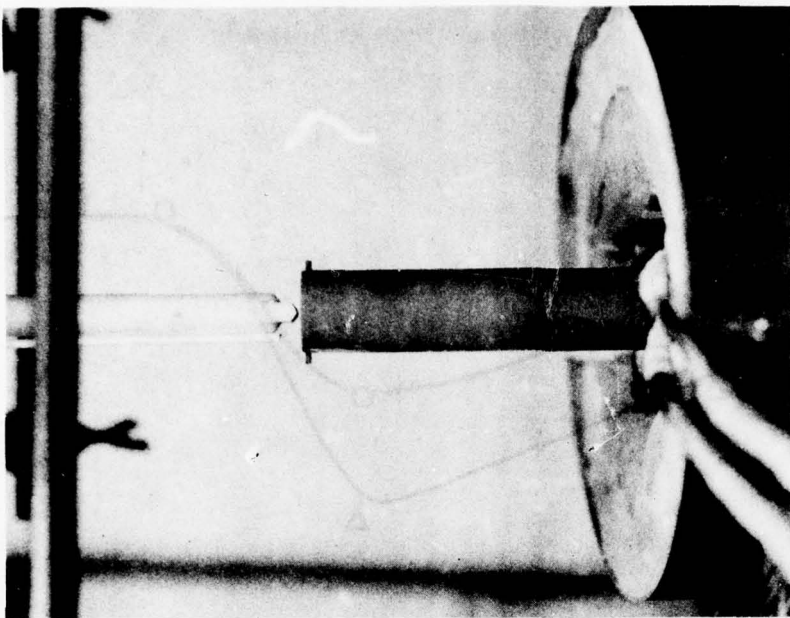
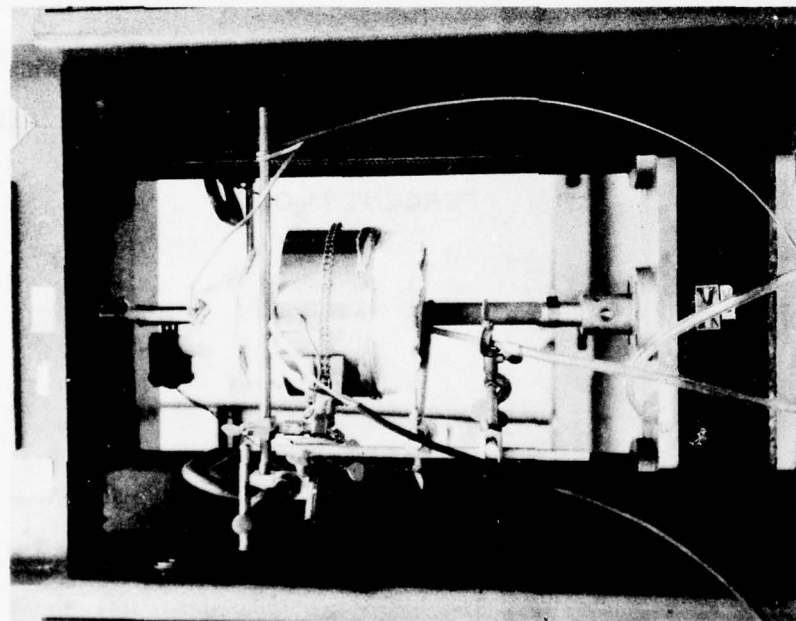


Figure 14. Assembled apparatus for elevated temperature testing with close-up view of specimen in place in the alumina ceramic 3-point bend-test fixture.

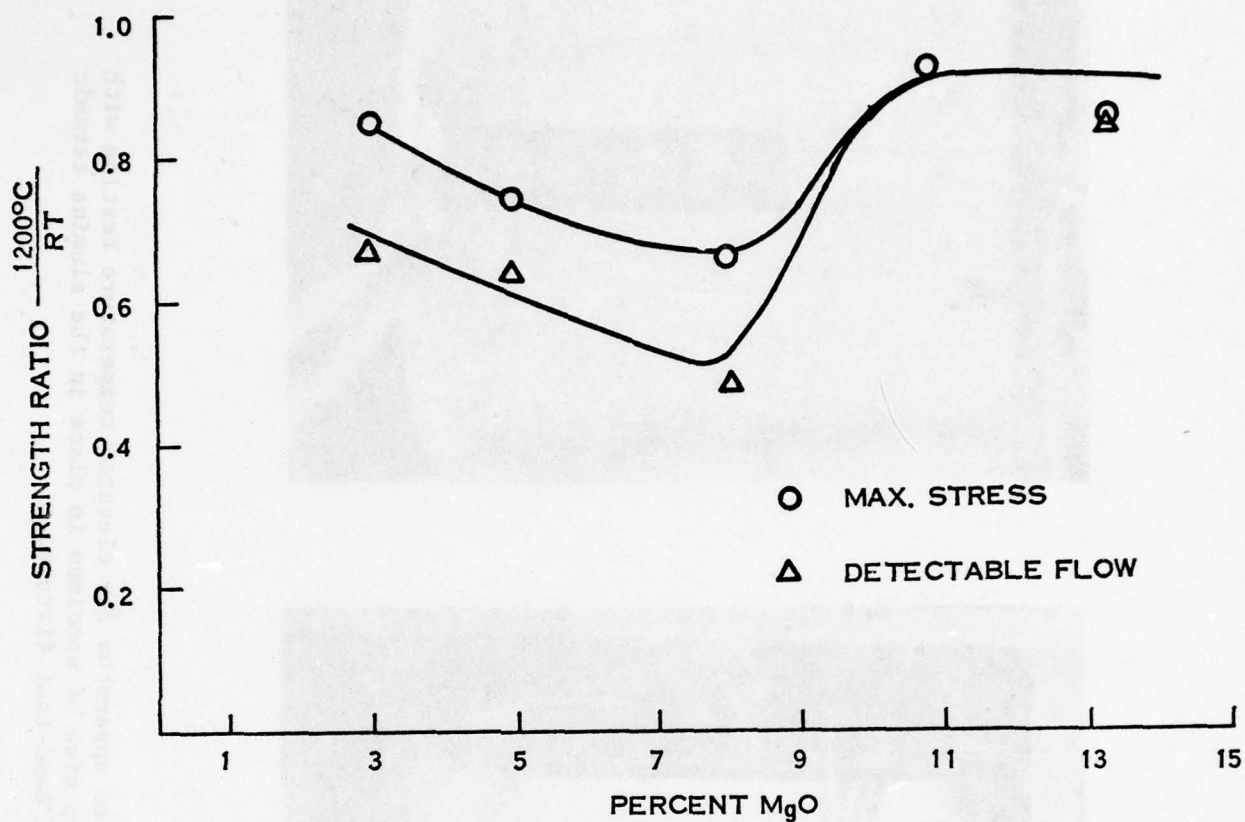


Figure 15. The relationship between strength retention as measured at 1200°C and magnesia content of Sialon materials.

TABLE 6. THREE-POINT BEND TEST RESULTS FOR
MgO-Doped Sialons (ALL BASED ON
60% Si₃N₄ + 40% Al₂O₃ BY WEIGHT)

%MgO	Test Temp °C	Max Stress MPa(psi)	Avg. MPa(psi)	Stress Ratio 1200 C/RT	Detectable Yielding Avg MPa(psi)	Stress Ratio 1200 C/RT MPa(psi)	Stress Ratio 1200 C/RT
3	RT	151(22600)					
3	RT	117(17500)	147(22125)				
3	RT	151(22600)		.85			
3	RT	145(21800)					
3	1200	135(20200)	126(18850)		108(16200)	98(14750)	.67
3	1200	117(17500)			87(13300)		
5	RT	111(16700)					
5	RT	87(13300)	100(14933)				
5	RT	99(14800)		.74			
5	1200	65(9800)			55(8300)		
5	1190	71(10700)	73(11000)		63(9500)	63(9500)	.64
5	1200	79(11800)			67(10000)		
5	1215	79(11700)			69(10300)		
8	RT	138(20700)	129(19300)				
8	RT	120(18000)		.81			
8	1200	121(18200)	105(15700)		81(12100)	77(11500)	.58
8	1200	87(13200)			73(11000)		
10.8	RT	129(19400)	118(17700)				
10.8	RT	107(16000)					
10.8	1200	119(17900)		.89	116(17400)	105(15750)	.89
10.8	1200	91(13600)	105(15750)		91(13600)		
13.3	RT	192(28800)	189(28300)				
13.3	RT	186(27900)		.91			.91
13.3	1200	174(26100)	171(25700)		174(26100)		
13.3	1200	169(25300)			169(25300)		

high enough to form appreciable spinel during pre-firing (also shifting the sialon composition remaining to higher actual Si₃N₄ content than the standard 60/40 ratio) some spinel phase persisted which in effect depleted the grain boundaries of MAS glass and rendered them more refractory. In some specimens it was considered that only spinel existed as the second phase and perhaps no "liquid" MAS was present as shown by the brittle fracture behavior at least at temperatures up to 1280 C.

These strength data show clearly the importance of the nature of

second phases on the high temperature properties of the materials produced. Such tests were continued as this program proceeded with improved materials (Section III-2 later) since they provided a more sensitive indication of the presence and extent of glassy second phases than would any of the normal characterization methods. Utilization of liquid phases for enhanced densification is of little value if these phases persist in the final product and prevent the achievement of high stress levels at desirable service temperatures. An improved test rig to accommodate specimens in four point bending at temperatures up to 1400 C was also employed in screening of suitable sintered specimens (Section III-2-later).

j. Nitrogen Atmosphere Sintering Experiments

Residual porosity was attributed above, in part, to the release of N_2 during the high temperature heating of Si_3N_4 . The hydrogen atmosphere employed in sintering would not significantly reduce this decomposition and in fact may enhance it by the reduction of SiO_2 . Accordingly, a few experiments were attempted using N_2 atmosphere with BN-coated sealed graphite hot-pressing dies heated by induction. It was felt that the increased partial pressure of N_2 in the system would minimize N_2 release from the Si_3N_4 . However, as observed by others, (4,5,6) porosity remained in the fired specimens and indications were that the hydrogen atmosphere during firing gave more control of composition and structure than did nitrogen at least for the materials and conditions studied in these experiments. Control of the relative partial pressures of hydrogen and nitrogen as well as the total ambient pressure appeared desirable for complete control of the sintering environment.

k. Sintering Behavior of Sialons Containing CeO_2 , ZrO_2 and La_2O_3

The utility of liquid-phase sintering of sialons is well established and indeed if sialon is formed from alumina and Si_3N_4 without AlN additions (and often even with them) a liquid phase is unavoidable. MgO , the most popular

sintering aid produces MAS glasses and, at best, poor refractory compounds which affect both the creep resistance and the oxidation resistance of sialons at temperatures above 1200 C. Other additives which should provide the same function as MgO but might form more refractory glasses or preferably intermediate compounds include Y_2O_3 , CeO_2 , ZrO_2 and La_2O_3 . The utility of such additives in the processing of hot-pressed Si_3N_4 was shown by Gazza⁽²⁷⁾ and others⁽²⁸⁾ and have become part of the state-of-the-art for Si_3N_4 processing.

Mixtures of 60 Si_3N_4 - 40 Al_2O_3 with additions of CeO_2 , ZrO_2 and La_2O_3 at 5, 10 and 15 percent levels were made and 6 mm thick x 19 mm diameter disks were formed by cold pressing at 67 MPa (10 Ksi) in a steel die. Specimens were fired by the standard procedure. Data on shrinkage, weight loss and final density were obtained and are shown in Figure 16, (data for MgO additions, Table 3, show that MgO is a more effective sintering aid for this type of powder mixing). As can be seen the three additives exhibit similar density and weight loss characteristics but different shrinkage behavior. X-ray diffractometer traces of the resulting sialon bodies with 10% additive are shown in Figures 17(a), 17(b), and 17(c). The CeO_2 and La_2O_3 containing materials were essentially single-phased β' -sialon while the ZrO_2 bearing material was a multi-phased structure of β' -sialon and ZrO_2 . All three additives were effective sintering aids for sialon, however, ZrO_2 dopant appears less likely to result in achievement of single-phased sialon.

1. Sintering Behavior of Sialon Using GTE-Sylvania and Plessey Si_3N_4 Powders

Three types of Si_3N_4 powder were used in these experiments. Amorphous Si_3N_4 from Sylvania (Lot #T-20437), Si_3N_4 from Sylvania (Lot #T-20437), and Plessey Si_3N_4 (Batch #6). The sinterability of these materials was compared by making 60 Si_3N_4 -32 Al_2O_3 , 8% MgO sialons which were well characterized under normal fabrication procedures using the AME controlled-phase " α " powder.

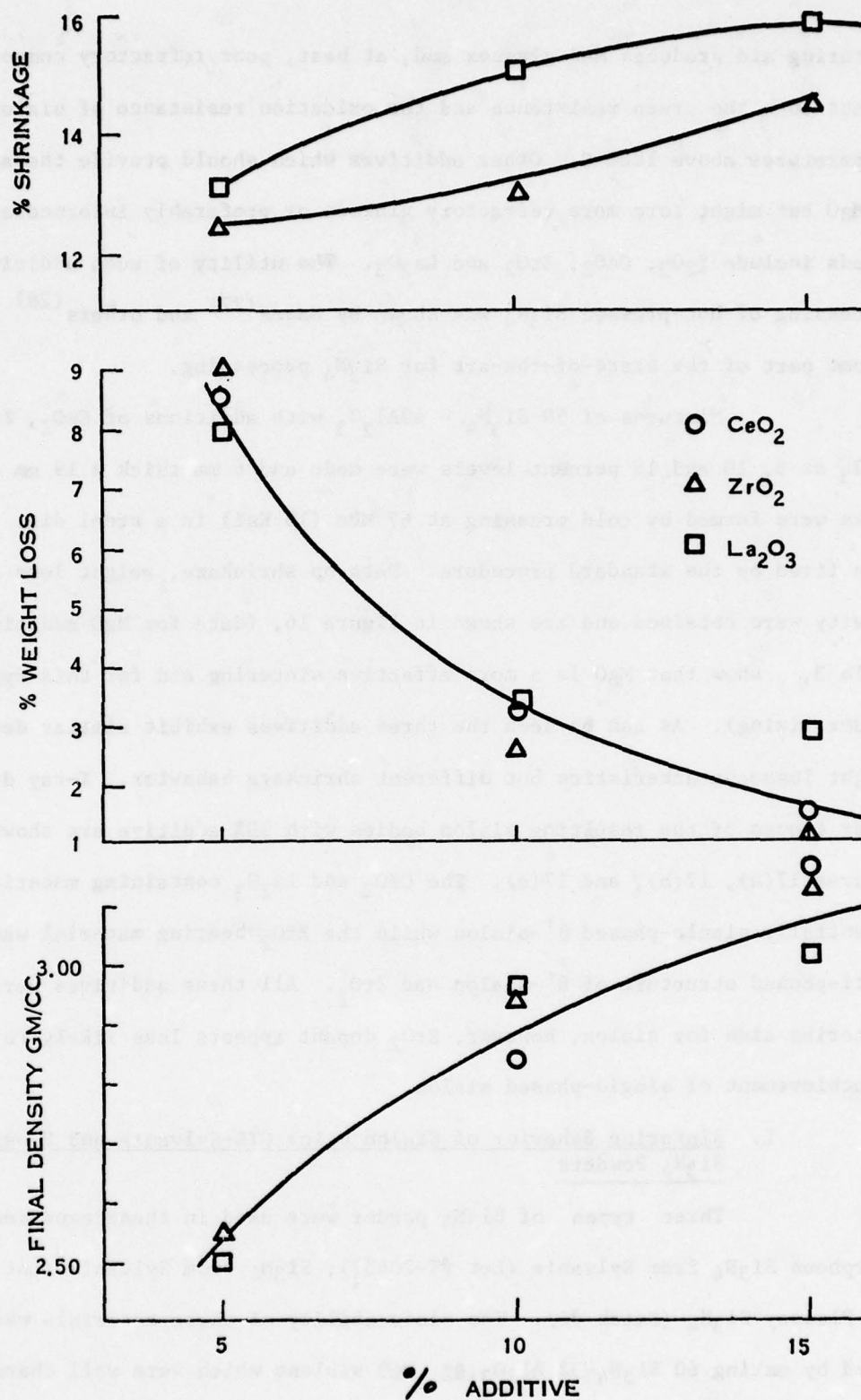


Figure 16. Linear shrinkage, % weight loss and measured final density of Sialon containing CeO_2 and La_2O_3 sintered in $\text{H}_2\text{-H}_2$ at 1700°C for 2 hours.

- CODE
1. α - Si_3N_4
 2. β - Si_3N_4
 3. β' - Sialon
 4. Al_2O_3
 5. γ Phase
 6. γ Phase
 7. MgAl_2O_4
 8. ZrO_2
 9. $3\text{Al}_2\text{O}_3 \cdot 2\text{SiO}_2$

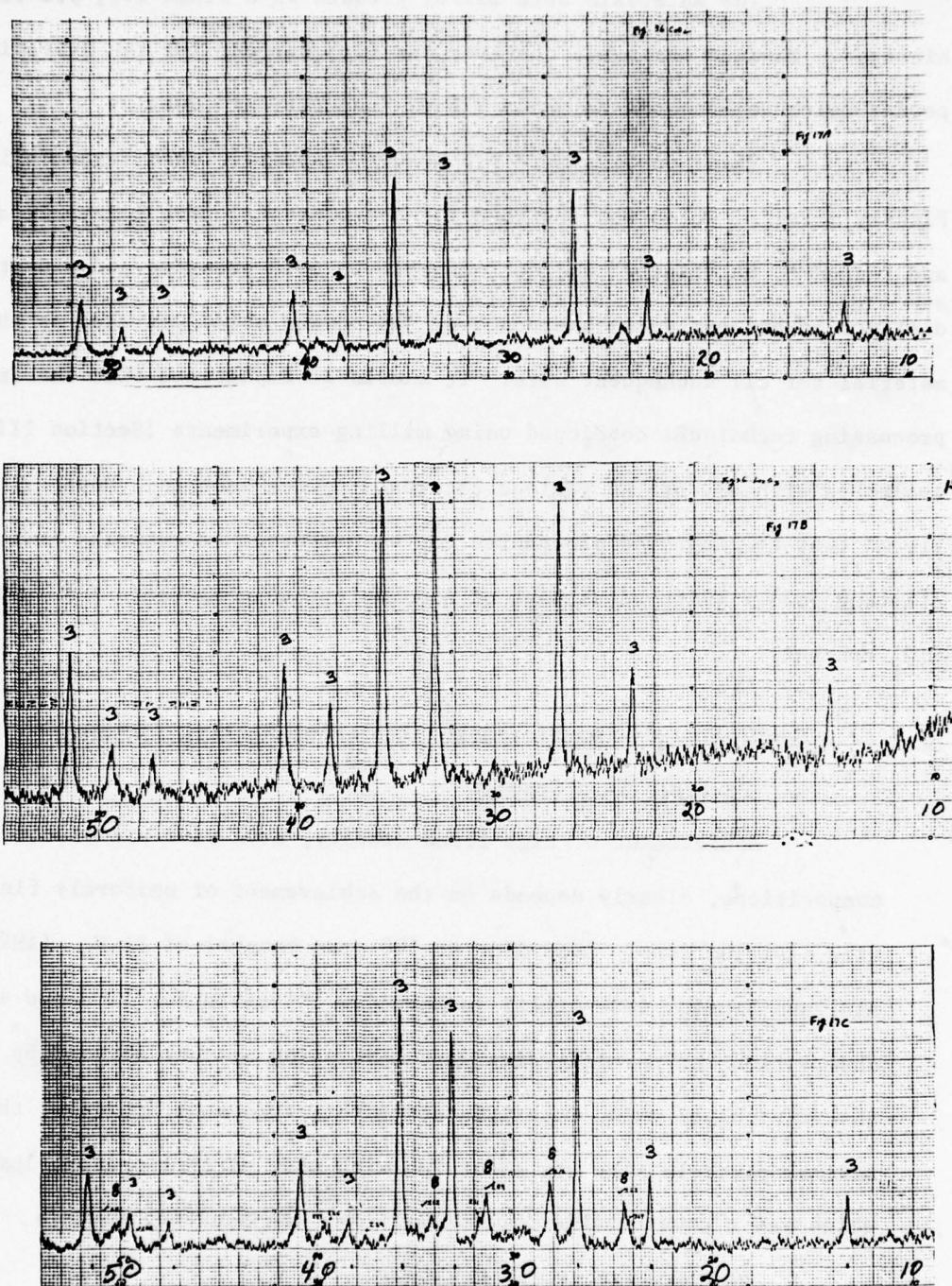


Figure 17. X-ray diffractometer traces from Sialon material containing (a) 20 W/O CeO_2 , (b) 10 W/O La_2O_3 , (c) 10 W/O ZrO_2 .

The materials were mixed, pressed in a steel die, pre-fired and sintered. Maximum shrinkage observed was 11.5 percent for the Sylvania α - Si_3N_4 powder which corresponds to about 72% of "theoretical" density.

These powders were prepared for specific uses (especially the Plessey material which was designed for hot-pressing) were generally agglomerated, and tended to be "fluffy" and not amenable to cold pressing and sintering. No distinct advantages were observed over AME powder which was used as the baseline material for all subsequent work. It should be emphasized that the improved processing techniques developed using milling experiments (Section III-2) were not evaluated with all of the various alternate powder sources. However, it is believed that the improved procedures can be performed essentially independent of starting powder (with adjustment of AlN content to compensate for variations in SiO_2 content).

2. Controlled Sialon Processing Employing Milling Techniques

a. Particle Size Studies

Achievement of high fired density, even with pre-reacted sialon compositions, clearly depends on the achievement of uniformly fine particle size distributions. Accordingly, 100 gram batches of Si_3N_4 (AME material), AlN, and alumina were milled in Borundum^(R) mills for 24 hours and observations of particle size were made using optical microscopy. Typical observations of these materials after this treatment indicated that the maximum particle size was about $2\mu\text{m}$ with most particles about $1\mu\text{m}$ or less, which was a considerable improvement over the starting powders.

b. Pre-Reacted Sialon Material:

(1) Milling

Sialon composition 60/40 $\text{Si}_3\text{N}_4/\text{Al}_2\text{O}_3$ + 8% MgO was pre-reacted at 1700 C in N_2/H_2 for one hour, crushed in a steel mortar and pestle, and milled for 72 hours in propanol. The mill and balls were Borundum^(R) (Norton Company)

of the composition 85% Al_2O_3 , 11% SiO_2 , 2% MgO , 1.2% CaO , balance TiO_2 , Fe_2O_3 , Na_2O , K_2O (.89%). After milling the batch had more than doubled in weight, (a typical 100 gram charge weighed 215 grams). This ratio of about 1-1/2 grams of mill wear per hour was fairly constant throughout the study when either Si_3N_4 , β' sialon, or AlN was milled. These milling experiments were thus more a study of mill contamination effects than comminution effects but nevertheless the results provided clues to the nature of the achievement of high density in sintered sialons .

The probable composition of this milled material was changed considerably from the starting batch and was now 28% Si_3N_4 , 60% Al_2O_3 , 5% MgO , 6% SiO_2 and 6% CaO (based on mill composition and pick-up. The composition was now alumina rich, the relative amount of MgO was reduced, and significant amounts of SiO_2 and CaO were added. An x-ray diffractometer trace of this material (as milled) is shown in Figure 18; the pre-formed and well-developed β' sialon phase is evident together with excess Al_2O_3 acquired during milling and some MgAl_2O_3 spinel. The SiO_2 appeared to be present as an amorphous phase since there was evidence of low angle scattering and neither mullite nor cristobalite were identified. The CaO contribution was too small to detect.

(2) Sintering Studies

20 mm dia. x 6 mm high discs of "MX" series material (designated "X" to denote that the MgO -content was known only approximately because of milling contamination) were pressed at 20 tsi and shrinkage data, micro-structures, and x-ray diffraction traces were obtained. This material sinters to full density at 1550 C which represents a linear shrinkage of 19%. Material sintered above 1600 C experienced bloating reminiscent of the "foaming" in the preliminary studies. Figure 19 shows the progress of the bloating reaction as

- CODE
1. α - Si_3N_4
 2. β - Si_3N_4
 3. β' - Sialon
 4. Al_2O_3
 5. γ Phase
 6. γ' Phase
 7. MgAl_2O_4
 8. ZnO
 9. MgAl_2O_4 7x10²

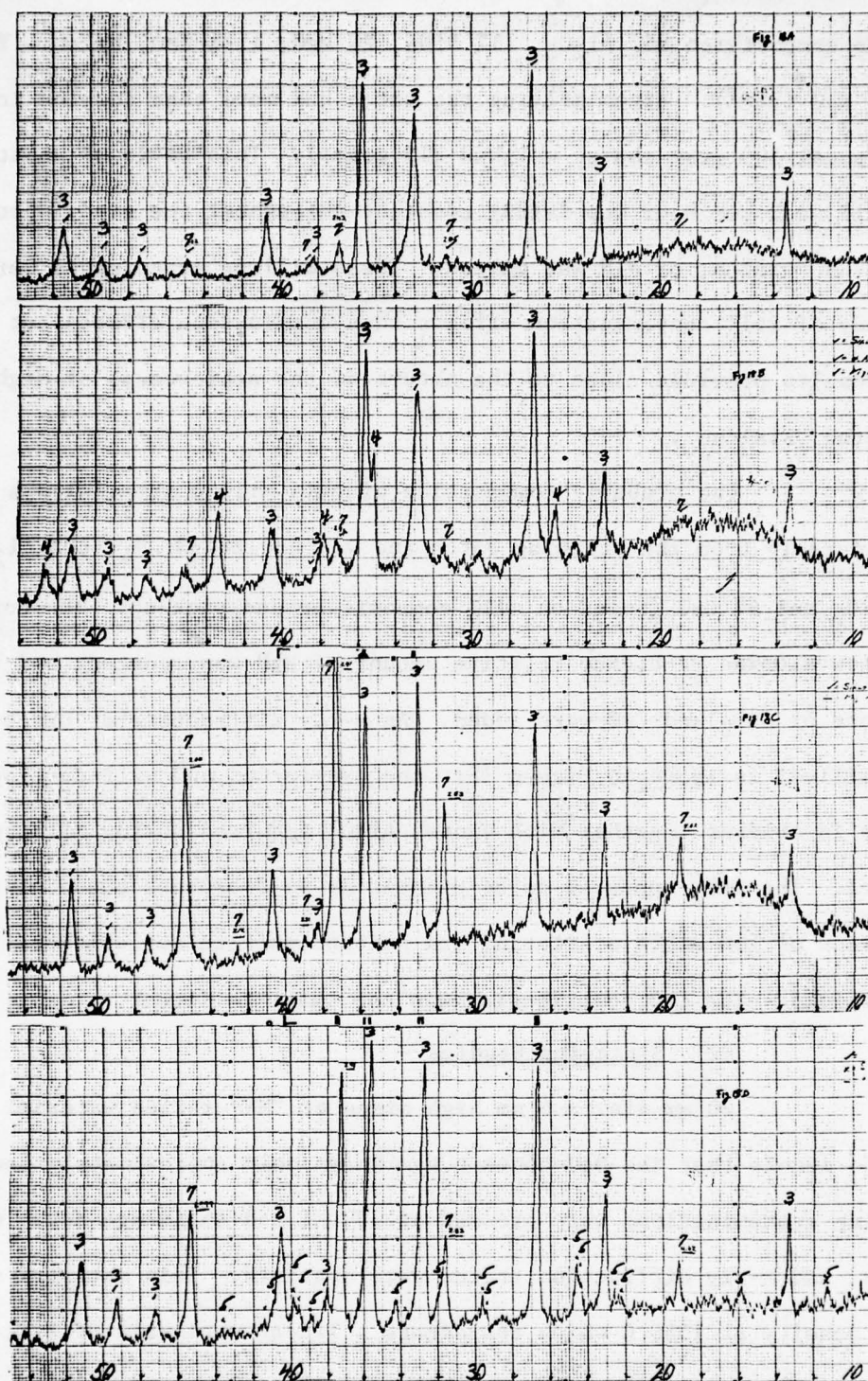


Figure 18. X-ray diffractometer traces of (a) pre-reacted 8% MgO Sialon, (b) as-milled Mx showing original 8% MgO Sialon pattern and additional Al_2O_3 , (c) Mx after sintering showing β' Sialon and MgAl_2O_4 , and (d) "X" phase β' Sialon and no Al_2O_3 after "aging" heat treatment.

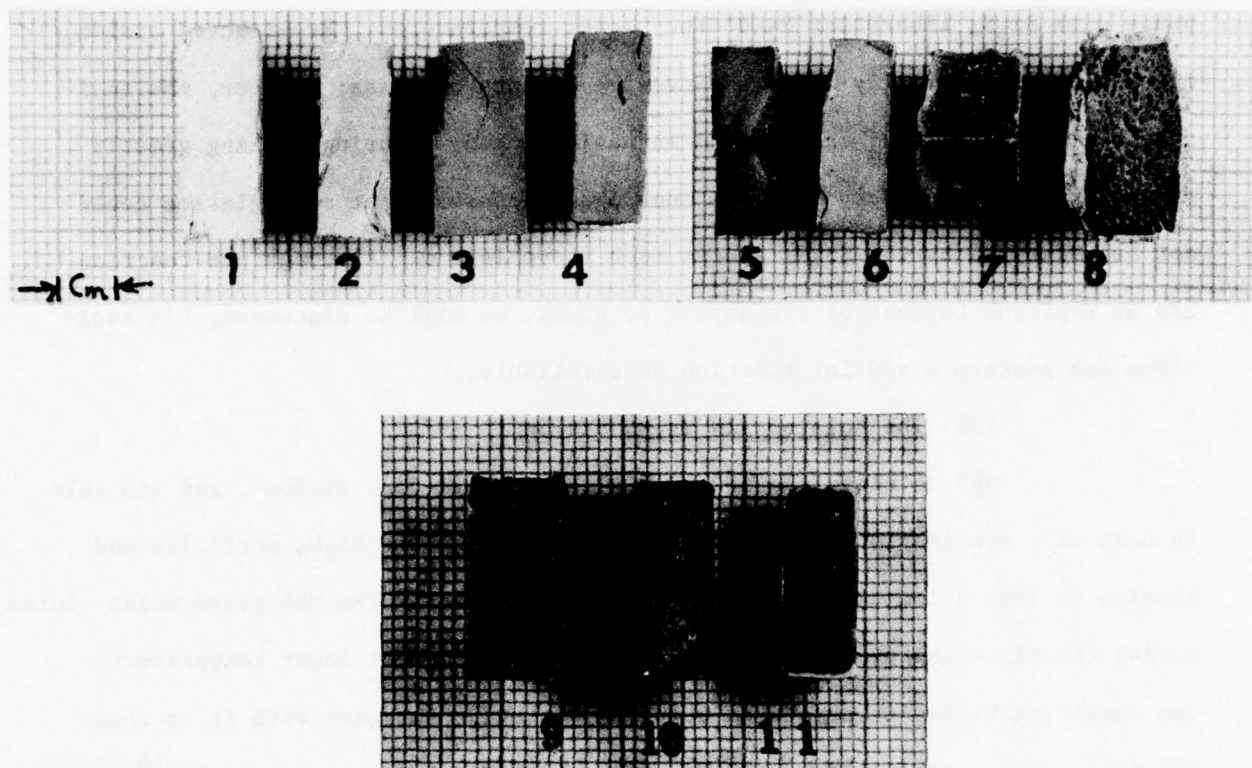


Figure 19. Cross sections of Mx Sialon after sintering in N_2-H_2 for 2 hours at (a) $1450^{\circ}C$, (2) $1500^{\circ}C$, (3) $1550^{\circ}C$, (4) $1600^{\circ}C$, (5) $1625^{\circ}C$, (6) $1650^{\circ}C$, (7) $1675^{\circ}C$, (8) $1700^{\circ}C$, (9) $1700^{\circ}C + 5\text{ AlN}$, (10) $1700^{\circ}C + 10\% \text{ AlN}$, (11) $1700^{\circ}C + 15\% \text{ AlN}$.

temperatures were increased to 1700 C (cross-sections of discs photographed after firing for 2 hours at the designated temperature in N_2/H_2 are shown).

The bloating was no doubt a result of reaction of the glassy phase with Si_3N_4 liberating N_2 at the higher temperatures. Pre-reacted sialon mixes would not normally contain excessive amounts of glass; however, the additional alumina, silica, calcia, and magnesia picked up during milling greatly enhanced the glass supply. It was once again apparent that such glasses could not be tolerated by the Si_3N_4 system much above 1600 C. Although pre-reaction can be employed to control the amount of glass, as will be discussed, AlN additions can perform a similar function more reliably.

(3) The Role of AlN in MX Sialon

MgO is clearly a powerful sintering aid for sialon, and its role is seen as a combination with surface SiO_2 present on the Si_3N_4 particles and alumina to form a low viscosity, low melting MAS glass. The MAS glass which forms during the sintering process and enhances densification at lower temperatures can remain at higher temperatures where Si_3N_4 begins to react with it to cause bloating. The established remedy for this phenomena has been to add AlN^(8,10,20) which reacts with the available silica to form additional sialons and reduces the quantity of glass considerably if not totally. The MX series was produced by indirectly adding SiO_2 and MgO during milling so that excessive MAS glass was introduced to the body and bloating resulted (as shown in Figure 19). The milled material sintered to full density at relatively low temperatures before the bloating reaction was observed. When AlN was added to this readily sinterable milled material, inhibition of initial sintering was not observed. In addition, the bloating during final high-temperature firing was controlled and ultimately stopped as shown in Figure 19. Of course, the overall composition was changed again and large quantities of "X"-phase were produced. (This is the source of the mottled

microstructure seen in the samples of Figure 20). The results obtained with the MX series also provided the first clue that mineralizing the sintering aid would retard the formation of X-phase in the presence of AlN addition. Otherwise, AlN would simply limit the amount of liquid phase and effectively retard sintering.

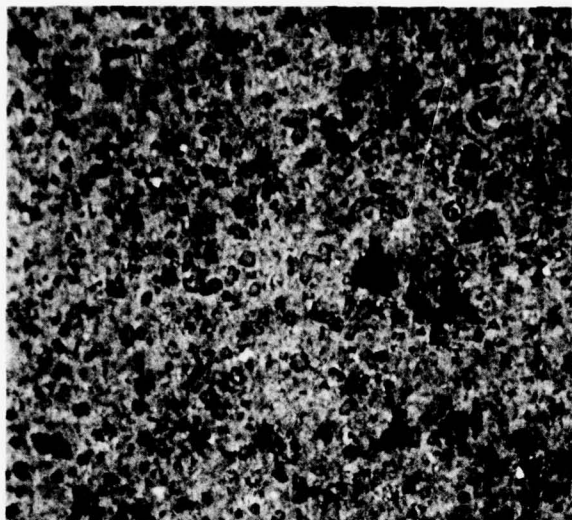
(4) Micro-Structure Analysis of MX Material

Figure 18 is a composite of x-ray diffraction traces of (1) pre-reacted MX material (nominally 8% MgO) showing the original pattern from the 8% MgO material; (2) as-milled MX showing the original 8% MgO pattern and the addition of Al_2O_3 ; (3) MX after sintering for 2 hours at 1600 C showing residual Al_2O_3 and MgAl_2O_4 phase formation; and (4) the x-ray trace of MX material with 15% AlN added and fired at 1700 C for 2 hours showing further formation of sialon, MgAl_2O_4 , the elimination of free alumina, and the appearance of "X"-phase.

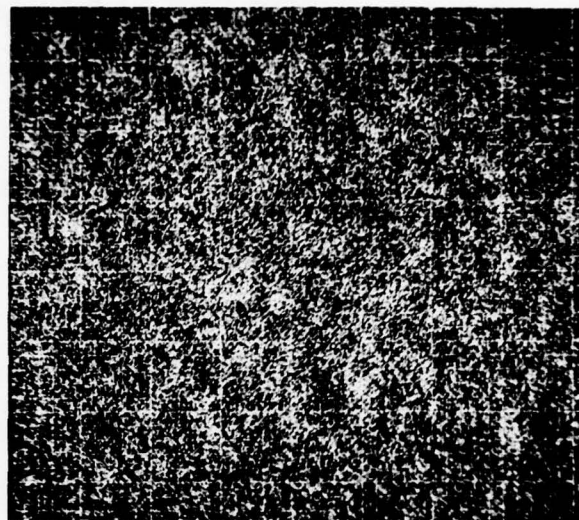
Figure 20 shows a photomicrograph of typical MX material fired at 1600 C for 2 hours and images of the same specimen examined by electron microprobe. These data show the distribution, size, and shape of the three phases β' sialon, X-phase, Al_2O_3 , and MgAl_2O_4 , detected in the x-ray studies.

(5) Mechanical Tests of MX Material

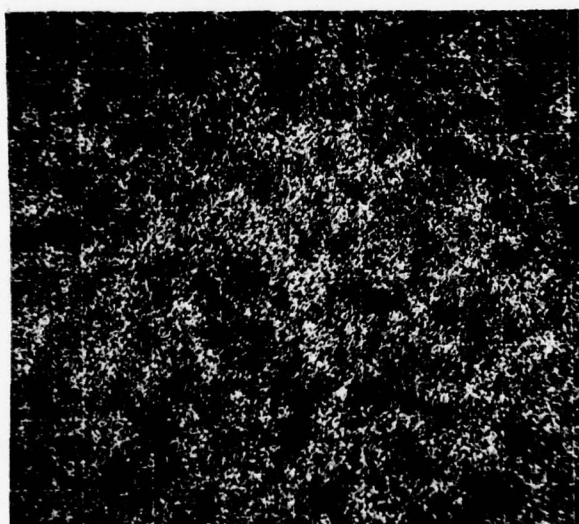
Although never considered an ideal material, some test bars of MX were fired for 2 hours at 1600 C and were used for property evaluations. Bars were cut and ground smooth on 400 grit diamond wheels of sufficient length to test one-half of a specimen at room temperature and the other half at 1200 C in 3-point bending. The results are shown in Table 7. For five tests, the average room temperature strength was 212 MPa(31,800 psi) with a maximum of 240 MPa(36,000 psi). The strength at 1200 C averaged 141 MPa(21,140 psi) with a maximum of 165 MPa(24,700 psi). The ratio of 1200 C strength to room temperature strength averaged 0.66 with the maximum ratio of 0.78. All failures were of a purely elastic brittle nature with no evidence of plastic deformation (as determined from the load/time trace) under short time loading at 1200°C).



SPECIMEN

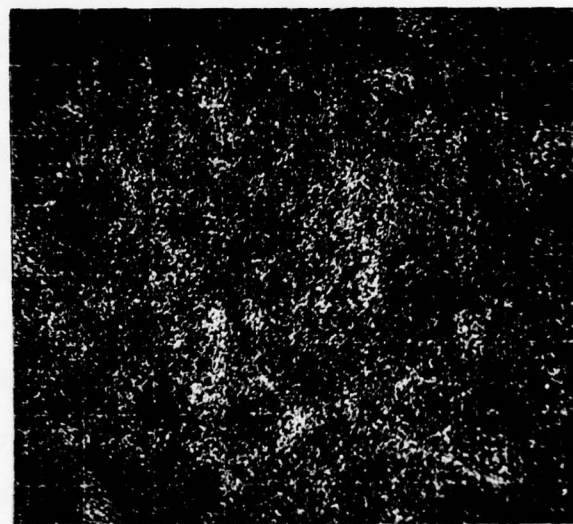


AL



Si

10 μ m



Mg

Figure 20. Optical microstructure and electron microprobe images obtained from Mx material fired at 1600°C for 2 hours in N₂-H₂.

TABLE 7. FOUR-POINT BEND STRENGTH
OF MX MATERIAL AT 20°C
AND 1200°C

<u>Spec #</u>	<u>Bend Strength at 20 C(psi)MPa</u>	<u>at 1200 C(psi)MPa</u>	<u>Strength Retention Ratio</u>
MX-1	(27,400) 183	(20,900) 135	.76
MX-2	(31,200) 208	(17,500) 117	.56
MX-3	(31,600) 210	(24,700) 165	.78
MX-4	(32,800) 219	(19,400) 129	.59
MX-5	(36,000) 240	(23,200) 155	.64

c. Unreacted Sialon Material Studies

(1) "W" Series

A parallel study was performed concurrently with the MX series discussed above in which AME Si_3N_4 , Linde-A Al_2O_3 , and Cerac AlN powders were blended in the ratio 50-25-25. (This composition was studied by Wills et al⁽²⁹⁾ and was designated "W"). A 100 gm charge of powder was milled 72 hours in a Borundum^(R) mill with propanol as a vehicle, and gained considerable weight (118 gm) during milling. The approximate composition of the charge after milling was 23% Si_3N_4 , 59% Al_2O_3 , 11% AlN (+ 1% MgO, 6% SiO_2 and 0.3% Ca) (calculated from pick-up of known mill composition).

A test firing of this material was made at 1700°C for 2 hours in N_2/H_2 and was found to sinter to full density. The sample was examined by x-ray diffraction (Figure 21), metallographically (Figure 22(a)), and by electron probe analysis (Figure 22(b)). The structure produced was multiphased with a considerable amount of free alumina.

The electron probe micrographs confirm the 2-phase structure but more significantly show the distribution of the MgO in the system (Mg Scan). At this level ($\sim 1\%$), the MgO is concentrated almost exclusively as a solid

- SCHE.
1. α - Si_3N_4
 2. β - Si_3N_4
 3. β' - Sialon
 4. Al_2O_3
 5. X Phase
 6. Y Phase
 7. MgAl_2O_4
 8. ZrO_2
 9. $3\text{Al}_2\text{O}_3 \cdot 2\text{SiO}_2$

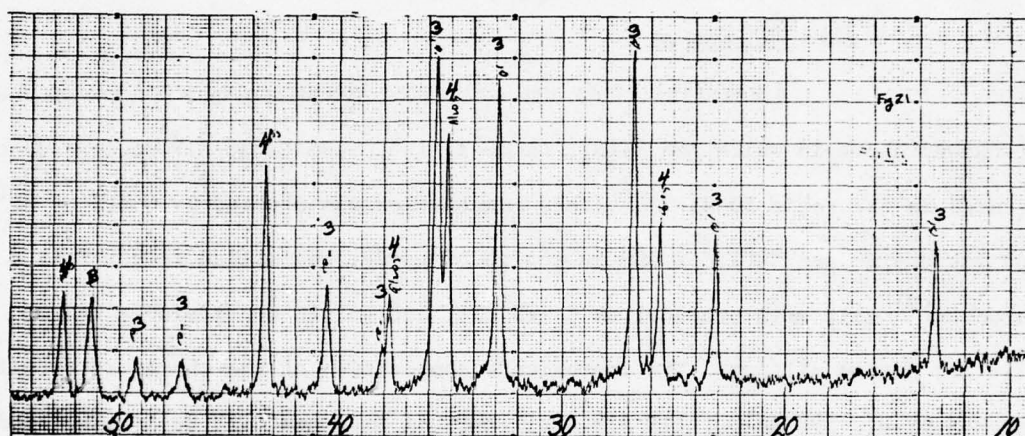
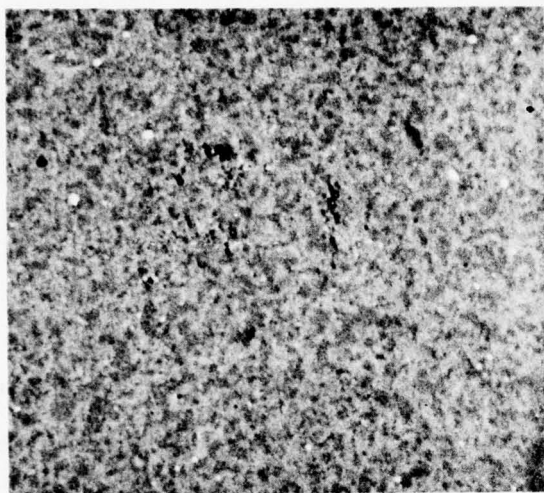
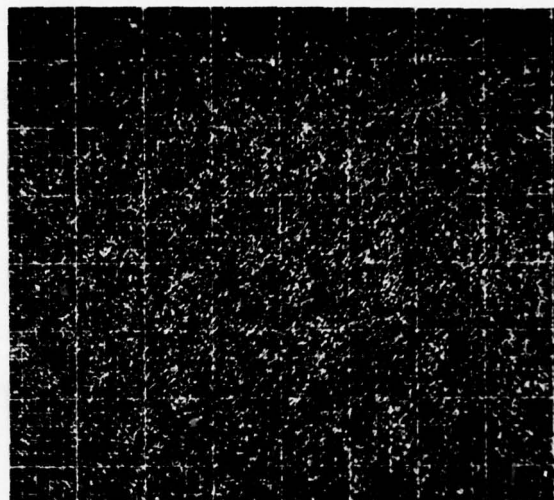


Figure 21. X-ray diffractometer traces of "W" series Sialon fired for 2 hours at 1700°C in $\text{N}_2\text{-H}_2$ showing β' Sialon and unreacted alumina.

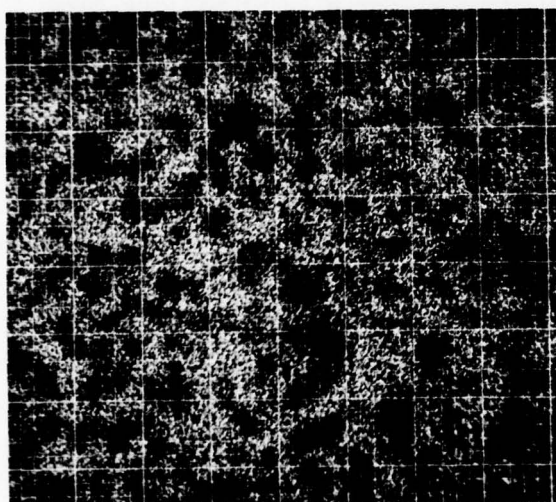


Optical Image (a)

20 μ m

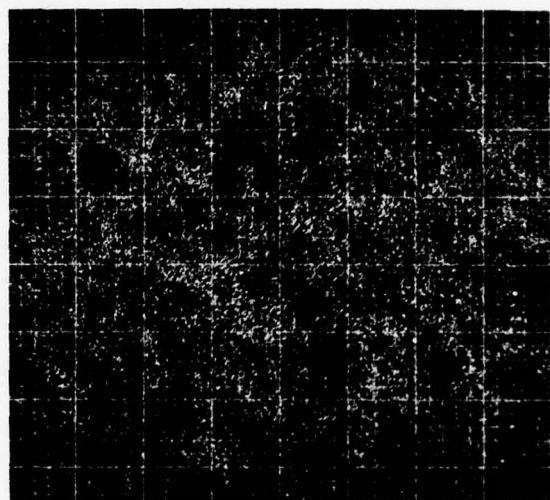


Al (b)



Si (b)

10 μ m



Mg (b)

Figure 22. Optical microstructure and electron-microprobe images of "W" material milled for 72 hours and fired at 1700°C for 2 hours in N_2-H_2 showing Mg concentration in Sialon phase.

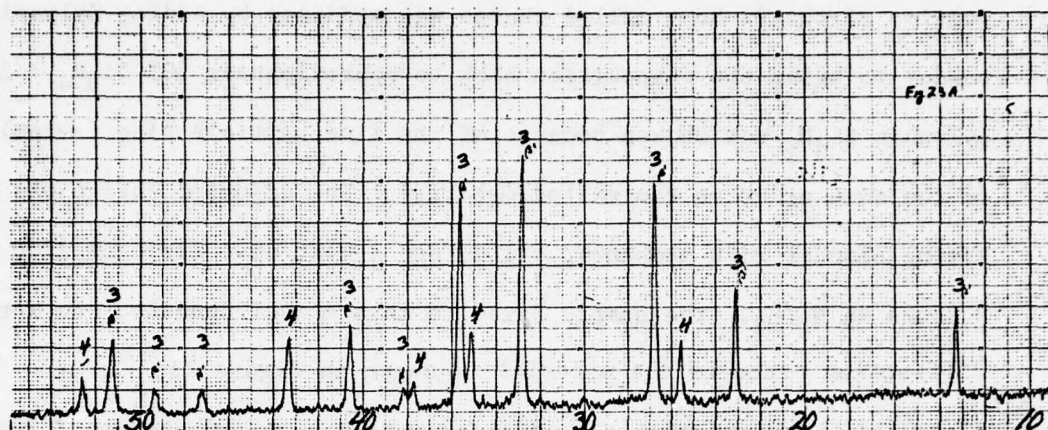
solution in the silicon-rich or Sialon Phase. Despite the large quantities of silica available in this composition, the amount of "X" phase was not significant. It appears that the available AlN was at the appropriate level to completely react with the available SiO_2 and convert to a sialon.

Since the milling for long times considerably shifted composition, the effects of shorter times were studied. A "W" charge was milled for 7 hours and picked up 15 gms of the mill. A calculated composition of this charge was then about 43% Si_3N_4 , 33% Al_2O_3 , 22% AlN (+ 1% SiO_2 + 0.3% MgO). A test firing of this material at 1700°C for 2 hours in N_2/H_2 only produced 8% shrinkage which corresponded to ~85% of theoretical density. The charge was returned to the mill and ground for an additional 17 hours for a total milling time of 24 hours. The approximate composition was then 30% Si_3N_4 , 54% Al_2O_3 , 15% AlN (+ 11% SiO_2 , 2% MgO and 0.6% CaO). This material fired to full density using the same firing schedule as above (2 hrs - 1700°C - N_2/H_2). A synthesis of this charge was made using AME Si_3N_4 , Linde-A Al_2O_3 , Bakers MgO, Cerac AlN, and Cab-O-Sil SiO_2 . The materials were mixed in a Waring Blender with propanol, dried and a test pressing fabricated and fired to 1700°C for 2 hours in N_2/H_2 . This synthesis resulted in a composition which did not sinter well and only reached about 85% of theoretical density. It was evident that a kinetic and mechanistic problem existed during sialon reaction/densification and that the manner in which the composition was initially formulated and mixed could critically determine the final fired condition. This may be considered similar to the phenomena seen in ceramic processing where "mineralizing" a batch can often increase the firing range and enhance uniformity of fired product.

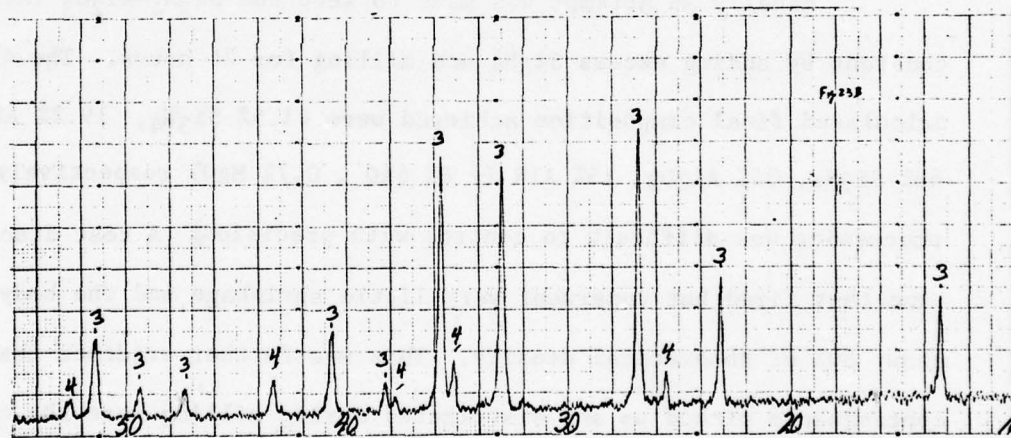
Two further experiments were performed during this series. First a portion of the 24 hour milled charge was modified by adding Sylvania α Si_3N_4 powder to bring the composition back to approximately 50% Si_3N_4 + 50% Al_2O_3 . Sylvania Si_3N_4 was chosen because of its fine particle size ($\sim 1\mu\text{m}$) which is of the same order as the milled material. The adjusted charge was mixed by Waring Blender with propanol, dried, and a test disc fired at 1700 C for 2 hours in N_2/H_2 . The sample fired to theoretical density. An x-ray diffraction trace of the material is shown in Figure 23. It is interesting to note that the additional Si_3N_4 was absorbed to form Sialon but that the Al_2O_3 peaks (although diminished somewhat) were not eliminated. Further sintering at 1700°C for three additional hours produced no change in the material as determined by x-ray diffraction.

Finally an attempt was made to keep the Si_3N_4 - Al_2O_3 ratio fairly constant by adding excess Si_3N_4 and milling for 24 hours. The initial and calculated final composition achieved were 61.5% Si_3N_4 , 19.2% Al_2O_3 , 19.2% AlN , and 48% Si_3N_4 , 34% Al_2O_3 , 15% AlN (+ 4% SiO , 0.7% MgO) respectively (the processing was difficult to control with precision). A test disc was made and test fired but underwent very little shrinkage and the body was only about 80% of theoretical density. This was further evidence that the contaminants picked up and distributed during milling were the controlling factors and not composition alone and further indicated that in order to reach full density as a β' -sialon the body must be densified early, perhaps even before the sialon-forming reaction takes place.

CODE
 1. α - Si_3N_4
 2. β - Si_3N_4
 3. α' - Sialon
 4. Al_2O_3
 5. X Phase
 6. Y Phase
 7. MgAl_2O_4
 8. ZrO_2
 9. $3\text{Al}_2\text{O}_3 \cdot 2\text{SiO}_2$



(a)



(b)

Figure 23. X-ray diffraction traces of "W" material milled for 24 hours then (a) fired at 1700°C for 2 hours and (b) Si_3N_4 added, milled and fired for 2 hours at 1700°C showed that unreacted alumina still persists after this treatment.

(2) Fabrication of Sialon Grinding Media using "W" Series Material

It was apparent that milling highly abrasive Si_3N_4 in Borundum mills or indeed any other mill would lead to pick up of material and hence contamination of the batch. Although considerable knowledge was gained using crude grinding media, it was imperative that the composition of sialon be brought under greater control so that mixtures could be more precisely formulated to minimize additional phases, excess glass content, etc. and thus produce strong, dense material of controlled composition. Accordingly, large quantities of sialon material were milled for 72 hours to produce a starting powder of approximately 40% Si_3N_4 , 50% Borundum and 10% AlN by weight. Large quantities of various diameter cylinders were isostatically pressed at 67 MPa (10,000 psi) from these powders so that sialon grinding balls could be made. Figure 24 is an illustration of a portion of these fabricated cylinders, cut-up green balls, and fired balls. The balls, actually round-ended cylinders, were fired at 1700°C for 1 hour in N_2/H_2 and were fully dense. They approximate the structure seen in "W" material milled for an equal amount of time (X-ray diffraction, pattern, Figure 23). Sufficient balls were made to give a 55% ball charge in either a low-ash rubber lined mill or a polyurethane lined mill of 2 liter capacity (purchased from Norton Company). Particle size reduction after 24 hours running was comparable to Borundum milling.

Of course, the sialon material of which these balls were made was fabricated using mill-contaminated material so that some carry over was to be expected. However, the level of contamination was reduced considerably with no free SiO_2 pick-up (since the additions of AlN to the original mix converted SiO_2 to 'X'-phase and/or β' sialon. Some MgO pick-up was inevitable but was at low level since it was only about 1 percent in the balls themselves.



Figure 24. Photographs of sialon cylinders and sialon balls for use in rubber or soft urethane-lined mills to minimize contamination, all "W" material, milled 24 hours.

(3) "SM" Series

The MX and W studies showed conclusively that the milling components (Borundum ^(R)) were contributing to sialon formation and the attainment of high density without need for additional sintering aids. (The high-alumina porcelain body of which the mill was made sinters readily at 1500°C).

A series of "synthetic milled" experiments were done (designated SM) using the principle of calcining the alumina addition of a composition approximately Borundum ^(R) ceramic and milling the Si_3N_4 and AlN separately. The "Borundum" was synthesized by blending together 6.4 gms of Sierrallite talc, 23.3 gms Kyanite, and 69.6 gms of Linde-A Alumina. This mixture had the composition (weight percent) 85% Al_2O_3 , 11% SiO_2 and 2% MgO the balance being small quantities of Fe_2O_3 , TiO_2 and CaO. These oxides were calcined at 1500°C in air for 16 hours and then ball milled for 24 hours with propanol vehicle. The Si_3N_4 and AlN were made in 150 gm and 100 gm batches, respectively and each was milled separately for 24 hours also using a propanol vehicle. This processing allowed control of composition since the Borundum pick-up during milling could be determined for each additive separately and compensated for in the final formulation: also only three additives were involved. Five compositions 0, 2.5, 5, 10 and 15 w/o AlN added to a basic 50% Si_3N_4 , 44.5% Al_2O_3 , 5.5% SiO_2 , 1% MgO, body were made by Waring blending of appropriate quantities of each milled batch in propanol. Discs of these 5 compositions were fabricated and fired to 1700 C for 2 hours in N_2/H_2 and examined by x-ray diffraction. The results are shown in Figure 25. All fired discs reached at least 95% of theoretical density, SM-15 reached 98% of theoretical. It is curious here that even without AlN additives no

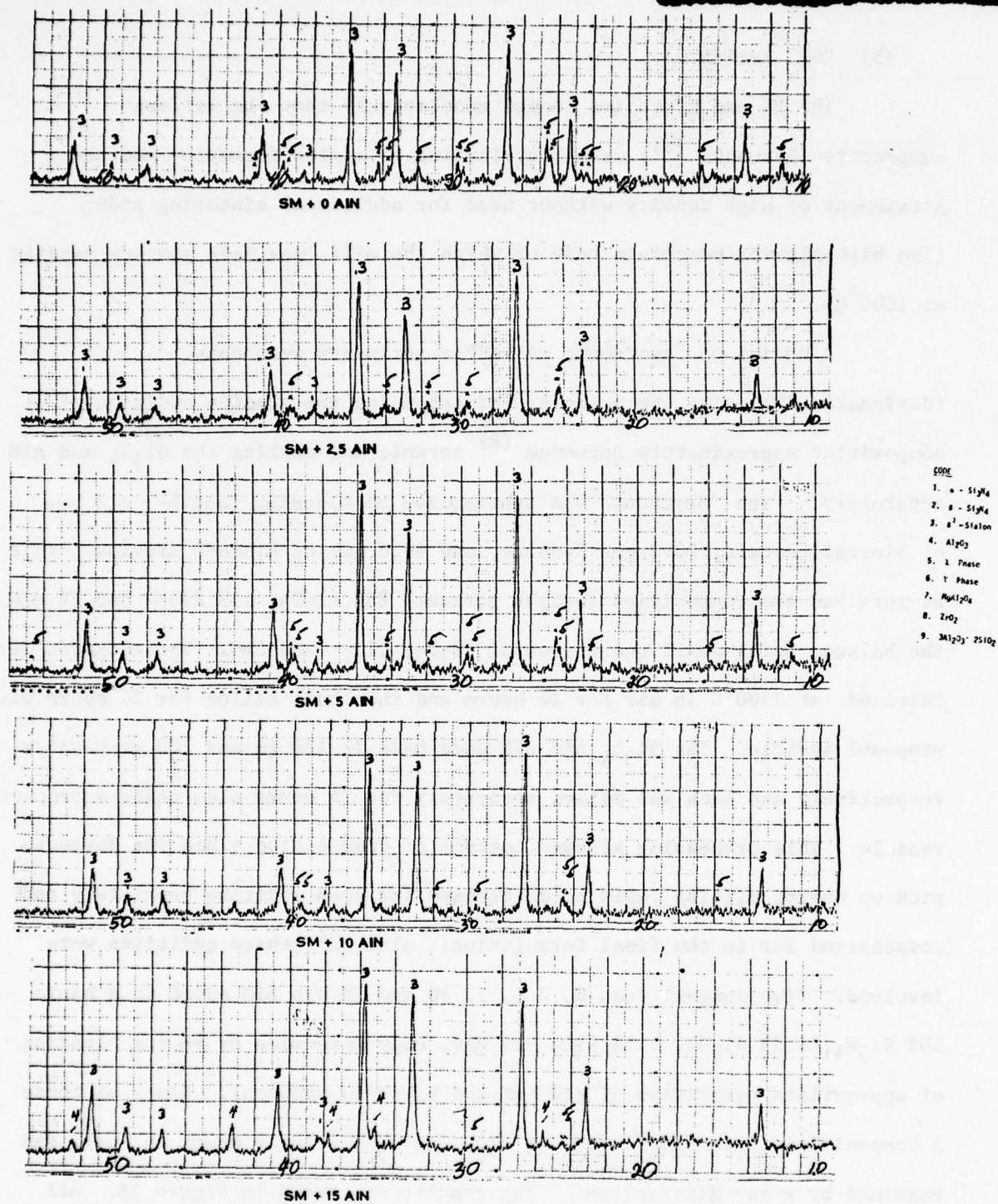


Figure 25. X-ray diffractometer traces of SM series Sialon showing relationships between β' Sialon, "X" phase, AlN and Al_2O_3 .

adverse reaction occurred due to Si_3N_4 decomposition (no bloating) and further retardation of sintering was not observed as a result of using the AlN additive. It appeared that pre-heating the Alumina addition with SiO_2 and MgO , produced a MAS glass of higher refractoriness and high viscosity, possible because of greater Al_2O_3 solution or because some SiO_2 was present as mullite. The detection of "X" phase in the SM-0 sample showed that the reaction $\text{SiO}_2 + 2\text{Al}_2\text{O}_3 + \text{Si}_3\text{N}_4 \rightarrow 4\text{SiO}_2\text{-AlN}$ ("X" phase) could occur without initial AlN additions.

The SM series also showed that AlN additions controlled the formation of "X" phase; as more AlN was added, "X" diminished. When excess AlN was present, then Al_2O_3 was stabilized. This is consistent with the phase diagram of Gauckler, et al⁽¹⁵⁾ and the work of Lumby⁽⁸⁾ where β' sialon is shown as a narrow band and where the addition of AlN can be effective in determining which side of the band the fired compositions will lie.

The SM series sintered well but did not fully achieve the high density (approximately theoretical) achieved with the ball-milled material. There are at least two reasons for this. First the Waring Blender cannot mix as thoroughly as long time milling, also the Waring Blender uses an aluminum blade which wears in the process and can add significant amounts of aluminum metal to the mix. Since the mixes were never fired in air, the reaction of the atmosphere (H_2/N_2) with the dispersed metal particles can form fine "puffball" porosity in the fired body. This observation was documented by Bruch⁽³⁰⁾ during extensive studies of defects seen in Lucalox^(R) alumina. (Initial work in this program employed a low temperature pre-fire in air to produce Al_2O_3 from Al metal contaminant from the Waring Blender).

(a) Sintering Behavior of SM-15

The sintering behavior of SM-15 sialon material was studied by following shrinkage, weight loss (packed in Si_3N_4), and resulting sialon formation as a function of firing temperature and atmosphere. The firing time in every case was one hour. Table 8 and Figure 26 summarize these data.

(b) Strength of SM-15

Table 9 summarizes the results obtained on SM-15 material at room temperature and at 1400 C. A maximum strength of 280 MPa (42,000 psi) was observed at room temperature using the three-point bending apparatus described earlier.

Tests at 1400 C showed the material to deform plastically to a degree sufficient to prevent fracture. The plastic behavior indicated that weak, glassy, grain-boundary phases were present in this material, presumably a MgO-bearing glass or low melting crystalline phases such as forsterite.

(4) Studies on Sialon Bodies Other Than SM-15

The sinterability of sialons was related to the total alumina content such that bodies containing low amounts of Al_2O_3 did not sinter as readily as high alumina bodies. Using the "SM" approach, it was seen that the excess SiO_2 and AlN added to the system also contributed to the total amount of " Si_3N_4 " in the system during sialon formation. Therefore, by decreasing the amount of Si_3N_4 in the initial batch more favorable sintering conditions may be encountered. SM-15, for example, was initially 50% by weight Si_3N_4 but after firing would be at least 61% " Si_3N_4 ". Such bodies sintered to between 91-95% of theoretical density. By starting with 40 W/O Si_3N_4 , the resultant bodies sintered to between 95-98% of theoretical density and the fired composition was ~45% Si_3N_4 .

Table 10 summarizes the compositions studied in this phase of the work while Figure 27 summarizes the x-ray diffractometer data. Notice that changes in SiO_2 or MgO additions did not affect the sinterability or fired crystalline composition of these materials: they are all apparently single-phased β' sialon. It was hypothesized that at least the minimum amount of liquid

TABLE 8. WEIGHT LOSS (%) AND SHRINKAGE (%)
VS. FIRING TEMPERATURE (°C) FOR
SM-15 MATERIAL

Temperature °C	% Shrinkage	% Weight Loss
1300	1.0	2.2
1400	2.0	2.5
1500	4.9	3.9
1600	10.0	4.5
1700	17.0	5.5

TABLE 9. FOUR-POINT BEND STRENGTH RESULTS
ON SM-15 MATERIAL

Specimen #	Temp. °C	Max. Stress MPa(psi)
SM-15-M	20	274(41,100)
SM-15-A	20	209(31,300)
SM-15-B	1400	84(12,600)
SM-15-C	20	259(38,800)
SM-15-D	20	139(20,800)
SM-15-D	1400	79(11,800)
SM-15-E	20	281(42,200)
SM-15-F	20	235(35,300)

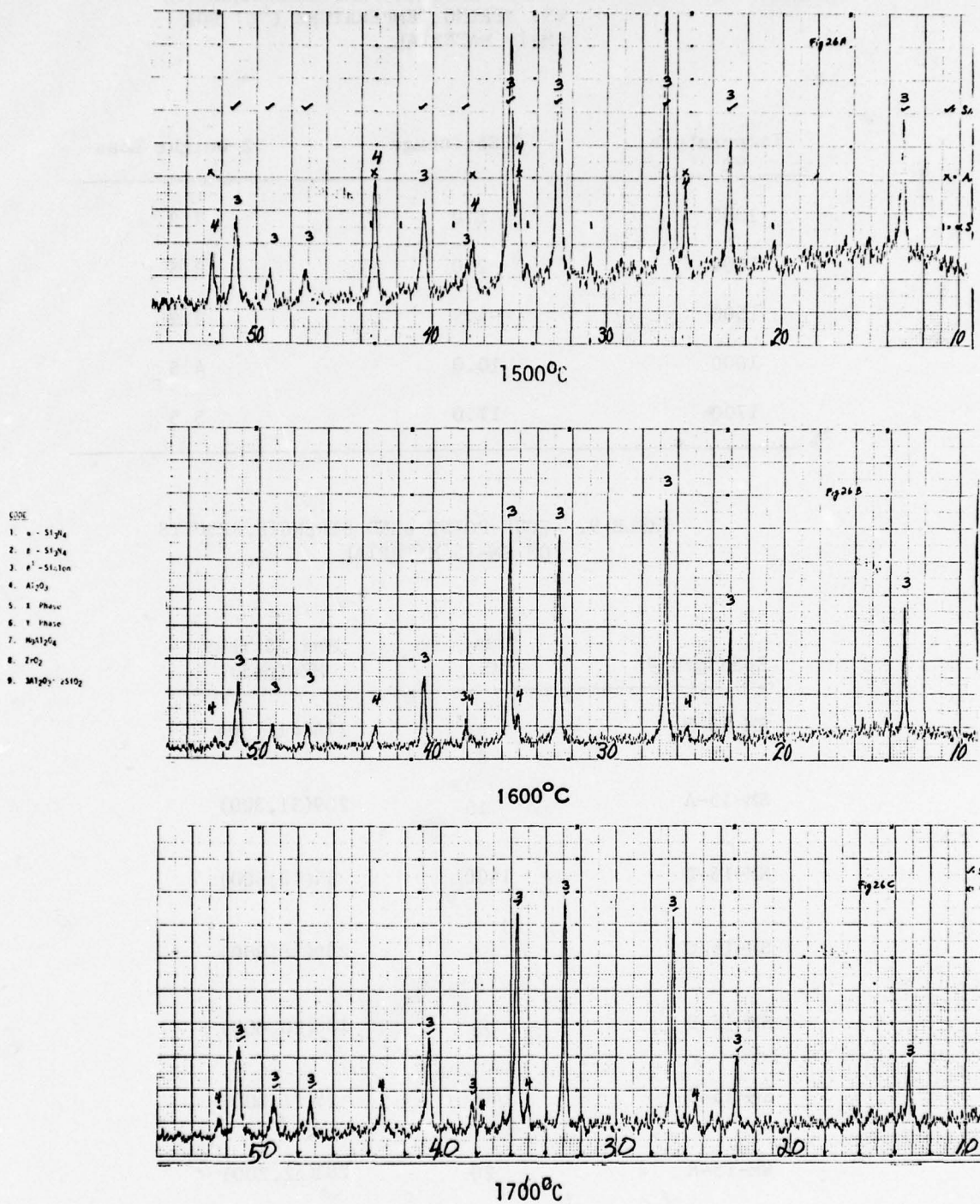


Figure 26. X-ray diffractometer traces of Sm-15 showing affect of temperature on formation of β' Sialon phase.

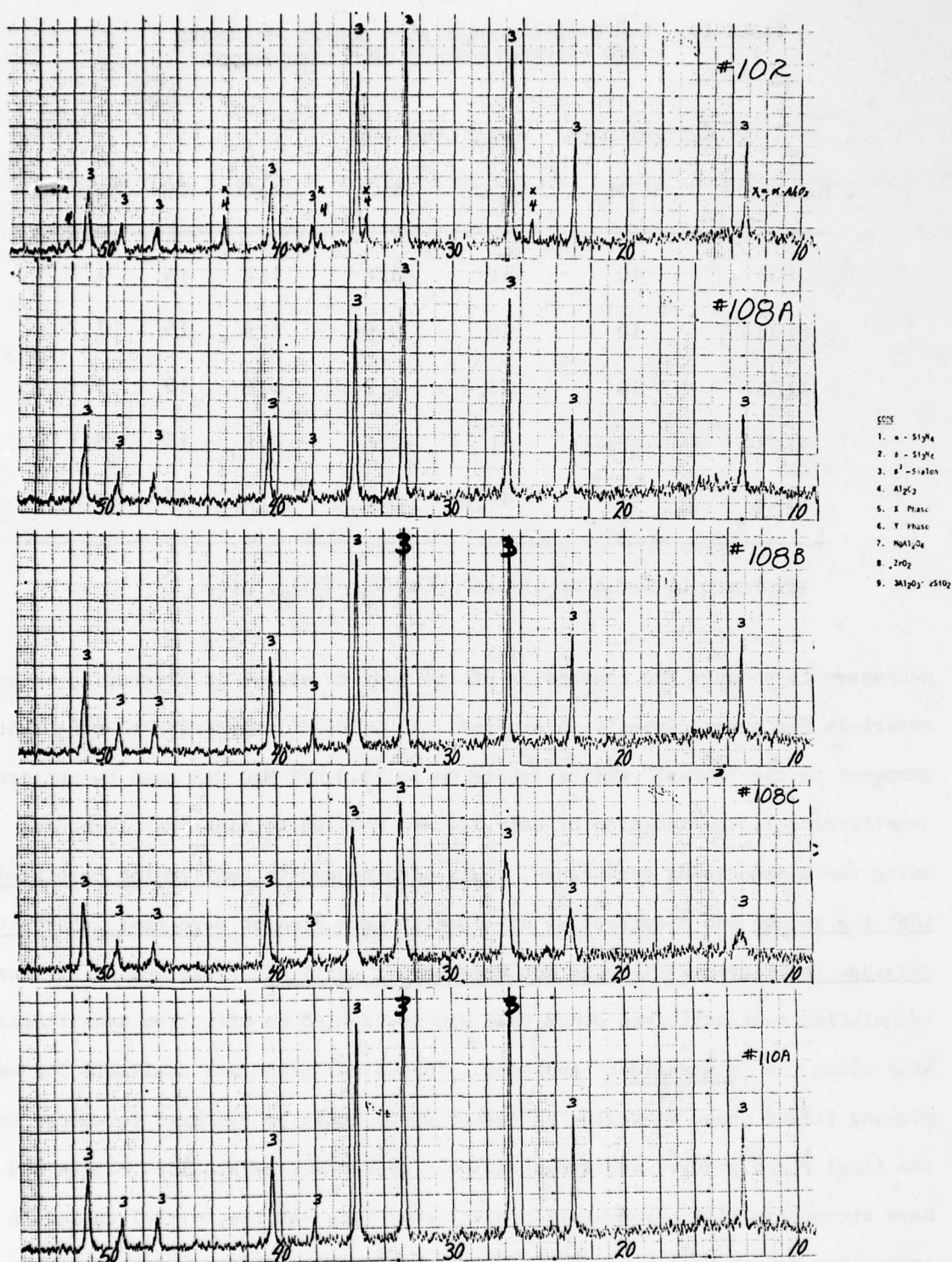


Figure 27. X-ray diffractometer traces of Sialon materials in which the glass forming volume was varied by adjusting the Al_2O_3 - SiO_2 - MgO content showing single phase β' Sialon formation as specimen numbers increase.

TABLE 10. COMPOSITIONS OF SIALON BODIES PROCESSED
WITH VARYING AMOUNTS OF "GLASS-FORMER"

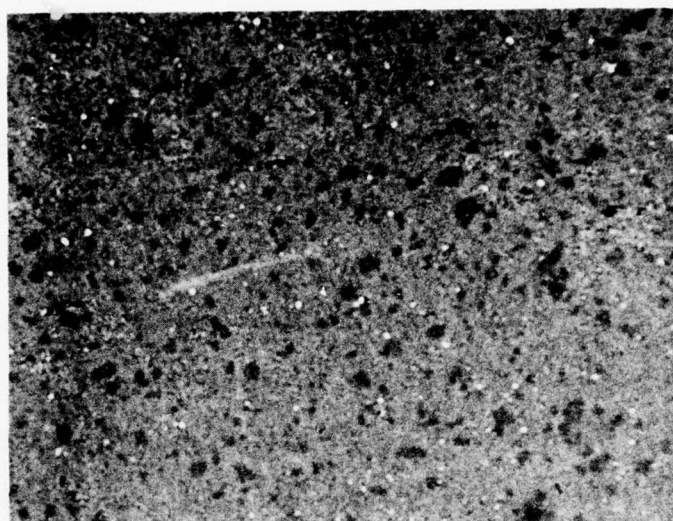
Composition: Weight percent						
Sample #	Si_3N_4	Al_2O_3	SiO_2	MgO	AlN	Balance*
#102	40	51	6.6	1.2	15	1.2
#108A	40	48	9.0	1.8	15	1.2
#108B	40	53.4	4.2	1.8	15	0.6
#108C	40	51	6.6	1.8	15	0.6
#110	40	49.8	6.6	3.0	15	0.6

*Balance is made up of CaO , Fe_2O_3 , TiO_2 , etc.

necessary to enhance the conversion of the body to sialon is present in these materials for every composition studied. It is also interesting to note that compared to the "normal" series (where up to 13.3 W/O MgO was used to achieve densification), the addition of only 1.2 W/O MgO led to high density bodies using these processing techniques. This also tended to confirm the hypothesis that the volume and distribution of glass formers present were most important and that their composition was not necessarily critical. This led to further speculation that additives other than MgO would also be effective densification aids using the "mineralized" approach. Thus a mechanism was available for employing liquid phase sintering processes which could be tailored to ensure that the final fired product would contain only refractory crystalline phases and thus have attractive high temperature properties. This was the initial rationale for converting MgO to MgAl_2O_4 in the earlier work but, as noted, this may not be necessary and compositional control can be assured at much lower "additive"

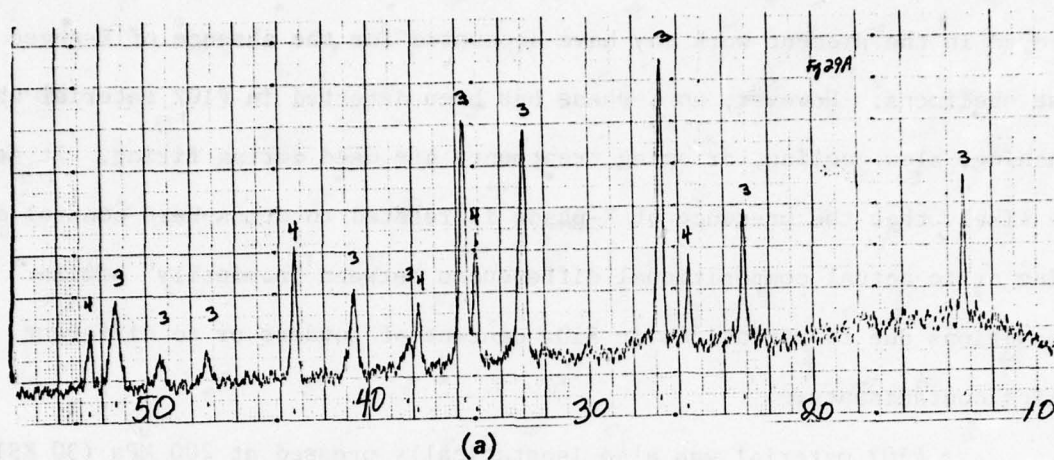
(5) #102 Material

#102 material was a Sialon produced using MgO as a sintering aid (Table 10). It was well behaved in that it could be readily and reproducibly sintered to high density. Figure 28 is a typical microstructure of this material. Although it was felt earlier that MgO additives were not suitable because of their unfavorable effect on creep properties, later work indicated that this disability may be corrected by proper aging to transform any residual grain-boundary glass phases into crystalline or solid-solution form. The philosophy to treat MgO as an undesirable additive nevertheless continued and its use either deliberate or as an incidental contaminant (i.e. from ball mills) was minimized in other compositions as far as possible. Figure 29(a) is a typical x-ray diffractometer trace of #102 material after sintering for 2 hours at 1700°C. There is evidence of residual Al_2O_3 in the structure but the β' sialon phase is major and very sharp. Figure 29(b) is #102 sialon which was again sintered 2 hours at 1700°C but then aged for 16 hours at 1400°C and then furnace cooled. Notice that the β' peaks have diminished and have broadened indicating either further formation of Sialon crystallites or recrystallization. Also in Figure 29 the sharp peaks formed during initial firing can be seen to be replaced by wider trace made up of smaller multiple peaks. The Al_2O_3 peaks have also increased in intensity. As will be shown in a later section, aged #102 Sialon had an improved high temperature bend strength at 1370°C, and less plastic deformation compared to the normally processed material, suggesting that the suspected residual glassy phases were crystallized or otherwise removed or reduced. No evidence for new crystalline phases is evident, however, on x-ray diffractometer traces. However, the multiple peaks suggest that Sialons of varying composition have formed from the initial more-homogeneous sialon.



20μm

Figure 28. Typical microstructure of #102 Sialon material after firing for 2 hours at 1700°C.



- CODE
1. α - Si_3N_4
 2. β - Si_3N_4
 3. β' - Sialon
 4. Al_2O_3
 5. X Phase
 6. Y Phase
 7. MgAl_2O_4
 8. ZrO_2
 9. $3\text{Al}_2\text{O}_3 \cdot 2\text{SiO}_2$

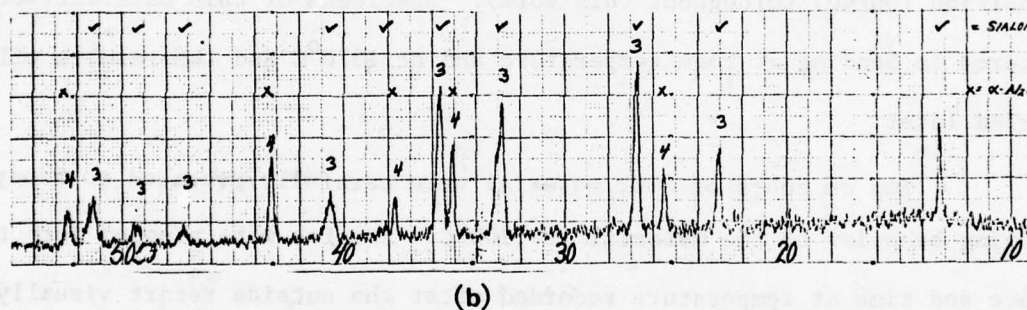


Figure 29. (a) A typical x-ray diffractometer trace of #102 Sialon material fired at 1700°C for 1 hour, (b) after aging for 16 hours at 1400°C all in $\text{N}_2\text{-H}_2$ atmosphere. Showing broadening of β' Sialon peaks after aging.

Wimmer (31) consistently detected X-phase in similar Sialon materials processed at AFML and it was considered that the rapid cooling employed in the present work may have accounted for the absence of X-phase in these specimens. However, no X-phase has been detected in #102 material whether quenching, slow cooling, or aging treatments are used during firing. It seems more likely that the presence of X-phase is related to atmosphere control during firing or to actual compositional differences between "nominally" similar compositions due to variations in SiO_2 content of powders or to different milling contaminants.

#102 material was also isostatically pressed at 200 MPa (30 KSI) and 333 MPa (50 KSI) to increase green density since "standard" processing used 67 MPa (10 KSI) only. The fired specimens did reach somewhat higher densities (3.2 gm/cc) (which for convenience was the "theoretical" density used for this composition (60/40) throughout this work). Specimens of this material were fractured in bending at room temperature and at 1370°C and the results will be reported later.

Two cm cubes of #102 material were carefully prepared to study the sintering behavior of the material at 1700°C. Samples were plunged into the furnace and time at temperature recorded after the outside retort visually appeared to have reached temperature (usually within 5 minutes). The data obtained are shown in Figure 30 as both the actual time in the furnace and the estimated time at which the specimens were at temperature. This was done since the true specimen temperature could not be measured because of the retort structure and powder packing. The first detection of a density change is recorded as zero time but which was in fact 20 minutes after furnace plunging. The letters A through I on the Figure 30 corresponds to the X-ray traces made during the study. Notice that at (point F) (Figure 31) $\alpha\text{-Si}_3\text{N}_4$ was still

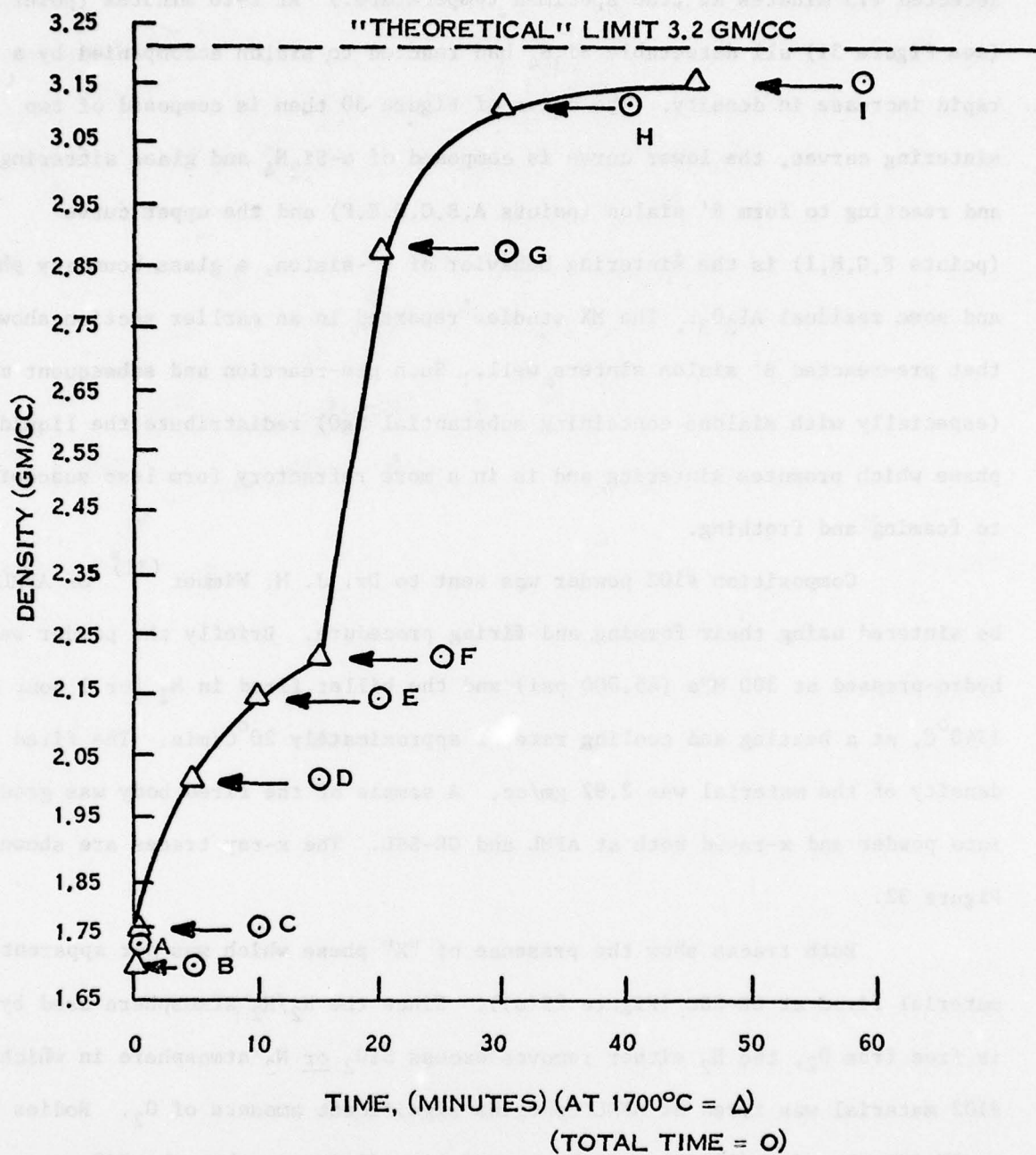
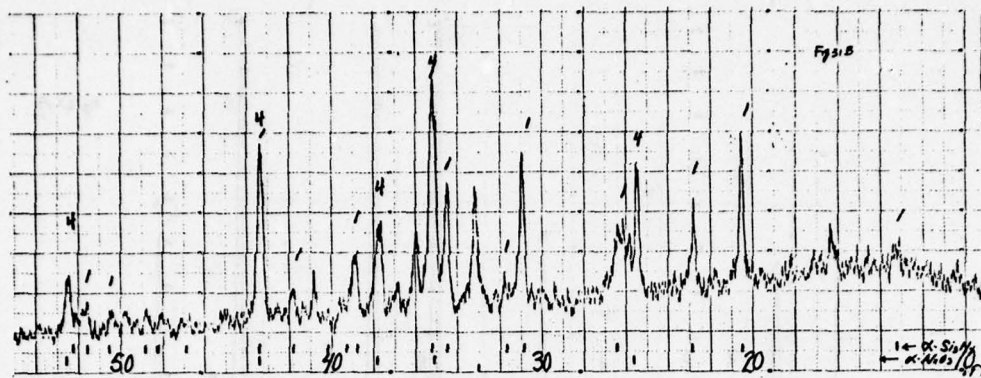


Figure 30. Density vs. sintering time data for #102 material sintered at 1700°C using the standard firing procedure with Mo retort and N₂-H₂ atmosphere.

detected (15 minutes at true specimen temperature.) At $t=20$ minutes (point G) (see Figure 31) all detectable Si_3N_4 had reacted to sialon accompanied by a rapid increase in density. The curve of Figure 30 then is composed of two sintering curves, the lower curve is composed of $\alpha\text{-Si}_3\text{N}_4$ and glass sintering and reacting to form β' sialon (points A,B,C,D,E,F) and the upper curve (points F,G,H,I) is the sintering behavior of β' -sialon, a glass boundary phase, and some residual Al_2O_3 . The MX studies reported in an earlier section showed that pre-reacted β' sialon sinters well. Such pre-reaction and subsequent milling (especially with sialons containing substantial MgO) redistribute the liquid phase which promotes sintering and is in a more refractory form less susceptible to foaming and frothing.

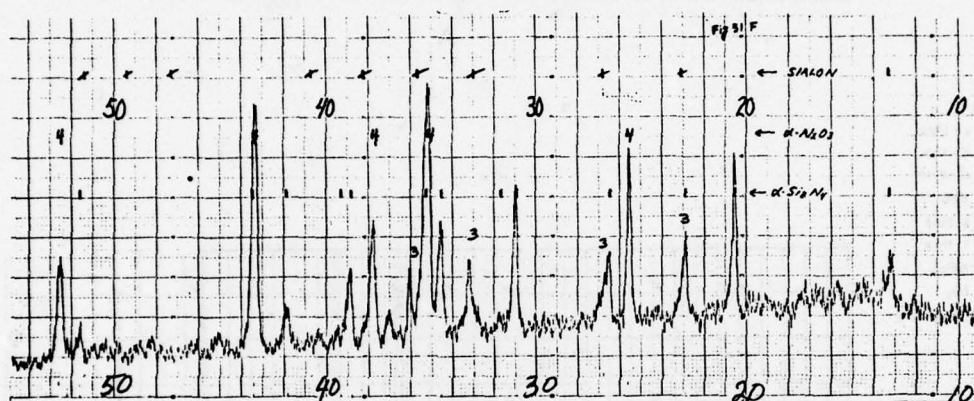
Composition #102 powder was sent to Dr. J. M. Wimmer⁽³¹⁾ of AFML to be sintered using their forming and firing procedure. Briefly the powder was hydro-pressed at 300 MPa (45,000 psi) and the billet fired in N_2 for 1 hour at 1740°C , at a heating and cooling rate of approximately $20^\circ\text{C}/\text{min}$. The fired density of the material was 2.92 gm/cc. A sample of the fired body was ground into powder and x-rayed both at AFML and GE-SSL. The x-ray traces are shown in Figure 32.

Both traces show the presence of "X" phase which was not apparent in material fired at GE-SSL (Figure 29(a)). Since the N_2/H_2 atmosphere used by GE is free from O_2 , the H_2 either removes excess SiO_2 or N_2 atmosphere in which the #102 material was fired at AFML contains significant amounts of O_2 . Bodies fired at GE-SSL showed negligible weight loss during firing so that the SiO_2 removal hypothesis does not appear valid. If the N_2 atmosphere did indeed add O_2 during sintering, then it can be appreciated that both the composition and glass content

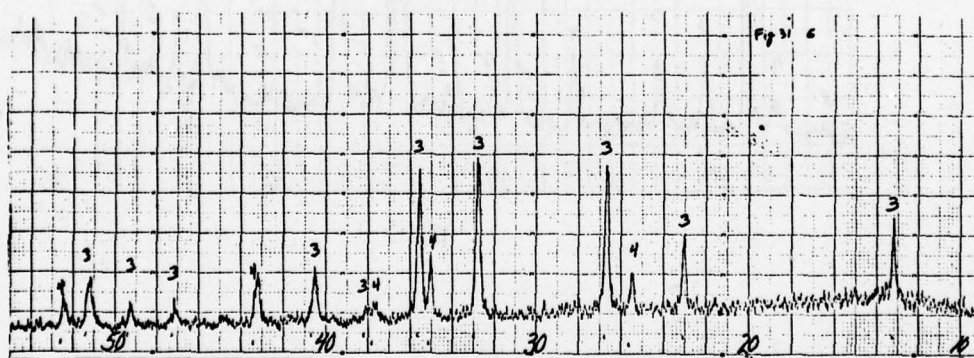


(B)

- KEY
1. α - Si₃N₄
 2. β - Si₃N₄
 3. α' - Si₃N₄
 4. Al₂O₃
 5. Z Phase
 6. Y Phase
 7. MgAl₂O₄
 8. ZnO₂
 9. Mg₂O₂ · 7SiO₂

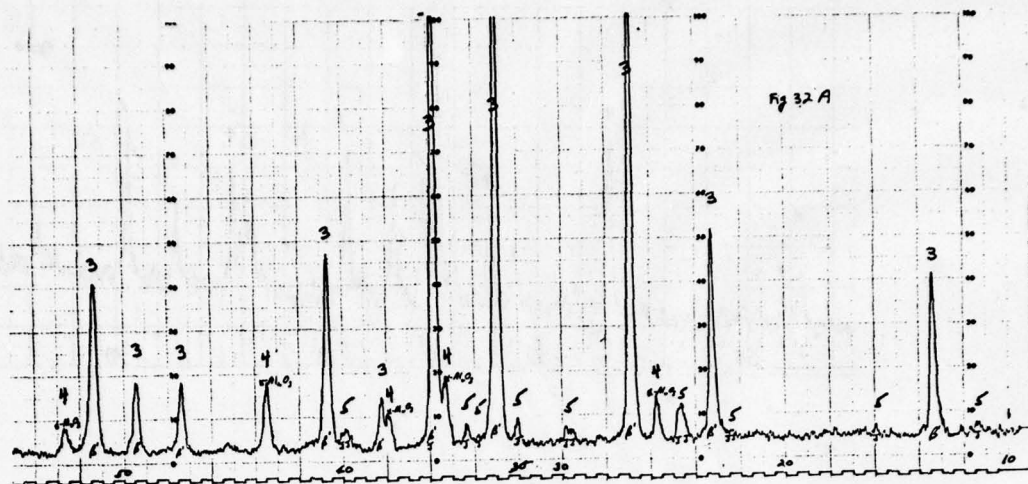


(F)



(G)

Figure 31. X-ray diffractometer traces of #102 material sintered at 1700°C for increasing times showing progressive elimination of α Si₃N₄ (see also Figure 30).



A

- CODE
- 1. α - Si_3N_4
 - 2. β - Si_3N_4
 - 3. α' - SiAlON
 - 4. Al_2O_3
 - 5. X Phase
 - 6. Y Phase
 - 7. MgAl_2O_4
 - 8. ZrO_2
 - 9. $3\text{Al}_2\text{O}_3 \cdot 2\text{SiO}_2$



B

Figure 32. X-ray diffractometer traces of #102 material fired in N_2 atmosphere at AFML. A - AFML trace, B - GE trace.

of fired materials may not be controlled. As will be seen later (Table 12) other sialons of high-Si₃N₄ content fired under both conditions generally attained higher densities at AFML suggesting again the possibility of slightly greater glass content under the "N₂" conditions. (AFML firing temperature was generally higher than at GE and the heating schedule differed markedly.)

(6) Sialons Containing Y₂O₃ and ZrO₂

Yttria and zirconia sialons were made and sintering characteristics studied using the mineralization technique. Their fabrication techniques, firing schedules and compositions are reported elsewhere in this report (also Figure 33 and Table 11). No extensive mechanical property studies were made however. Yttria sialons have been studied by McLean, et al⁽³²⁾ fired at 1600°C rather than the 1700°C used here; however, their processing conditions and possible contaminants were not detailed and although bend strengths near 600 MPa (90,000 psi) were measured at room temperature the strength fell rapidly at temperatures above 1000°C. Layden⁽¹³⁾ also reports bend strength values as high as 533 MPa (80,000 psi) for sialons containing Y₂O₃ and mixtures of Y₂O₃ and ZrO₂. However, severe contamination due to mill wear in high alumina mills was reported and may in fact be the controlling factor in promoting densification as was discussed here. Severely impaired oxidation resistance was observed in several Y₂O₃-containing sialons in these studies^(11,32). The reasons for this have recently been explained by Lange⁽³³⁾ who showed that the fired composition must end within the Si₃N₄-Si₂N₂O-Y₂Si₂O₇ compatibility triangle if stable behavior is required under oxidizing conditions. Similar work in the MgO system by Lange⁽³⁴⁾ and by Jack⁽³⁵⁾ have shown a similar marked dependency between oxidation resistance and composition, specifically the MgO/SiO₂ ratio.

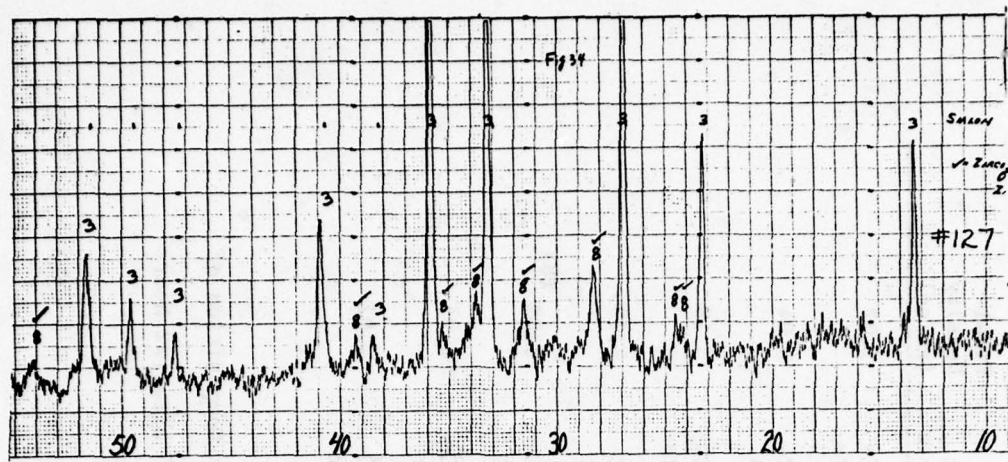
TABLE 11. COMPOSITIONS, FIRING SCHEDULE AND FINAL SINTERED DENSITY OF HIGH-Si₃N₄ CONTENT SIALONS

Specimen #	Composition in w/o (c)					Milling Time (Hours)	Mill Pick-up (grams)	Firing Schedule	Final Density (gm/cc)																																								
	Si ₃ N ₄	Al ₂ O ₃	AlN	Borundum	ZrO ₂	Y ₂ O ₃																																											
102	40		15	60			1.5	1700°C- 2 hours	3.07																																								
124	64	12		24		2	1.5	1600°C- 16 hrs.	3.04																																								
127	70		7	30	10		1.5	1750°C- 2 hours	3.18																																								
128	66	24	10				1.6	1740°C- 1 hour	2.10																																								
128	66	24	10			72	20	1740°C- 1 hour	3.08 (b)																																								
129	88.7	8	3.3			72	21	1740°C- 1 hour	2.91																																								
130	94.5	4	1.5			72	20	1740°C- 1 hour	2.92																																								
<table> <tr> <td></td><td></td><td></td><td></td><td></td><td>SiO₂</td><td>MgO</td><td>CaO</td><td colspan="2"></td></tr> <tr> <td>128</td><td>64.0</td><td>26.0</td><td>8.3</td><td></td><td>0.9</td><td>0.6</td><td>0.1</td><td colspan="2">Correcting for Composition of</td></tr> <tr> <td>129</td><td>83.0</td><td>13.0</td><td>2.7</td><td></td><td>0.9</td><td>0.6</td><td>0.1</td><td colspan="2">Mill "Pick-up" after 22 hours</td></tr> <tr> <td>130</td><td>87.0</td><td>10.0</td><td>1.0</td><td></td><td>0.9</td><td>0.6</td><td>0.1</td><td colspan="2"></td></tr> </table>															SiO ₂	MgO	CaO			128	64.0	26.0	8.3		0.9	0.6	0.1	Correcting for Composition of		129	83.0	13.0	2.7		0.9	0.6	0.1	Mill "Pick-up" after 22 hours		130	87.0	10.0	1.0		0.9	0.6	0.1		
					SiO ₂	MgO	CaO																																										
128	64.0	26.0	8.3		0.9	0.6	0.1	Correcting for Composition of																																									
129	83.0	13.0	2.7		0.9	0.6	0.1	Mill "Pick-up" after 22 hours																																									
130	87.0	10.0	1.0		0.9	0.6	0.1																																										

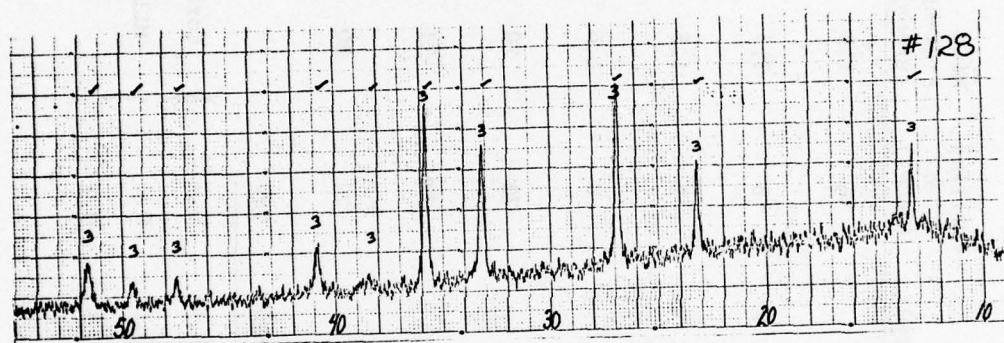
(a) Mineralized Al₂O₃

(b) Theoretical Density of this Composition (7)

(c) 100 gram batches

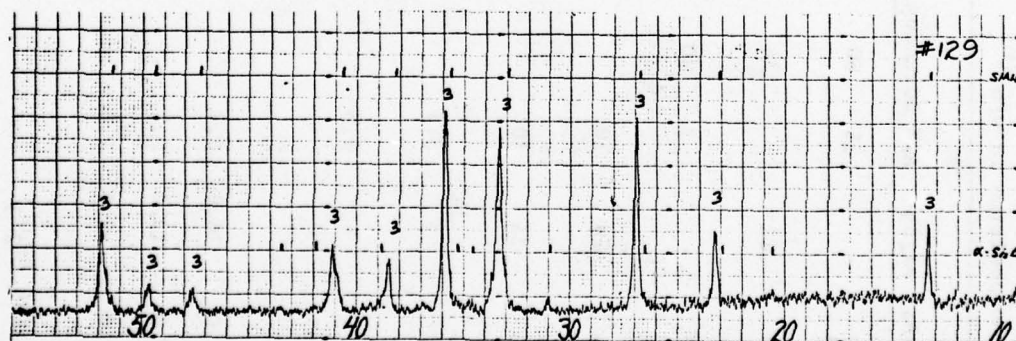


127



128

- CODE
1. α - Si_3N_4
 2. β - Si_3N_4
 3. β' - Sialon
 4. Al_2O_3
 5. γ Phase
 6. γ Phase
 7. MgAl_2O_4
 8. ZrO_2
 9. Mg_2O_3 - ZrO_2



129

Figure 34. X-ray diffractometer traces of Sialons #127, #128, #129 showing retained ZrO_2 (127), single-phased β' Sialon (128) and single-phase β' Sialon and α - Si_3N_4 (129).

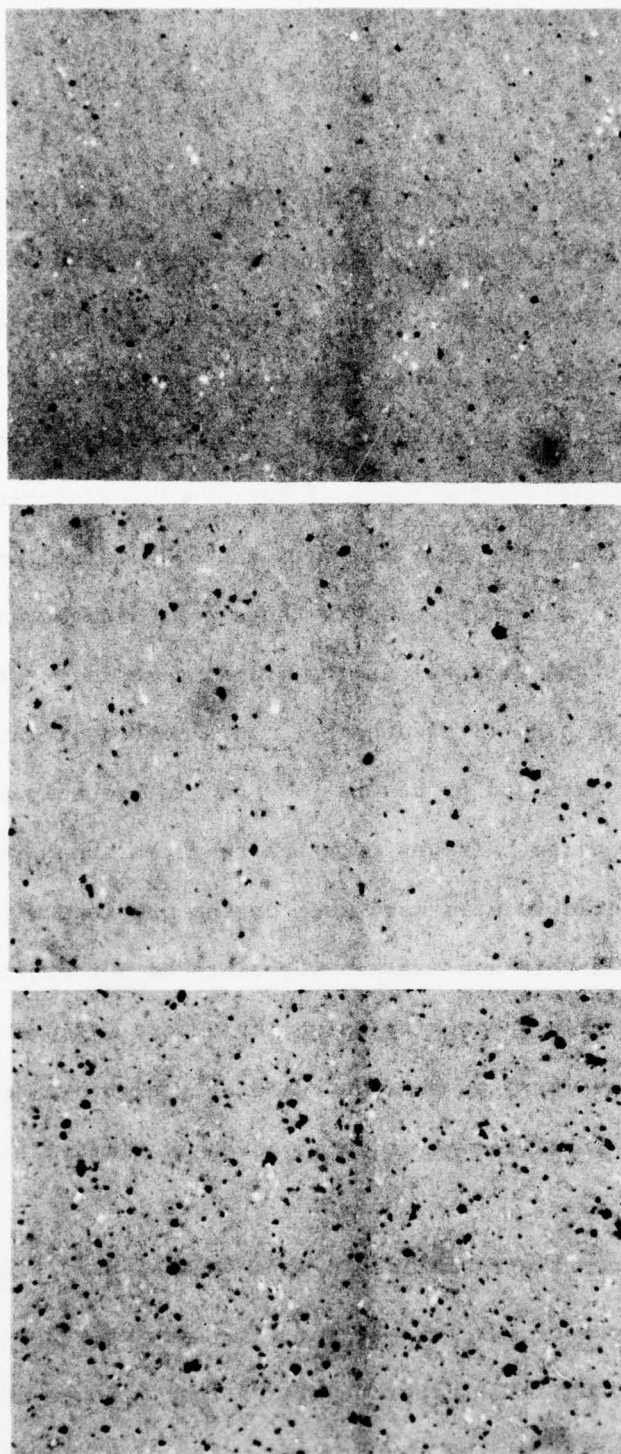


Figure 35. Photomicrographs of Sialons #128, #129, #130 showing increasing porosity with increasing Si_3N_4 content for identical firing procedures.

AD-A054 043

GENERAL ELECTRIC CO PHILADELPHIA PA SPACE DIV
METHODS OF FABRICATING CERAMIC MATERIALS.(U)
NOV 77 A GATTI, M J NOONE

F/G 11/2

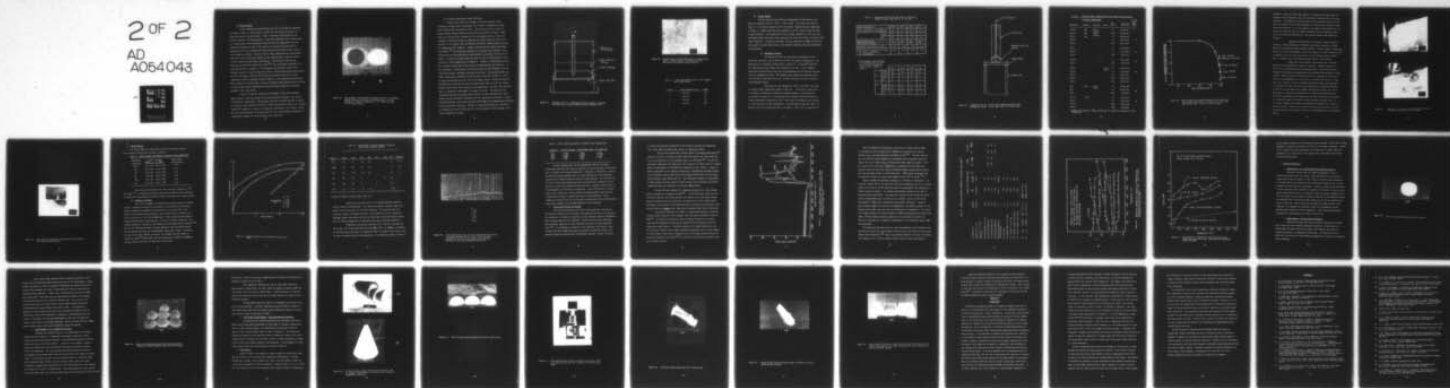
UNCLASSIFIED

AFML-TR-77-135

F33615-74-C-4073

NL

2 OF 2
AD
A054 043

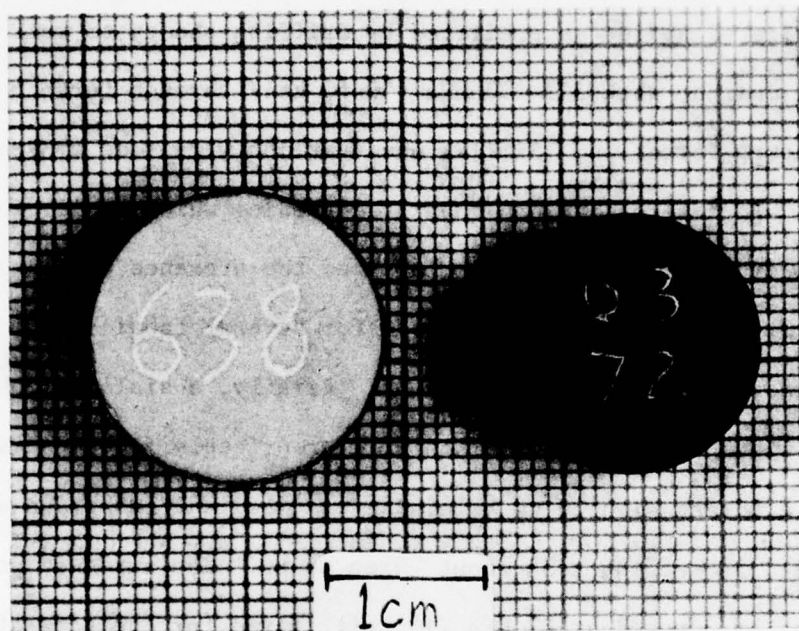


END
DATE
FILMED
6-78
DDC

(7) Milled Sialons

Sialon compositions studied using mill wear as an additive mechanism are shown in Table 11, while Figure 34 shows the x-ray traces and Figure 35 shows some typical microstructures. Table 11 includes firing schedules and sintered densities of these materials. Note that composition #127 contains ZrO_2 as a second phase, while composition #128 and #129 are single-phased sialons. Mineralized alumina was used as the means of introducing sintering aids in composition #127 while compositions #128, #129 and #130 relied on mill pick-up as the additive variable. The mill used in these compositions was polyurethane-lined with sialons balls and propanol as the grinding media. Material milled 72 hours readily achieved high fired density. This method of introducing sintering aids has been reported by others⁽²⁹⁾ and is probably unavoidable if a long milling time is required. It was apparent from the above results that excessive amounts of liquid formers were used in the previous mineralizing studies (in #102 for example) and this can explain why sintered structures of those compositions usually contained porosity formed by a pore agglomerating mechanism which allowed the sintered body to achieve reasonably high average density but also to retain large, widely dispersed pores which severely limited the achievable strength of the fired bodies.

Figure 36 shows the variation in shrinkage of body #128 processed under identical conditions except for milling time and, therefore, mill pick-up (overall milled composition). The material milled for 72 hours achieved a density of 3.08 gm/cc while material milled for 8 hours only reached a density of 2.10 gm/cc. Composition changes as a result of milling were restricted to two sources, sialon ball wear and hydrolysis of the Si_3N_4 and AlN. By far the largest contributor to compositional changes in the processing was the ball wear.



(A)

(B)

Figure 36. Photographs of #128 material showing variation in shrinkage during firing as a function of milling time, i.e. as a function of "actual" composition. A = 8 hours milling, B = 72 hours milling.

(a) Screening Experiments Using #128 Sialon

Defects which limit the strength of brittle materials can be introduced through several mechanisms, one of which is agglomerates which pass through normal processing screens. Initial practice was to pass all milled batches through 400 mesh screens which contained $37\text{ }\mu\text{m}$ holes. These holes can obviously pass contaminants of this diameter which can limit the strength of fabricated bodies as predicted by Griffith theory to well below the goals of the current work 333-400 MPa (50-60 ksi) through further reaction and exaggerated pore formation. Similar observations were made by Prochaska of GE-CR&DC ⁽³⁶⁾ who developed techniques of screening which achieved a more uniform particle size distribution and minimized the presence of flaws in SiC bodies. A similar screening system was used for several fabrications in this work and is shown schematically in Figure 37. Briefly, a sialon-alcohol slurry was continually wiped over a nylon screen of appropriately fine mesh size. In one experiment, a screen with $10\text{ }\mu\text{m}$ hole size was used and 100 grams of sialon #128 was processed; screening took about three hours. The screened powder was dried, isostatically pressed at 67 MPa (10 ksi), fired for one hour at 1775°C in N_2/H_2 and machined into test bars for strength studies. Figure 38 shows the microstructure resulting from this processing while Table 12 gives the results obtained from 4-point bend testing at room temperature. As can be seen from the data, no significant improvement in strength was noted. The material still contained random gross porosity which resulted from non-uniformities in green density and was considered responsible for the relatively low strength. As was speculated earlier, the porosity may have been formed by an agglomeration mechanism during liquid phase sintering. Removal of coarse particulates may, therefore, be necessary but was not sufficient for the achievement of high strength in the sialon compositions studies.

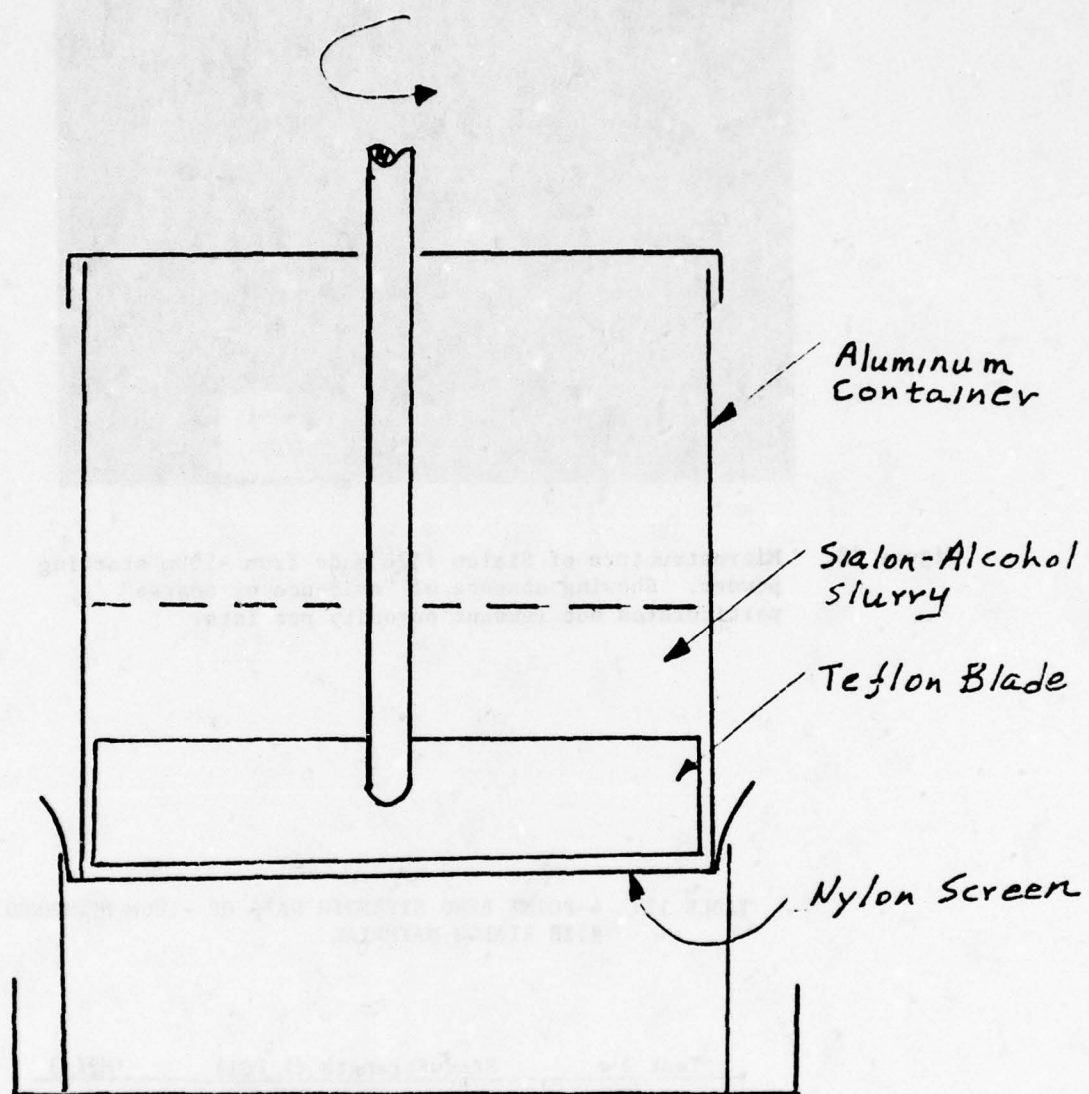


Figure 37. Schematic view of a screening apparatus capable of passing only particles of small diameter (after Prochaska (36)).

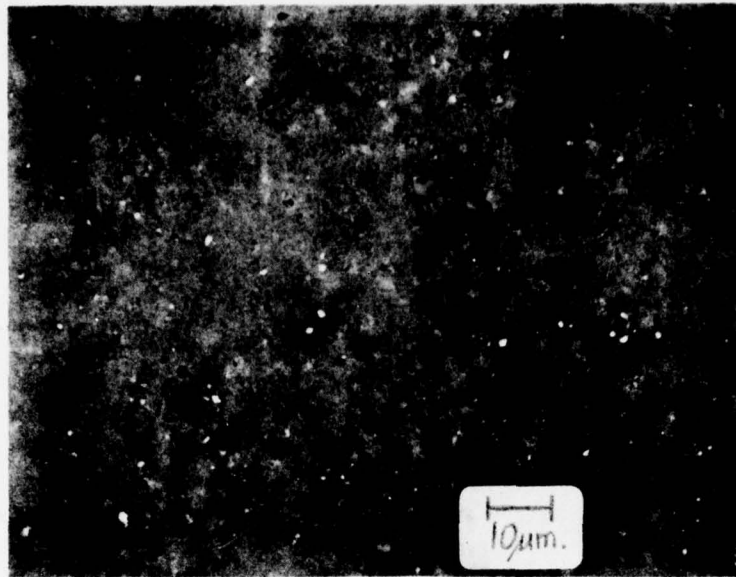


Figure 38. Microstructure of Sialon #128 made from $-10\mu\text{m}$ starting powder. Showing absence of "evidence of coarse" particulates but remnant porosity persists.

TABLE 12. 4-POINT BEND STRENGTH DATA OF $-10\mu\text{m}$ SCREENED #128 SIALON MATERIAL

Test #	Bend Strength (k PSI)	MP(a)
1	(38.350)	256
2	(47.765)	318
3	(45.090)	301
4	(41.930)	280

(b) Firing Studies

Further studies on the effects of atmosphere on fired density were made in cooperation with Dr. Peter L. Land of AFML. The results are shown in Table 13. The results obtained at GE from similar compositions were summarized in Table 11. Higher densities were achieved for all the sialons using the AFML firing techniques. The compositions fired in N_2/H_2 atmosphere (at GE) show less shrinkage during firing which would indicate that less liquid phase is present under these conditions. As noticed previously, the N_2 atmosphere (at AFML) could allow more liquid to exist during firing, thus markedly enhancing the sintering densification process.

(c) Mechanical Testing

The three-point bend test apparatus was modified so that four-point bend tests can be made at both room and elevated temperatures. The modification is described schematically in Figure 39. A Lucalox^(R) push-rod was fabricated with an inverse cone machined at one end. A 1/2" diameter Si_3N_4 ball bearing⁽³⁷⁾ was sliced into two hemispheres and one-half was machined into the configuration shown. The machined knife edges were suspended within the core with a platinum alloy wire. The ball seating in the cone provides a self-alignment feature.

Bend tests at room temperature, 1370 C, and 1400 C were made of various sialon compositions shown in Table 14. Data points using ratios of strength at temperature divided by average strength at room temperature are plotted in Figure 40. Yttria material and "unaged" 102-type material exhibits considerable weakening at 1370 C (some plastic deformation was observed in these materials at high temperature). Zirconia doped sialon and "aged" 102 material show only a modest decline in strength at 1370 C with no apparent de-

TABLE 13. COMPOSITIONS AND FINAL DENSITIES OF HIGH-Si₃N₄ CONTENT SIALONS FIRED BOTH BY GE AND AFML

Sample Designation		128-3	128-2	129-1	130
Green Composition in grams	Si ₃ N ₄	66	66	88.7	94.5
	Al ₂ O ₃	24	24	8.0	4
	AlN	10	10	3.3	1.5
Milling time hours		8	72	72	72
Mill pickup in grams		1.5	20	20	20
GE density for firing at 1740 C		2.10	3.08	2.91	2.92
AFML density in gm/cm ³ for firing at 1775 C in bottle N ₂ at 1 atmosphere.		2.30	3.10	3.10	2.96

The approximate green composition assuming the mill pickup to be 50 m/o Al₂O₃ and 50 m/o Si₃N₄. Weight in grams.

		123-3	128-2	129-1	130
w/o	Si ₃ N ₄	66	65	84	87
	Al ₂ O ₃	24	27	14	12
	AlN	10	8	3	1.3
m/o	Si ₃ N ₄	54	53	77	81
	Al ₂ O ₃	27	31	17	15
	AlN	19	16	6	4

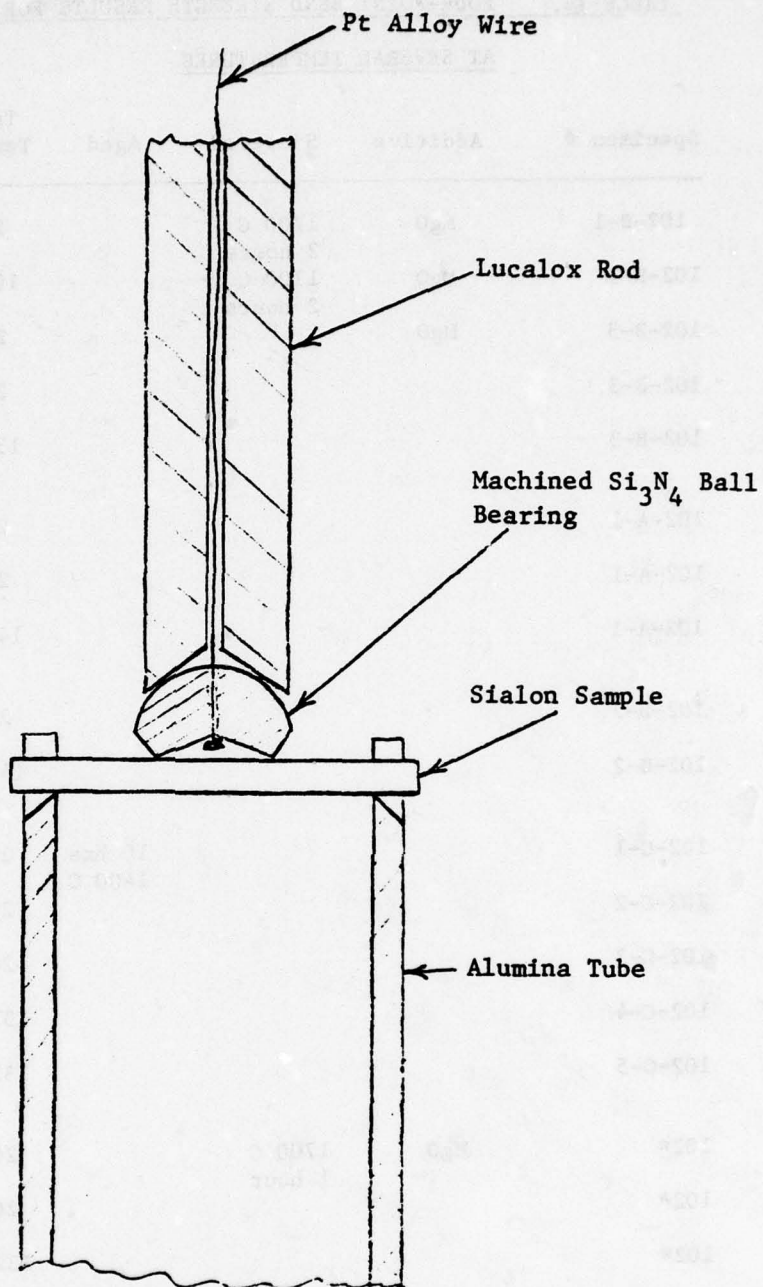


Figure 39. Schematic view of the four point bending apparatus used during this study. 15/16" outer span, 3/8" inner span.

**TABLE 14. FOUR-POINT BEND STRENGTH RESULTS FOR VARIOUS SIALON MATERIALS
AT SEVERAL TEMPERATURES**

Specimen #	Additive	Sintered	Aged	Test Temp °C	Max Stress MPa (psi)	Average Ratio: Test Room
102-B-1	MgO	1700 C 2 hours		20	202(30,300)	1
102-B-1	MgO	1700 C 2 hours		1000	244(36,600)	
102-B-3	MgO	"		20	228(34,200)	
102-B-3				20	225(33,700)	.78
102-B-3				1300	185(27,800)	
102-A-1				20	262(39,300)	
102-A-1				20	245(36,800)	.31
102-A-1				1400	78(11,700)	
102-B-2				20	227(34,090)	
102-B-2				1420	69(10,300)	.30
102-C-1			16 hrs 1400 C	20	265(39,700)	
102-C-2				20	252(37,800)	.65
102-C-3				20	240(36,000)	
102-C-4				1370	169(25,300)	
102-C-5				1370	158(23,700)	
102*	MgO	1700 C 1 hour		20	427(64,000)	
102*				20	301(45,200)	
102*				1370	72(10,800)	.20
114-A-1	Y ₂ O ₃			20	215(32,200)	
114-A-2				20	225(33,700)	.39
114-A-3				1370	92(13,760)	
114-A-4				1370	79(11,800)	

* Samples cold pressed at 333MPa (50,000 psi) all others cold pressed at 67 MPa (10,000 psi)

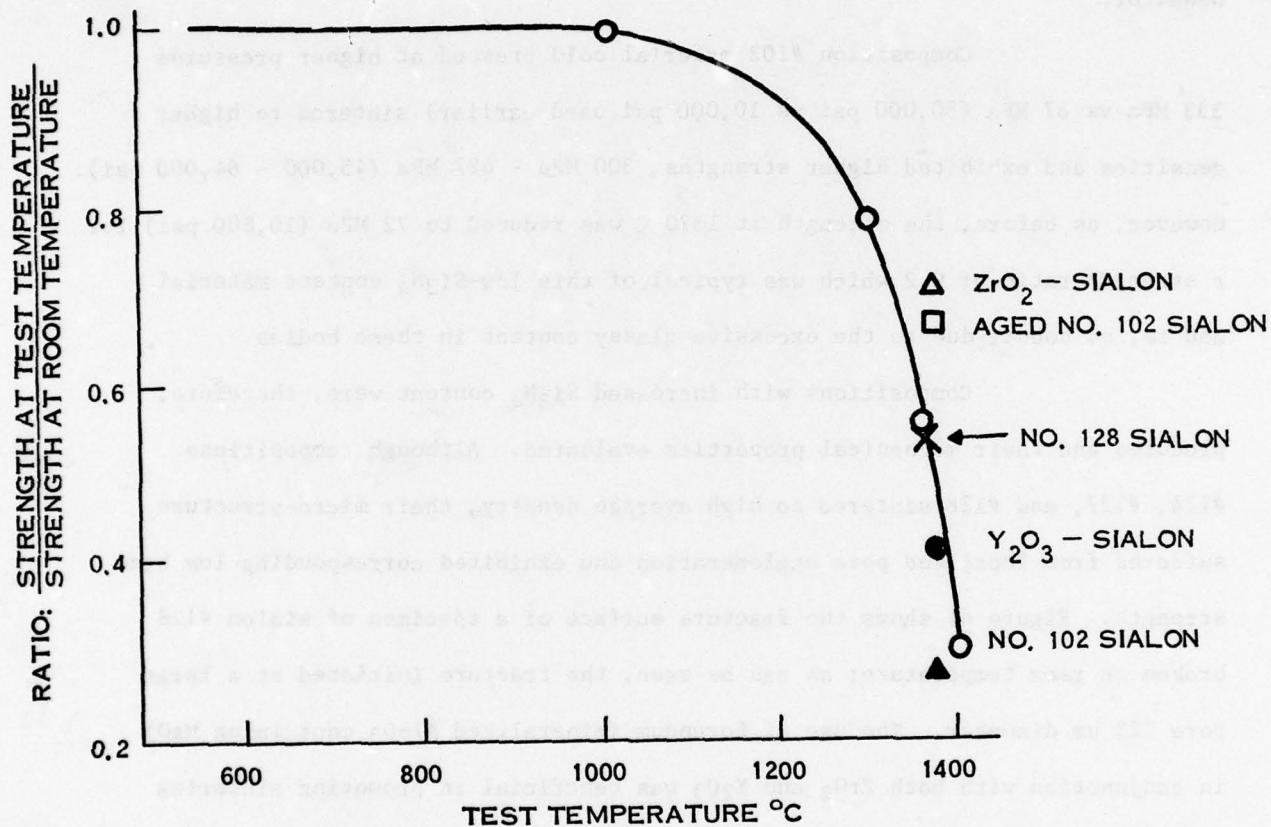


Figure 40. High temperature strength behavior of #102 Sialon with data on aged #102 materials, #128 Sialon and ZrO₂ and Y₂O₃ Sialons added. (All in 4-point bending).

formation. (Since the lower knife edges of the apparatus are Al_2O_3 , some deformation at high temperature may not be definitely correlated with the sialon specimen.) It appears that zirconia-sialon may be sufficiently refractory and free from "glassy" films at grain-boundaries to avoid plastic deformation under these test conditions. It is also apparent that aging of #102 material has also altered the nature of both the "glassy" boundaries and the crystalline structure of that material sufficiently to also exhibit improved high temperature behavior.

Composition #102 material cold pressed at higher pressures 333 MPa vs 67 MPa (50,000 psi vs 10,000 psi used earlier) sintered to higher densities and exhibited higher strengths, 300 MPa - 427 MPa (45,000 - 64,000 psi). However, as before, the strength at 1370 C was reduced to 72 MPa (10,800 psi) for a strength ratio of 0.2 which was typical of this low- Si_3N_4 content material and is, no doubt, due to the excessive glassy content in these bodies.

Compositions with increased Si_3N_4 content were, therefore, produced and their mechanical properties evaluated. Although compositions #124, #127, and #128 sintered to high average density, their micro-structure suffered from localized pore agglomeration and exhibited corresponding low bend strength. Figure 41 shows the fracture surface of a specimen of sialon #128 broken at room temperature; as can be seen, the fracture initiated at a large pore ~25 μm diameter. The use of Borundum (mineralized Al_2O_3 containing MgO) in conjunction with both ZrO_2 and Y_2O_3 was beneficial in promoting sintering of #127 but the high temperature strength improved only slightly over that of #102 material, indicating the persistence of a glassy grain boundary phase. The failure mechanisms at high temperatures was slow crack growth characterized by a significant amount of "plastic" strain occurring at constant load. If the load was removed, the specimen was permanently deformed and on occasion is partially cracked. Figure 42 is a typical fracture pattern showing an initial rough intergranular fracture path followed by smooth (predominantly transgranular) failure.

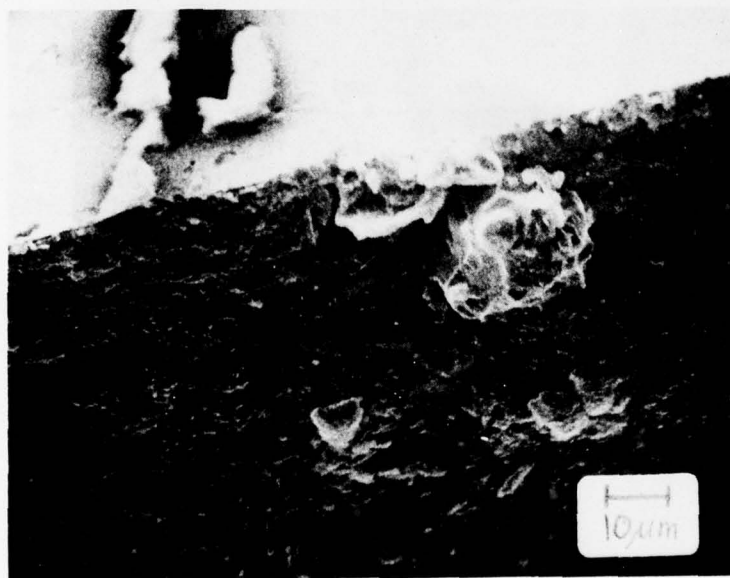


Figure 41. SEM images of a fracture area of #128 Sialon showing fracture initiation site at a large pore.

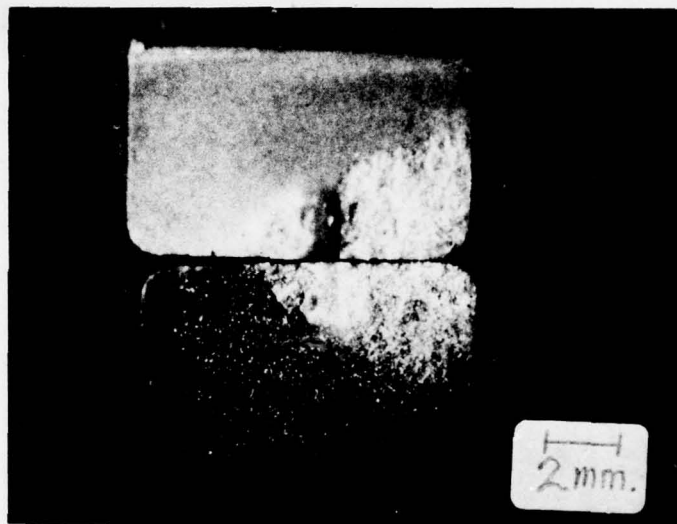


Figure 42. Fractograph of #128 Sialon showing typical evidence of slow crack growth behavior.

d. Young's Modulus

The Young's Modulus of some typical sialons were measured using a sonic resonance technique and are shown in Table 15.

TABLE 15. ELASTIC MODULUS AND DENSITY OF VARIOUS SIALON COMPOSITIONS

Composition	Elastic Modulus		Density gm/cc
	(MPa)	(PSI)	
SM-15	111×10^3	(33.3×10^6)	3.10
102	210×10^3	(31.6×10^6)	3.10
124	210×10^3	(31.6×10^6)	3.10
127	218×10^3	(32.8×10^6)	3.20
128	243×10^3	(36.4×10^6)	3.03
129	249×10^3	(37.4×10^6)	2.96

These values are consistent with those reported by Wills et al (38) and Lange (11) for pressureless sintered sialons and as expected show an increase in modulus with increasing silicon nitride content (and reduction in glass content).

(e) Oxidation of Sialons

Table 16 is a summary of the milled sialons which underwent oxidation testing. Specimens 2 mm thick by 16 mm square of each material were polished, measured, weighed and suspended by platinum wires in an alumina boat. Four samples of each material were included so that oxidation rates at 1400°C in air could be studied for 1, 10, 100 and 1000 hours. Some cycling tests were made to further survey oxidation characteristics. The data are shown in Figure 43. The oxidation behavior is similar to that exhibited by hot pressed silicon nitride (9,39). The data for #128 material shows a steeper dependence than the earlier sialons which contained less Si_3N_4 and correspondingly higher glass content. The reason for this is not clear, however, the result is consistent with the studies by Singhal and Lange (40) which showed that the weight gain of sialons was dependent on Al_2O_3 content and was in the same order as shown here.

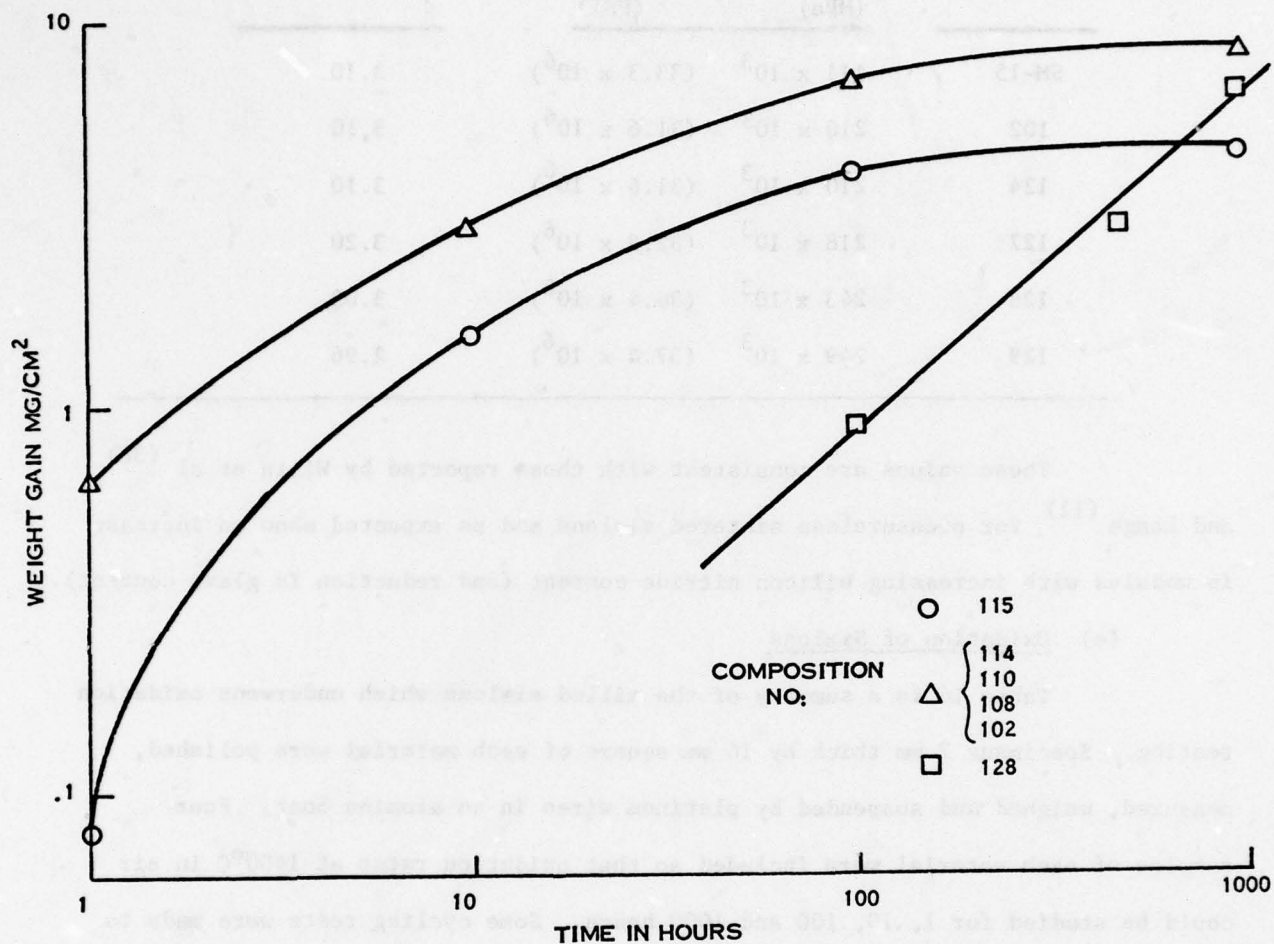


Figure 43. Oxidation behavior of Sialon materials in still air at 1400°C.

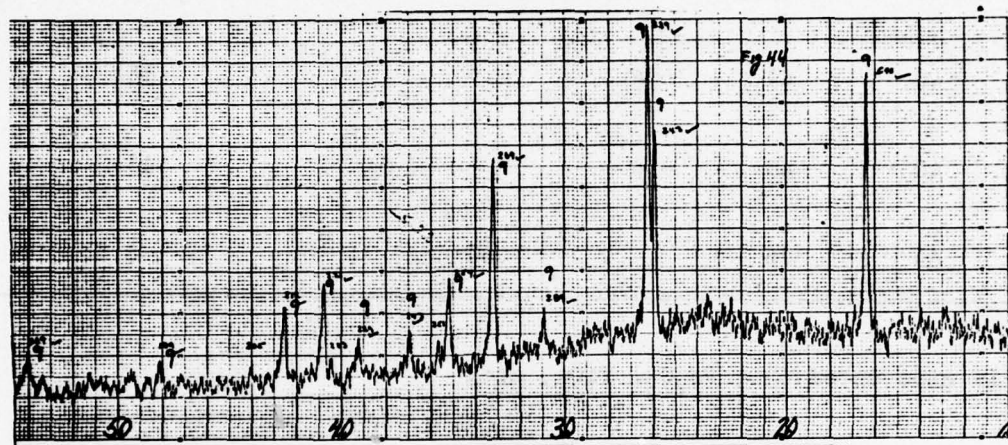
TABLE 16. COMPOSITION IN WEIGHT PERCENT OF SIALONS
USED DURING OXIDATION STUDIES

Sample #	Si ₃ N ₄	Al ₂ O ₃	SiO ₂	MgO	ZrO ₂	Y ₂ O ₃	AlN	Balance*
102	40	51	6.6	1.2			15	1.2
108A	40	48	9.0	1.8			15	1.2
110	40	49.9	6.6	3.0			15	.6
114	40	49	6			5	15	
115	40	49	6		5		15	
128	64	26	.9	.6			8.5	

* Balance is made up of CaO, Fe₂O₃, TiO₂, etc.

Figure 44 is an x-ray trace of the glassy-appearing oxidation product formed on #102 material. The coating was smooth, uniform, tightly adherent, and did not spall for this test condition. The data show that the oxidation product is primarily mullite. X-ray diffraction of all the milled specimens showed that mullite was the only detectable crystalline phase regardless of starting composition or additives under these oxidizing conditions.

Temperature cycling was conducted over a 100 hour time span for 100 cycles. The cycling apparatus and furnace (at 1400 C in air) were coordinated so that 20 minutes were spent at temperature with a 10 minute travel time in and out and a 20 minute hold at room temperature. The results are shown in Table 17.



- CODE
1. α - Si_3N_4
 2. β - Si_3N_4
 3. β' - Sialon
 4. Al_2O_3
 5. X Phase
 6. Y Phase
 7. HfAl_2O_4
 8. ZrO_2
 9. $3\text{Al}_2\text{O}_3 \cdot 2\text{SiO}_2$

Figure 44. X-ray diffraction trace of layer formed during oxidation of Sialons showing mullite as the only detectable crystalline phase but also evidence for amorphous material in the broad background distortion.

TABLE 17. CYCLIC OXIDATION BEHAVIOR OF SEVERAL SIALON COMPOSITIONS

Specimen #	Initial Wt (gms)	Final Weight (gms)	Wt Change (gm)
#102	1.0996	1.0081	-0.0915
#114	1.0012	0.8264	-0.1748
#115	0.8185	1.1078	+0.2893
#128	1.084	1.084	-0-

The data indicated that for the compositions richer in the glassy second phase (#102 and #114) there is evidence for loss by spalling of the coating due to a slight loss in weight perhaps due to formation of cristobalite. However, the mullite coatings remained intact for these compositions so that additional sialon was not oxidized during the 100 hour cycling exposure. The oxidation film of the #115 sialon (containing ZrO_2) which contained mullite apparently did not maintain its protective integrity and thus was able to oxidize further during the cycling exposure as indicated by a weight gain. Sialon #128 which has a greater Si_3N_4 content showed that a stable mullite-containing oxidation layer had been formed which was immune to damage under these cycling conditions. Visual examination indicated that all the coatings were unaffected by the cycling exposure and no gross changes in the coating appearance could be detected.

f. Electrical Properties of Sialons

The electrical properties of silicon nitride materials, specifically the dielectric constant and loss tangent, have generated interest in the material for construction of radomes for operation in high temperature erosive environments where alternate materials are inadequate. Reaction sintered Si_3N_4 , CVD- Si_3N_4 , and hot-pressed Si_3N_4 have all been considered as potential radome fabrication routes⁽⁴¹⁾. The advantages of sialons for this application are twofold. First, the ease with which radome shapes may be produced by conventional ceramic processing techniques and densified by pressureless sintering. Second, the ability

to tailor the electrical properties of the sialon by varying the composition over a wide range from high-Si₃N₄ content to high-Al₂O₃ content.

Work at GE has shown that sialons exhibit a pronounced Reststrahlen⁽⁴²⁾ reflection at about 10 microns in their reflection spectra but this reflection is not as pronounced as in hot-pressed Si₃N₄ or in CVD Si₃N₄⁽⁴²⁾. As with the electrical properties, the reflection can be tailored in amount, and to a certain degree in wavelength, by tailoring the composition of the sialon. Figure 45 shows a comparison of the specular reflectance of mechanically polished samples of two different sialons (#102 with 45 W/O Si₃N₄ and #129 with 83.0 W/O Si₃N₄) and hot-pressed Si₃N₄ (Norton NC-132). The reflectance maxima are proportional to Si₃N₄ content but also relate to other factors such as porosity and surface finish which were not identical in the three samples shown.

Sialon #102 was evaluated for comparison purposes in a laser thermal shock environment in a separate program⁽⁴³⁾. It was found that, under the test conditions employed, the sialon material was superior to all the glass-ceramic materials evaluated and was second only to fused silica in this thermal shock environment and retained its favorable dielectric properties and microwave transmission properties during severe temperature excursions under laser irradiation.

Dielectric properties of a number of Si₃N₄-based materials, including several sialons produced on this program, have been made by Westphal of MIT for AFML⁽⁴⁴⁾. The data were obtained on discs of material placed in a circular cross-section waveguide by measuring the phase shift and attenuation over the temperature range 20-800 C. Desirable properties for radome applications are low dielectric constant with a small temperature dependence and low loss tangent. In other studies, some relation between purity of the Si₃N₄ powder material and resultant properties was evident⁽⁴⁴⁾ but there are several other variables which may influence behavior.

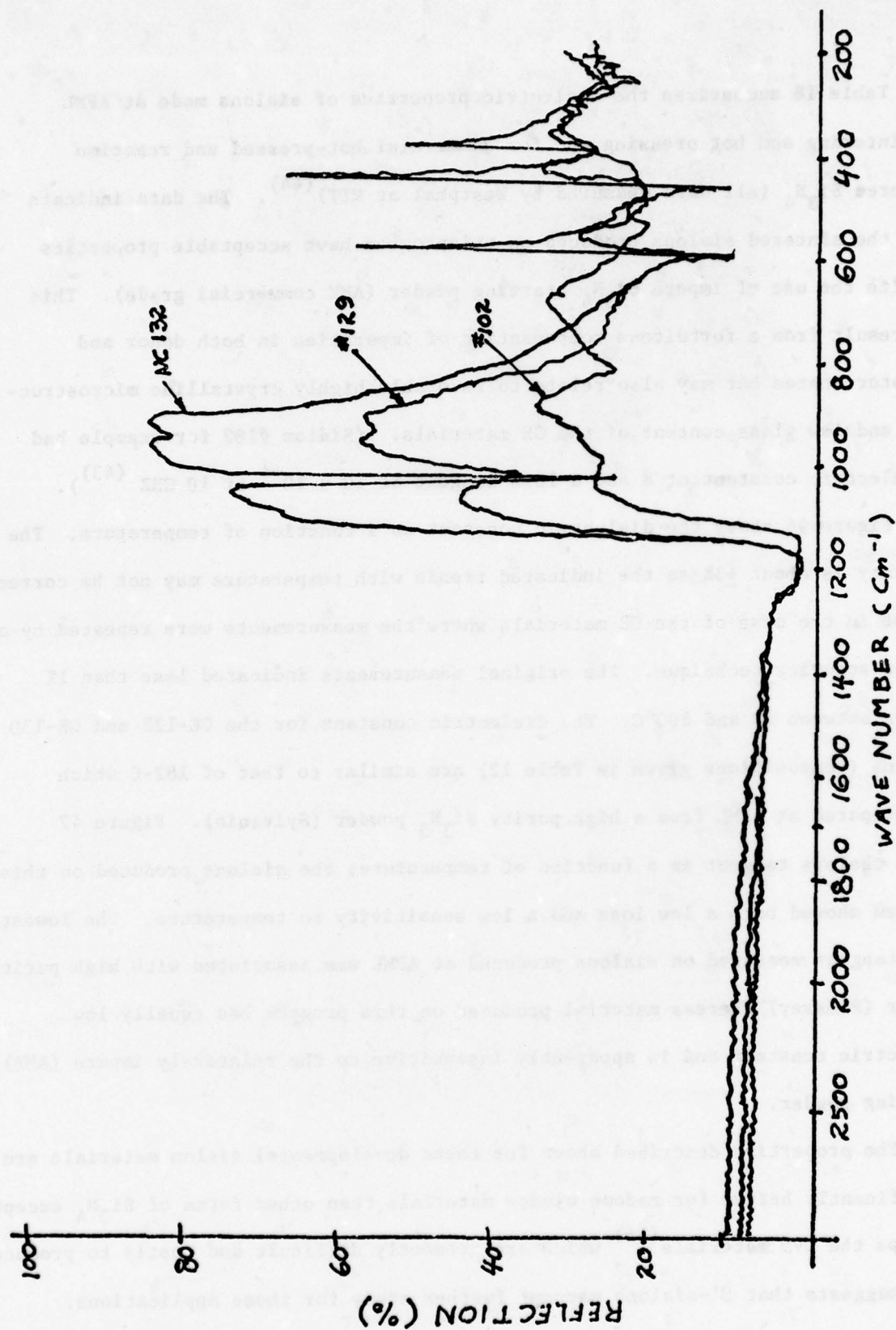


Figure 45. Comparison of specular reflectance of β - Si_3N_4 (NC132) with #102 and #129 Sialons. Showing reflectance peaks proportional to Si_3N_4 content.

Table 18 summarizes the dielectric properties of sialons made at AFML by sintering and hot pressing and for commercial hot-pressed and reaction sintered Si_3N_4 (all data measured by Westphal at MIT)⁽⁴⁴⁾. The data indicate that the sintered sialons produced on this program have acceptable properties despite the use of impure Si_3N_4 starting powder (AME commercial grade). This may result from a fortuitous compensation of impurities in both donor and acceptor states but may also relate to favorable highly crystalline microstructure and low glass content of the GE materials. (Sialon #102 for example had a dielectric constant of 8 and a loss tangent of 10×10^{-4} at 10 GHz⁽⁴³⁾).

Figure 46 shows the dielectric constant as a function of temperature. The accuracy is about $\pm 3\%$ so the indicated trends with temperature may not be correct except in the case of the GE materials where the measurements were repeated by a higher accuracy technique. The original measurements indicated less than 1% change between 20 and 800°C. The dielectric constant for the GE-128 and GE-130 sialons (compositions given in Table 12) are similar to that of 182-C which was prepared at AFML from a high purity Si_3N_3 powder (Sylvania). Figure 47 shows the loss tangent as a function of temperature: the sialons produced on this program showed both a low loss and a low sensitivity to temperature. The lowest loss tangent measured on sialons produced at AFML was associated with high purity powder (Plessey) whereas material produced on this program has equally low dielectric constant and is apparently insensitive to the relatively impure (AME) starting powder.

The properties described above for these developmental sialon materials are significantly better for radome window materials than other forms of Si_3N_4 except perhaps the CVD materials⁽⁴⁵⁾ which are presently difficult and costly to produce. This suggests that β' -sialons warrant further study for these applications.

TABLE 18. SUMMARY OF DIELECTRIC PROPERTIES OF SIALONS (AFTER LAND⁽⁴³⁾)

20 Samples HP	(gm/cm ³)	ϵ'	$\tan \delta \times 10^4$	ϵ'	$\tan \delta$	ϵ'	$\tan \delta$
SIALON up to 5 m/o	2.99-3.14	7.40-8.12	9-44				
AlN, 21% J, or 4 m/o Silicon							
Sintered SIALON, 5 w/o Si	2.90	7.42	47				
GE Sintered SIALON 128	3.10	7.67	34	7.65	31	7.62	22
GE Sintered SIALON 129	3.10	7.67	20	7.57	26	7.77	19
GE Sintered SIALON 130	2.99	7.45	19	-	-	7.35	14
Norton NC-350 Reaction Sintered Si ₃ N ₄	2.4	5.7-6.0	120-146				
NC 132 Si ₃ N ₄	3.2	8.39	39				
Hot Pressed AME + 4 w/o CeO ₂	3.14	8.45	41				
H.P. Plessey + 5 w/o CeO ₂	3.3	8.81	33				
H.P. Ventron (Alpha) 5 w/o CeO ₂	3.19	9.24	118				
H.P. Ventron (Alpha) 5 w/o Y ₂ O ₃	3.20	10.47	370				
GE 128 25-800°C	$\epsilon' = 7.6 - 8.2$	$\tan \delta = 15 \text{ to } 25$					
GE 130 25-800°C	$\epsilon' = 7.35 - 7.8$	$\tan \delta = 15 \text{ to } 25$					

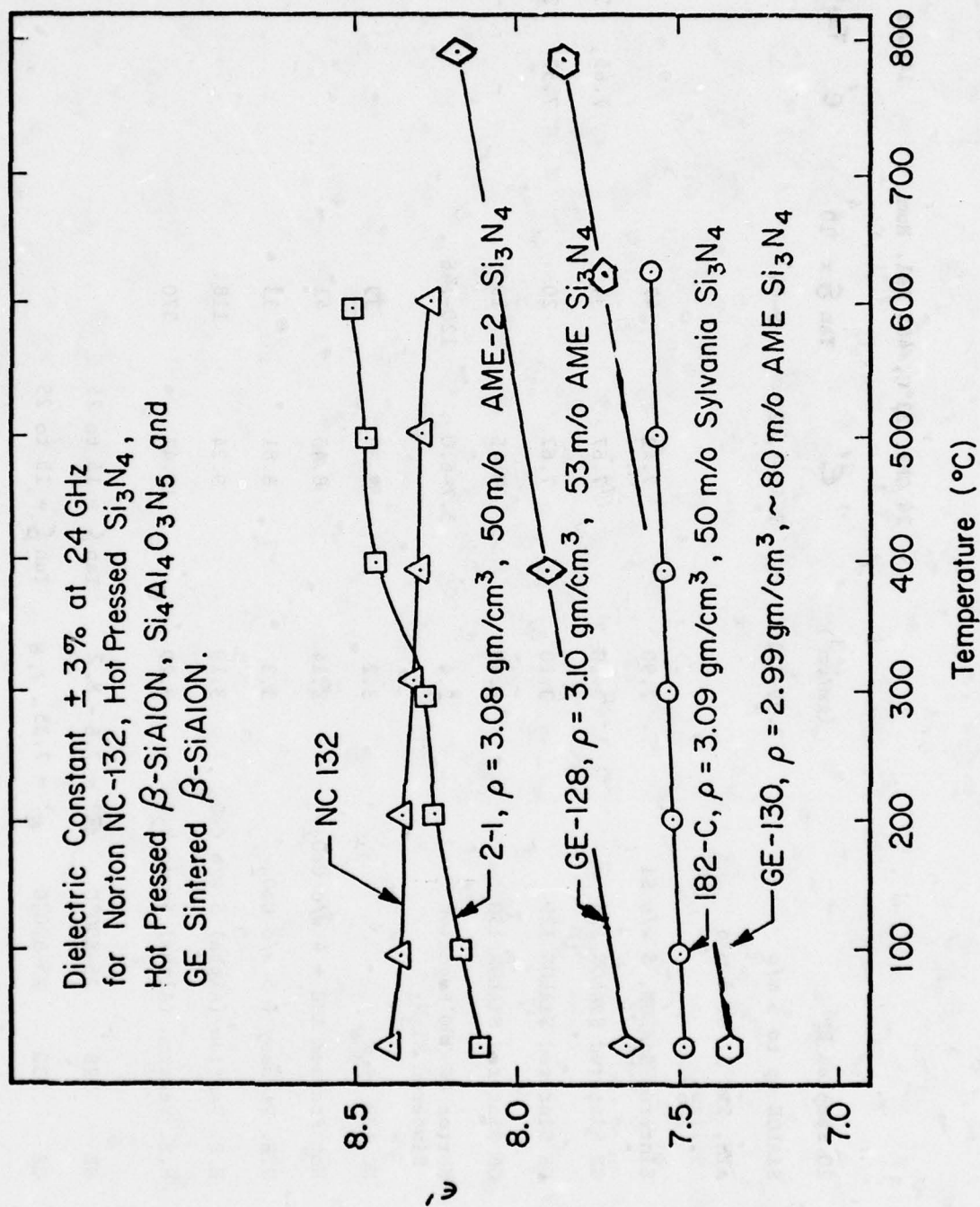


Figure 46. Dielectric constant as a function of temperature for several Sialons and hot-pressed Si_3N_4 (data obtained by Westphal at MIT for AFML).

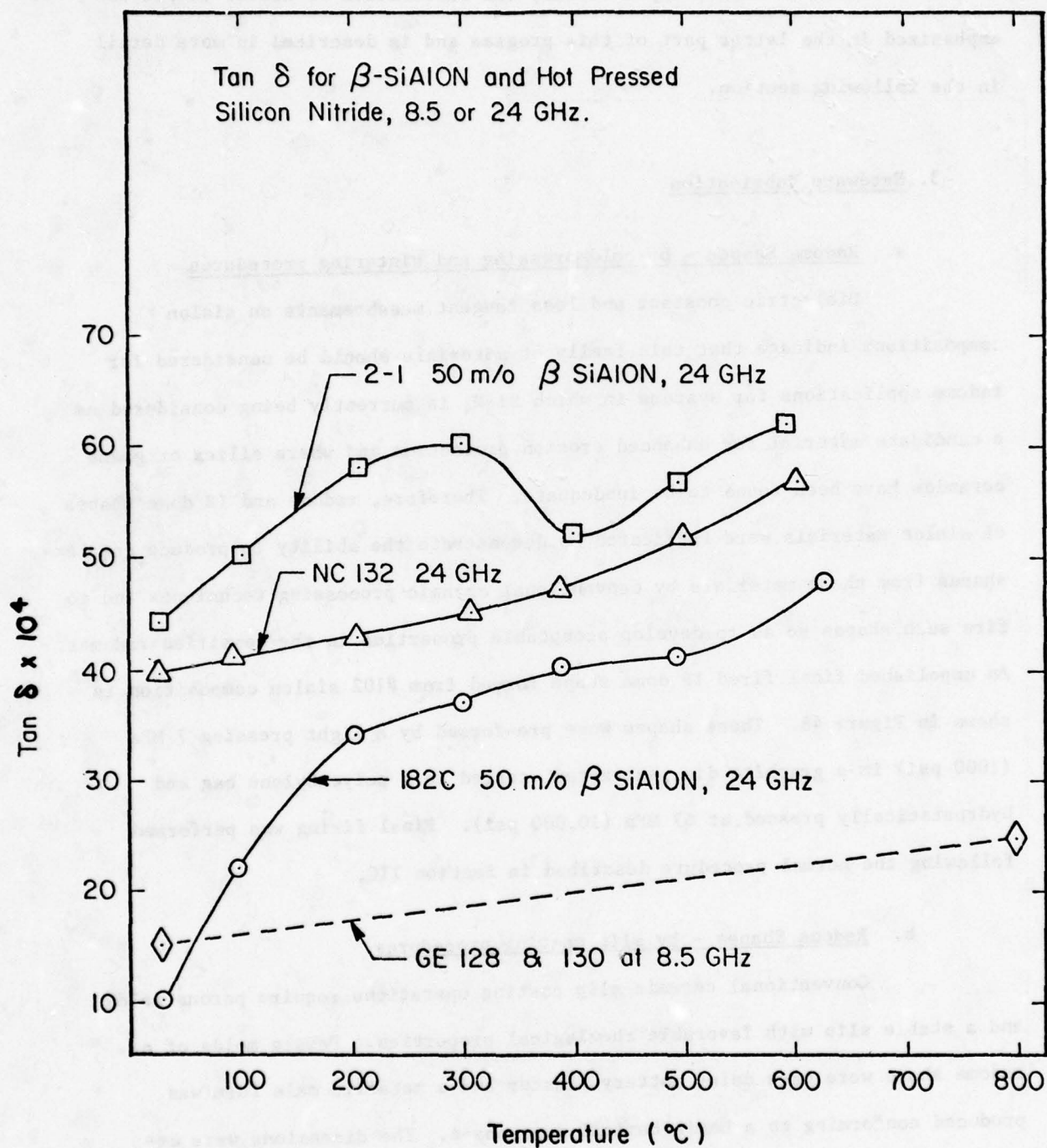


Figure 47. Loss tangent as a function of temperature for several Sialons and hot-pressed Si_3N_4 (data obtained by Westphal of MIT for AFML).

Several samples produced on this program are being evaluated at AFML under on-going programs to determine the potential of sialons in the radome environment. Because of this interest in radome applications, the fabrication of radome shapes was emphasized in the latter part of this program and is described in more detail in the following section.

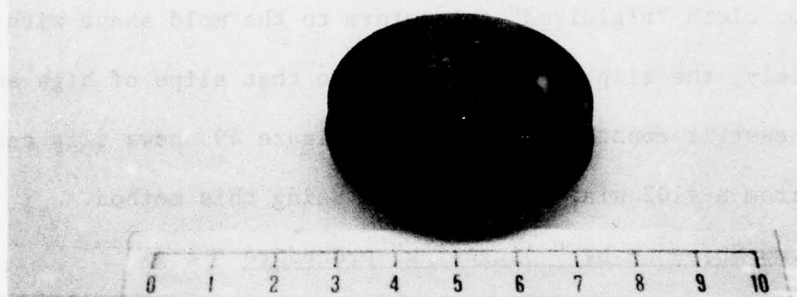
3. Hardware Fabrication

a. Radome Shapes - by cold-pressing and sintering procedures

Dielectric constant and loss tangent measurements on sialon compositions indicate that this family of materials should be considered for radome applications for systems in which Si_3N_4 is currently being considered as a candidate material for enhanced erosion protection and where silica or glass ceramics have been found to be inadequate. Therefore, radome and IR dome shapes of sialon materials were fabricated to demonstrate the ability to produce complex shapes from these materials by conventional ceramic processing techniques and to fire such shapes so as to develop acceptable properties in the densified radomes. An unpolished final fired IR dome shape formed from #102 sialon composition is shown in Figure 48. These shapes were pre-formed by a light pressing 7 MPa (1000 psi) in a graphite die, extracted, sealed in a polyethylene bag and hydrostatically pressed at 67 MPa (10,000 psi). Final firing was performed following the normal procedure described in Section IIC.

b. Radome Shapes - by slip casting procedures

Conventional ceramic slip casting operations require porous molds and a stable slip with favorable rheological properties. Female molds of a radome shape were made using pottery plaster and a metallic male form was produced conforming to a hemispherical dome shape. The dimensions were expanded 20% over those of an "actual" radome configuration to account for shrinkage during sintering.



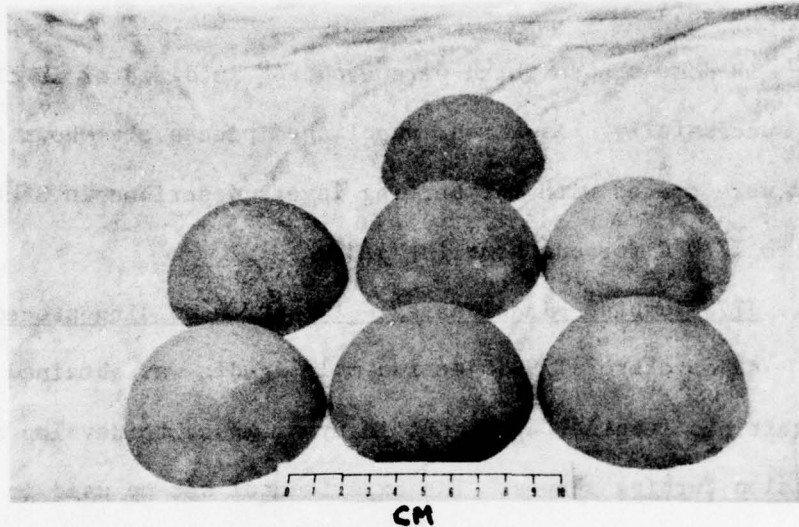
CM

Figure 48. As-Fired IR dome shape made from #102 sialon

Since sialon powder mixtures react in aqueous solutions, a non-aqueous slip was developed using isopropyl alcohol as the liquid media. Orange shellac was found to be both an excellent defloculant and binder for the slip and was used throughout the study (5 gms shellac per 100 ml alcohol was the standard mixture employed). Stable slips containing 50% by volume of solids were easily made. Some difficulty was experienced in removal of the shapes from the molds despite use of various "parting" aids. Also, slips of low viscosity (and thus low volume fraction sialon powder) shrank excessively during drying and produced shapes with radial cracks. The problems of separation of the casting from the mold were overcome by forming a liner of double-knit cotton cloth "rigidized" to conform to the mold shape with corn starch. Fortunately, the slip was thixotropic so that slips of high solid content could be cast if constantly agitated. Figure 49 shows slip cast radome shapes produced from a #102 sialon composition using this method.

c. Radome Shapes - by "jigging" procedure

Although slip casting proved to be a viable method for forming radome shapes the prospect of "jigging" these shapes using very viscous (clay-like) mixes also appeared feasible. Shellac/alcohol mixtures of 200 gm/1000 ml were used as the basic vehicle. A ratio of 3:1 by weight of sialon powder mix kneaded with the shellac/alcohol mix made an excellent workable "clay" for "jigging". The slip casting mold lined with cloth was used as the forming die and another male form also covered with cloth formed the inside cavity. The procedure was then to place the lined mold on a vibrating table, add the kneaded sialon "clay", start the vibrator table, insert the cavity forming die, jigging the shape while the "clay" was thixotropic, then stopping the vibrator to "freeze" the radome shape. The inside mandrel was then removed and as the shape dried, the cloth was peeled away from the shape and lifted from the



**Figure 49. Slip cast radome shapes made from Sialon materials.
(Shown after binder removal ready for final firing).**

mold cavity. After air drying the radome shape for 48 hours, the shellac was removed by burning in air at 400 C.

The "jiggering" technique was used to make larger radar dome shapes shown in Figure 50(a): the metal forms for making the plaster molds and cotton mold liners are shown in Figure 50(b). Various sections cut from the apex of this shape were fired since the full-sized dome was too large for the available furnaces.

IR dome shapes which were about 4" in diameter in the green state were fired successfully. As-fired, unpolished pieces are shown in Figure 51. These domes were coated with the parting layers described in Section II-C and were fired to 1770 C for one hour in N_2/H_2 .

d. JT79 Turbine Blade Shapes - Injection molding procedures

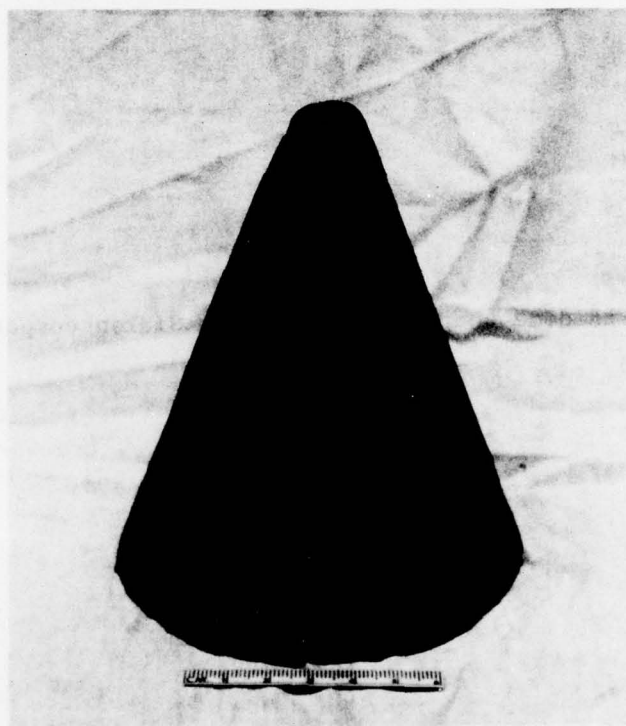
An obsolete JT79 injection molding die was obtained from the GE Small Aircraft Gas Turbine Department in Lynn, Mass. to develop a molding process for sialon turbine shapes. The experimental set-up used is shown in Figure 52 and a typical molded shape is shown in Figure 53. The sialon-wax mixture was loaded into the upper mold shown in Figure 52, heated to 65 C and injected within 2 seconds into the lower cold die. Shapes containing 55 volume percent sialon were readily formed by this procedure. A fired sample of a #102 sialon blade (minus the shroud portion) is shown in Figure 54.

4. Deliverables

Figure 55 shows fired samples of sialon composition #128 on the right and two of #129 on the left which were originally hydropressed to ~400 MPa (60,000 psi) by AFML. These samples were fired at GE and shipped to AFML for cutting into specimens for further evaluation. Similar slabs 1.5" x 1.5" x 1/8", 1/4", and 3/8" thick (8 of each thickness) were shipped to AFML for evaluation.



(a)



(b)

Figure 50. (a) Metal forms, plaster mold and cotton liners used to "jigger" radome shapes, (b) radome shape formed by "jiggering" technique.

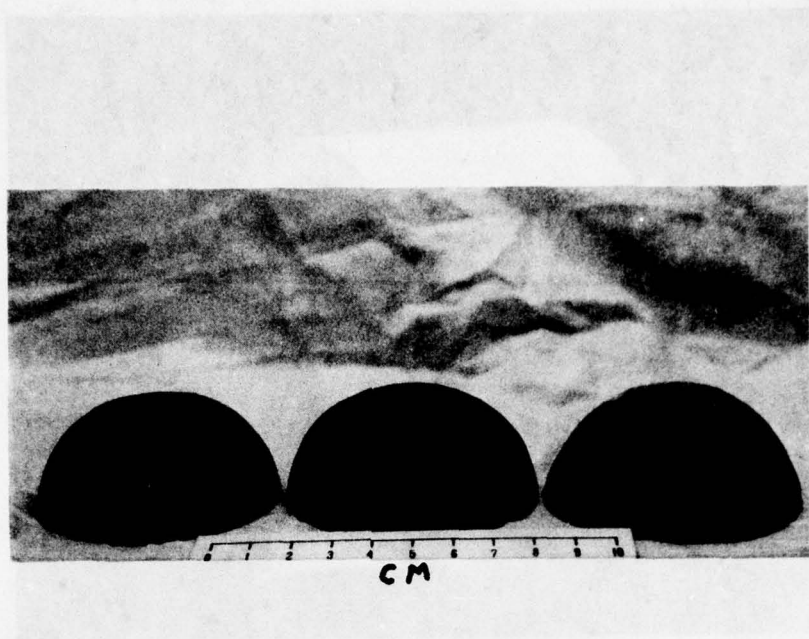


Figure 51. Fired IR dome shapes produced from Sialon compositions.

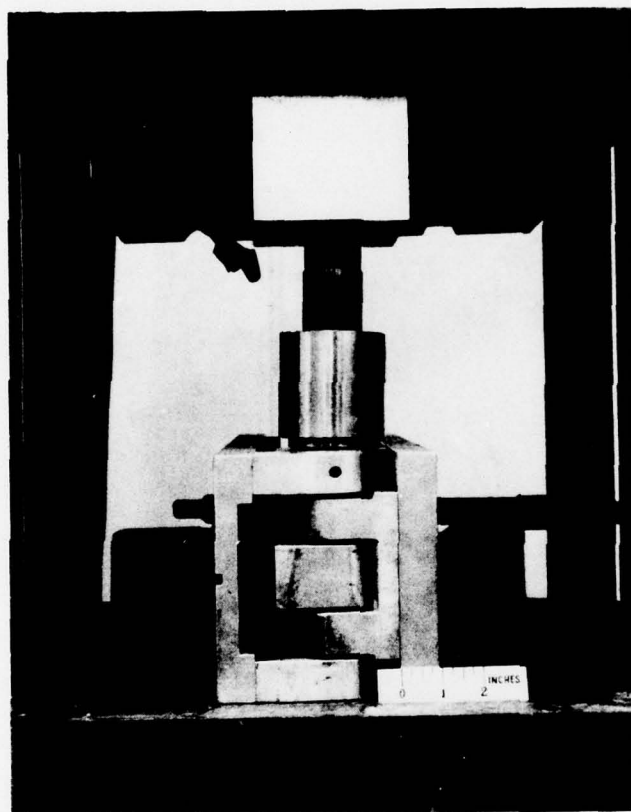


Figure 52. Photograph showing material container positioned ready for injection into mold for formation of turbine blade shape.

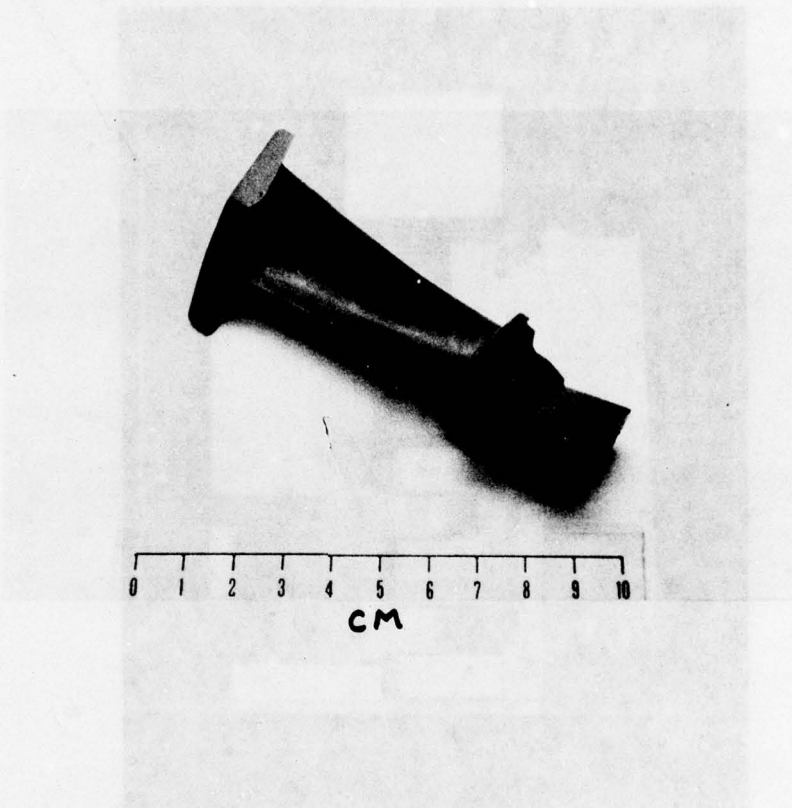


Figure 53. Injection molded Sialon-wax JT79 turbine blade.

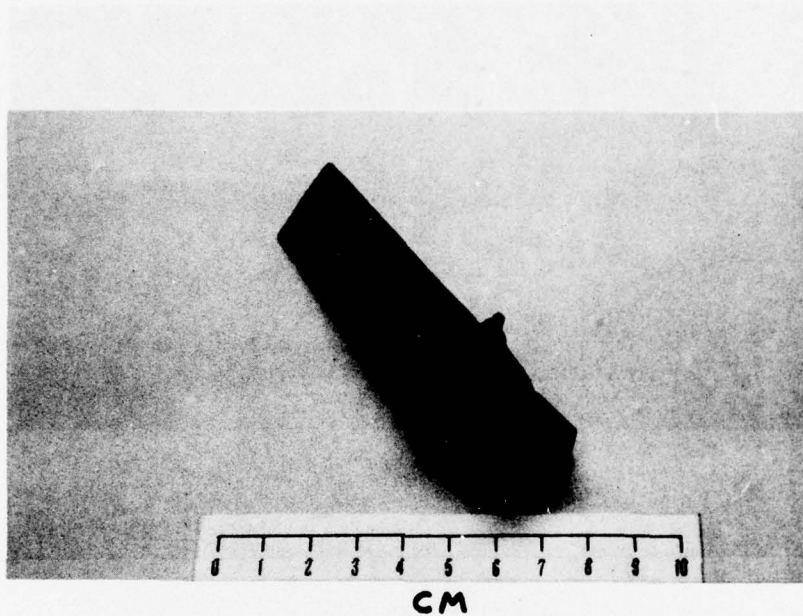


Figure 54. A Sialon JT79 blade after firing to 1700°C for 2 hours (minus shroud portion).

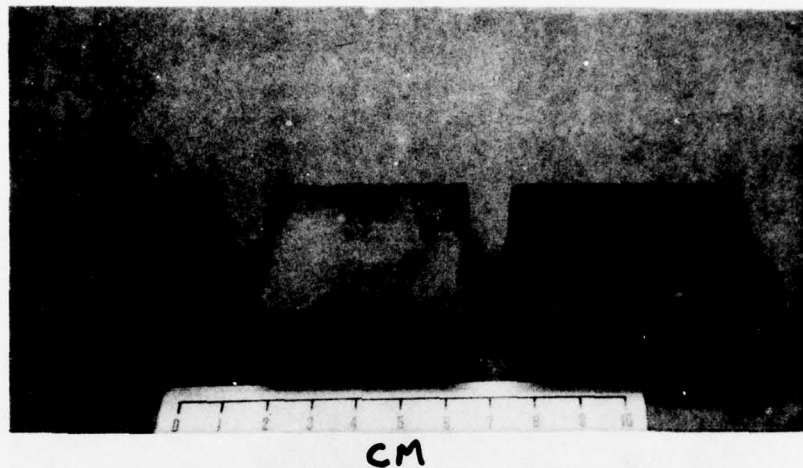


Figure 55. Fired Sialon #128 body on right and two Sialon #129 bodies on left before machining into flat plate specimens for laser irradiation and rain erosion testing.

Additional specimens produced on this program have been shipped to GE Aircraft Engine Group and to GE Gas Turbine Department for evaluations in on-going programs to evaluate ceramics in corrosive and erosive environments where ceramics show potential for application in advanced gas turbines. Also a series of cubes have been prepared for fabrication of balls for evaluation in a ceramic bearing⁽⁴⁶⁾. Evaluation of these and other specimens are continuing and will be reported elsewhere on other relevant programs.

SECTION IV

CONCLUSIONS

Preliminary experiments pointed to an important parameter which was referred to as mineralization and which appears to be an important mechanism in the effective sintering of sialon compositions. As was shown, mineralization could be accomplished by many paths including pre-reaction of sialon compositions by pre-firing and/or firing and regrinding; by comminution of separate elements of a composition and picking up mineralized material in each through contamination; and by contamination of the mixture through hydrolization of AlN and Si_3N_4 constituents while simultaneously adding mineralized contaminants from mill wear. It was difficult to separate these processes and, therefore, it was difficult to gain complete control of their effect on the sialon processing. However, an appreciation that such processing variables exist and a knowledge of their magnitude was employed to manipulate their influences on the ultimate batch composition and was utilized to achieve high densities in sintered sialon bodies. It was also apparent that if contamination were not completely controlled, then the role of "sintering aids" could not be correctly interpreted since these studies showed that very small amounts of mineralized MgO can be extremely effective even for sialons of high Si_3N_4 concentration when the mixes are highly milled (and presumably considerably hydrolized). It is further apparent that strict adherence to "phase diagram" composition is

virtually impossible without awareness of these influences, and the direction in which they all, separately and collectively, can move the assumed composition toward the eventual fired composition. For example, the addition of AlN to sialon compositions retards sintering unless the sintering aid is mineralized and/or the AlN particles become sufficiently hydrolized to delay their "adverse" reaction of liquid elimination during the initial phases of sintering. It has been shown that pressureless consolidation of Si_3N_4 systems is difficult and perhaps not possible without a liquid phase so that reactions which restrict liquid formation must be retarded (at least in the initial stages of sintering in order to permit the material to densify). The Si_3N_4 system is further complicated by the instability of Si_3N_4 at the high temperatures where rapid densification is possible. At these temperatures a significant dissociation pressure of nitrogen exists which can be aggravated by surrounding liquid reactants. This can lead to significant material loss during sintering, excessive bubble formation, or the random presence of large pores which tend to limit the strength of fired specimens. Techniques were developed to minimize these effects by coating the specimens during firing with layers of Al_2O_3 and combinations of Si_3N_4 , Al_2O_3 and AlN and then firing the coated specimens loosely packed in sialon-type coarse-grain powder materials in a N_2/H_2 atmosphere.

The very mechanisms which allow the attainment of high density in Si_3N_4 systems also affects the high temperature behavior of the products and most of these materials suffer from excessive creep at temperatures above 1200 C because of the viscous behavior of residual glassy second phases. The ability to minimize the influence of these unfavorable second phases by aging treatments (to encourage crystallization) and/or reduction of quantity by incorporation into the fired sialon structure was the primary goal of this program.

The elimination of the liquid phase at high temperatures has recently been termed "Transient Liquid Phase" sintering by Layden⁽¹⁰⁾ and has been employed in similar sialon studies to produce dense specimens under controlled small-scale conditions.

The properties of the sialon compositions fabricated during the program were comparable to those in the literature and reported in similar programs in terms of thermal expansion, oxidation resistance, strength and modulus. Exceptionally high strength was not consistently achieved. However, it is to be noted that the primary goal of this program was to develop processing techniques for sialon materials which could lead to their use in practical large-scale operations. Thus, mechanical properties were measured on bulk samples suitable for the fabrication of sizeable articles and were not in individually fabricated small test bars. Further work is required to refine the processing to reduce random porosity which was the predominate strength-limiting flaw observed during this work.

Ceramic processing techniques were developed which were based on conventional ceramic technology and were of sufficient scale to fabricate examples of radomes and IR-domes and turbine blade shapes without regard to starting powder or material suppliers resources. Further, no size limitations were encountered other than those imposed by available hydropressing facilities and furnace chamber capacity. Specimens suitable for further evaluations of rain erosion, radar response, reflectivity, hot corrosion, etc. were readily fabricated and are the subject of on-going test programs.

REFERENCES

1. K. H. Jack and W. I. Wilson, "Ceramics Based on the Si-Al-O-N and Related Systems," *Nature Phys. Sci.* 238, 28-9 (1972).
2. A Correspondent, "Ceramics Based on Silicon Nitride," *Nature* 238, (No 5360), 128-9 (1972).
3. K. H. Jack, "Nitrogen Ceramics," *Trans. and J. Brit. Ceram. Soc.* 72, 376-84 (1973).
4. Y. Oyama and O. Kamigaito, "Solid Solubility of Some Oxides in Si_3N_4 ," *Japan J. Appl. Phys.* 10, 1637 (1971).
5. Y. Oyama, "Solid Solution in the Ternary System Si_3N_4 -AlN- Al_2O_3 ," *Japan J. Appl. Phys.* 11, 760-1 (1972).
6. Y. Oyama, "Solid Solution in the System Si_3N_4 -AlN- Al_2O_3 ," *Yogyo-Kyokai-Shi* 82, No. 7, 352-7 (1974).
7. W. J. Arrol, "The Sialons-Properties and Fabrication," 729-38 in "Ceramics for High Performance Applications," Eds. J.J. Burke, A. E. Gorum, and R. N. Katz, Brook Hill Pub. Co. (1974).
8. R. J. Lumby, B. North, and A. J. Taylor, "Chemistry and Creep of Sialons," 283-98, in *Special Ceramics 6*, Edited by P. Popper, The British Ceramic Research Association (1974).
9. F. F. Lange, "Fabrication and Properties of Silicon Compounds," Final Report on Contract N00019-73-C-0208, Feb. 1974.
10. G. K. Layden, "Process Development for Pressureless Singering of Sialon Ceramic Components," Final Report on Contract N00019-75-C-0232, Feb. 1976.
11. G. K. Layden, "Development of Sialon Materials," Quarterly Progress Reports on Contract NA53-19712, June 1975 to date.
12. P. L. Land, J. M. Wimmer, R. W. Burns and N. S. Choudhury, "Compounds and Properties of the Si-Al-O-N System," AFML-TR-209 (1976). (A paper based on this report is to be published in *J. Am. Ceramic Society*.)
13. R. J. Lumby, B. North, and A. J. Taylor, "Properties of Sintered Sialons for Some Applications in Metal Handling and Cutting" in "Ceramics for High Performance Applications-II," Proceedings of the Fifth Army Materials Technology Conference, Newport, R.I., March 1977 (to be published).
14. A. Tsuge, H. Inoue, and K. Komeya, Paper presented to the Japanese Ceramic Society, January 28, 1972, (also, Tenth Symposium on Basic Ceramics, Osaka, 1972).
15. L. J. Gauckler, H. L. Lukas, and G. Petzow, "Contribution to the Phase Diagram Si_2N_3 -AlN- Al_2O_3 - SiO_2 ," *J. Am. Ceram. Soc.*, 58, Nos. 7-8, 346-7 (1975).

16. K. H. Jack, "Review: Sialons and Related Nitrogen Ceramics," J. Matls, Sci., 11, 1135-1158, (1976).
17. I. C. Huseby, H. L. Lukas, and G. Petzow, "Phase Equilibria in the System Si_3N_4 - SiO_2 - BeO - Be_3N_2 ," J. Am. Ceram. Soc., 58, No. 9-10, 377-380 (1975).
18. A. Gatti, "Development of a Process for Producing Transparent Spinel Bodies," Final Report on Contract N00019-69-C-0133, (1969).
19. A. Gatti, R. L. Mehan, and M. J. Noone, "Development of a Process for Producing Transparent Spinel Bodies," Final Report on Contract N00019-71-C-0126, (1971).
20. L. J. Gauckler, S. Boskovic, I. K. Naik, and T. Y. Tien, "Liquid Phase Sintering of β - Si_3N_4 Solid Solutions Containing Alumina," in Proceedings of the Workshop on Ceramics for Advanced Heat Engines, Orlando, (Jan. 1977). ERDA Report: Conf-770110, (1977).
21. German Patent 234129, 29 April 1911.
22. H. Suzuki, "The Synthesis and Properties of Si_3N_4 ," Bull. Tokyo Inst. Tech. No. 54, 1963.
23. H. W. Jacobson of DuPont, private communication, "Amorphous Si_3N_4 Composition Containing Carbon: U.S. Patent Application B581564, March 1976.
24. I. C. Huseby, General Electric CR&DC, Personal Communication, January 1975.
25. G. R. Terwilligen, F. F. Lange, "Pressureless Sintering of Si_3N_4 ," J. Mat. Sci., 10, 1169-1174 (1975).
26. G. K. Layden, "Process Development for Pressureless Sintering of Sialon Ceramic Components," 1st Quarter Report, Contract N00019-25-C-0232, NASC May 1975.
27. G. E. Gassa, "Effect of Yttria Additions on Hot-Pressed Si_3N_4 ," Am. Ceram. Soc. Bull., 54 (9) 778-81 (1975).
28. R. W. Rice and W. J. McDonough, "Hot-Pressed Si_3N_4 with Zr-Based Additions," J. Am. Ceram. Soc., 58 (5) 264 (1975).
29. R. R. Wills, R. W. Stewart and J. M. Wimmer, "Fabrication of Reaction Sintered Sialon," J. Am. Ceram. Soc., 60 (1) 64 (1977).
30. C. A. Bruch, "Preparation of Translucent Alumina from Powder," GE Report 58-RL-2122, November 1958.
31. J. M. Wimmer, Personal Communication, April 1976.
32. A. F. McLean, et al, "Brittle Materials Design, High Temperature Gas Turbine," AMMRC-CTR- 75-28, 84-88, October 24, 1975.
33. F. F. Lange, S. C. Singhal and R. C. Kuznicki, "Phase Relations and Stability Studies in the Si_3N_4 - SiO_2 - Y_2O_3 Pseudoternary System," J. Am. Ceram. Soc., 60 (5-6), 249-252 (1977).

34. R. J. Bratton, C. A. Anderson, F. F. Lange, Westinghouse Electric Corporation, "Progress on ARPA-ERDA Si_3N_4 Materials Development," in Ceramics for High Performance Applications - II, Newport, R.I., March 1977, to be published.
35. A. W. J. M. Rae, D. P. Thompson, and K. H. Jack, "The Role of Additives in the Densification of Nitrogen Ceramics," in Ceramics for High Performance Applications - II, Newport, R.I., March 1977, to be published.
36. S. Prochaska, C. A. Johnson and R. A. Diggings, "Investigation of Ceramics for High Temperature Components," Final Report on Contract N62269-75-C-0122, NADC, Dec. 1975 (Report #NADC-76004-30) GE CR&DC.
37. Courtesy of Dr. Harish Dalal of SKF Industries (1976).
38. R. R. Wills, R. W. Stewart and J. M. Wimmer, "Effect of Composition and X-Phase Upon the Intrinsic Properties of Reaction Sintered Sialon," Am. Cer. Soc. Bull. 56 (2) 19 Feb. 1977.
39. S. C. Singhal, "Thermodynamics and Kinetic of Oxidation of Hot Pressed Si_3N_4 ," J. Mat. Sci., 11 500-509 (1976).
40. S. C. Singhal and F. F. Lange, "Oxidation Behavior of Sialon," J. Am. Cer. Soc., 60, (3-4) 190-191 (1977).
41. P. Land, AFML, Personal Communication, Oct. 1976.
42. R. A. Tanzilli, GE-RESO, Personal Communication 1976.
43. M. J. Noone and H. W. Rauch, Sr., "Improved Glass Ceramics for High Temperature Environments," Final Report on Contract N00014-74-C-0422, June 1976.
44. P. L. Land, AFML, Personal Communication, May 1977.
45. J. J. Gebhardt, R. A. Tanzilli, T. A. Harris, "Chemical Vapor Deposition of Si_3N_4 ," Pub. Elect. Chem. Soc. Proceeding 5th Int. Conference on Chemical Deposition, Slough, England, Sept. 21-25, 1975.
46. H. Dalal, SKF Industries, Private Communication, Nov. 1976.